(1)

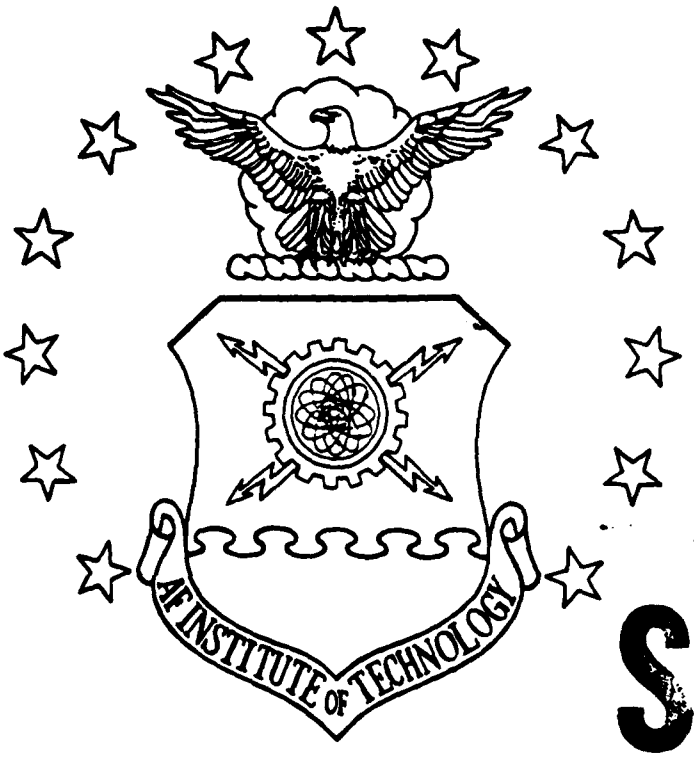

RESPONSE EQUIVOCATION ANALYSIS FOR THE SMART STICK CONTROLLER

THESIS

John M. Pracher
Captain, USAF

AFIT/GE/ENG/88D-38

DEPARTMENT OF THE AIR FORCE
AIR UNIVERSITY
AIR FORCE INSTITUTE OF TECHNOLOGY

Wright-Patterson Air Force Base, Ohio

RESPONSE EQUIVOCATION ANALYSIS

FOR THE

SMART STICK CONTROLLER

THESIS

John M. Pracher
Captain, USAF

AFIT/GE/ENG/88D-38

AFIT/GE/ENG/88D-38

RESPONSE EQUIVOCATION ANALYSIS FOR THE SMART STICK CONTROLLER

THESIS

Presented to the Faculty of the School of Engineering
of the Air Force Institute of Technology
Air University
In Partial Fulfillment of the
Requirements for the Degree of
Master of Science in Electrical Engineering

John M. Pracher, B.S.E.E.
Captain, USAF

November 1988

Preface

Anyone who has been through an effort as imposing as a thesis fully understands that completion depends not only on how much you accomplish, but also on the support you receive from others along the way. I would specifically like to thank my thesis advisor Major David Norman not only for his guidance, but also for having the confidence to give me a free hand in nearly all aspects of this project. I'd also like to thank Dr Dan Repperger of the AAMRL who sponsored this project for his many hours of support and his unfailing ability to consistently put things in perspective. Also, many thanks to my "cohort in crime", Capt Al Cozzone, who was always there when I needed to bounce another idea off of someone. But, I would especially like to thank my wife, [redacted] for tolerating all of those evenings I spent glued to [redacted] computer and for providing that shoulder to lean on whenever I needed it. Thank you all very much.

John M. Pracher

Table of Contents

List of Figures

List of Tables

Abstract

This ~~research~~ thesis provides an analysis of response equivocation (lost information) for subjects who use the "smart stick controller" -- an aircraft stick controller designed by the Armstrong Aerospace Medical Research Laboratory (AAMRL) to improve a pilot's tracking performance. First, a control theory model of a compensatory tracking task is developed and analyzed. Then, using an information theory model of the pilot, the results are used to develop expressions for information theory parameters (input entropy, transinformation, and equivocation).

Six subjects were tested using the smart stick controller and experimental an apparatus developed by the AAMRL. Each subject was tested twice: first in the passive stick mode (normal stick operation), and again in the active stick mode. In the active stick mode, the smart stick actively exerts a force in the direction opposite to the desired stick motion. Power spectral densities of the display error and the operator response were used to calculate the information theory parameters.

The results indicated that by viewing the response equivocation alone, it was not possible to ascertain any

significant change in performance between passive and active stick mode operation. However, by viewing other parameters (entropy, transinformation, human operator transfer function, and human operator remnant), it is evident that a change in performance definitely occurs.

RESPONSE EQUIVOCATION FOR THE SMART STICK CONTROLLER

Chapter I. Introduction

1.1 Historical Perspectives

As more capabilities are added to aircraft cockpits, questions naturally arise concerning the pilot's ability to acquire and process the information provided by the new equipment: "How much information can the pilot take in?" and "At what point does the pilot's performance begin to degrade?". This thesis is only a small portion of the Armstrong Aerospace Medical Research Laboratory's (AAMRL) effort to study human performance and develop new techniques to enhance performance and to reduce the time required to learn a task.

In 1983, the AAMRL was conducting experiments on the centrifuge to evaluate pilot tracking performance using various stick controllers. An unexpected outcome of the experiment showed that when a G-force was exerted in the direction opposed to the original stick motion, tracking performance was substantially and consistently improved. The improvement was attributed to the fact that the opposing

G-force was actually providing a natural damping force which reduced the amount of "overshoot" introduced by the pilot while performing the tracking tasks. This unexpected result led to the development of a device called the "smart" stick controller. (10:2-3)

The "smart" stick controller is an aircraft stick controller that can operate either in a passive or active mode. It is essentially an electro-mechanical device whose internal parameters can be controlled via a computer. In the passive mode the smart stick performs like a typical displacement stick controller, with all forces on the stick being provided by the pilot. In the active mode, however, the stick actively exerts a force in the direction opposite to the desired stick motion. An alternate view is that the smart stick develops a force via an algorithm to adjust the amount of force the pilot exerts on the stick. Reference 9 contains information on design and operation of the smart stick controller. The intent was to emulate the conditions that occurred in the centrifuge with an eye towards improving tracking performance. (9:810-811)

Results of experimentation with the smart stick controller have demonstrated that tracking performance improves significantly; however, the reasons for the improvement are not yet fully understood. Two primary theories are given for the marked improvement. The first

has to do with human physiology. In the active mode, the smart stick changes the muscle activity required to perform the tracking tasks, smoothing the pilot's performance and resulting in less error. The second theory is that the smart stick is actually providing the pilot with additional information in the form of the opposing force; and since the pilot has more information available, he is able to make a more accurate response. Both theories are presently being studied by the AAMRL. This thesis deals primarily with the latter theory.

1.2 Problem Statement

The purpose of this thesis is to develop information theory needed to support smart stick experimentation developed by the AAMRL, and to use the information theory and the experimental apparatus to determine the response equivocation (lost information) of various subjects performing a compensatory tracking task. The tracking tasks will be performed using the smart stick in both the passive and active modes of operation.

1.3 Scope

This research is part of a larger effort being pursued by the AAMRL to characterize, quantify, predict, and improve human performance through a combination of control theory and information theory techniques. This thesis, dealing

only with response equivocation while performing tracking tasks using the smart stick controller, is one of two efforts dealing specifically with information theory aspects of human performance. A concurrent effort deals specifically with the information capacity of an individual performing the identical tracking tasks.

1.4 General Approach

A two-fold approach is used in this research. First, information theory and appropriate assumptions are used to develop an information theory model of the human operator. Secondly, the smart stick apparatus developed by the AAMRL is used to train and test the subjects who will be *performing* the tracking tasks. Before testing the subjects, it is necessary to provide a training period. This is necessary because the overall goal is to measure the response of the human motor system during the tracking task. So, the training ensures that the tracking task becomes a "highly learned" skill, ensuring a certain amount of predictibility in the task. Each subject is tested in both the passive and active stick operation modes. This will provide a measurement of the noise introduced by the operator in each mode. The response equivocation will be determined for each mode of operation. Since the human operator is the only element in the system where noise is

introduced, any change in performance as a result of using the active stick will show up as a change in the amount of noise introduced by the operator. This will, consequently, be reflected by a corresponding change in the response equivocation.

Overview of Remaining Chapters

This report consists of five additional chapters. Chapter II provides a brief background regarding the evolution of the use of information theory to characterize human performance. It also provides a short synopsis of some of the most significant research previously conducted. In Chapter III, the control theory model of the tracking task and the information theory model of the human operator are presented. Chapter IV details the experimental apparatus used to train and test the subjects. It also provides a discussion of the procedure used during testing. Chapter V contains the data analysis and results obtained from this testing. Conclusions and recommendations for further areas of study are provided in Chapter VI.

Chapter II. Background

2.1 Introduction

A branch of experimental psychology, called the study of human performance, analyzes the processes involved in developing skilled performance. It not only studies how the skills are developed, but also identifies what factors may limit or inhibit skilled performance with the overall objective of trying to predict human performance in specific situations and under specific circumstances. (4:1)

Before proceeding, it is important to distinguish skilled performance from a reflexive act. Although both are reactions (responses) generated by the human as a result of information (stimuli) provided by the environment, the discriminating factor is what happens between the stimulus and the response. In a reflexive action the stimulus is sensed by the central nervous system and a response is automatically generated without any conscious internal process required on the part of the individual. In skilled performance, however, when a stimulus is received (sensed by the central nervous system) the response is not automatic. The stimulus is first analyzed and then a decision is made concerning what the appropriate response should be. Only then is the response generated. So, skilled performance requires internal processing within the human system in

addition to direct sensory interaction with the environment. It is, therefore, a learned response which can be developed to the point of being so highly proficient that it mimics a reflexive action. The internal processing becomes so well organized and efficient that very little time is required to generate a response. Examples of this are a boxer's ability to "slip a punch" and a baseball batters ability to hit a fast pitched ball. These skills are so highly learned that they appear to be reflexive to the casual observer. (4:1-5)

2.2 Information Processing

Paul Fitts defined Human Performance Theory as the study of how man's central nervous system performs the internal processing of information as well as how the central nervous system communicates between man and his environment. He surmised that there are essentially three information processing tasks performed by the central nervous system: transmission of information, information reduction, and elaboration. (4:5)

Transmission of information is the particular information processing task of primary concern in this research. In this task the objective is to take the input (stimulus) and reproduce it as precisely as possible at the output, but in a different form. Examples of this type of processing are reading out loud or translating from one

language to a another. In this research a human operator will be attempting to manually track a moving object on a video display using an aircraft stick controller (the smart stick).

Information reduction involves processing the input (stimuli), sorting out the extemporaneous and irrelevant information, and reassembling the information to produce the response. Examples are problem solving and reasoning. Elaboration involves the process of taking a stimulus and generating an output (response) which has a higher degree of complexity and a greater amount of information than that provided by the input. This is usually associated with the ability to generalize. (11:25-26)

2.3 Information Theory

In information transmission tasks, a human operator essentially behaves like an information processor -- accepting inputs (stimuli) from the environment, performing some internal processing of the information received from the stimuli, and producing specific outputs (responses). This process is very similar to the phenomenon exhibited by a physical communications channel such as a telephone channel or radio channel. Thus, for the purpose of modelling human behavior while performing an information transmission task, it is possible to draw a direct analogy

between the human operator and a physical communications process. (11:26)

Information theory, pioneered by Claude E. Shannon in 1948 in his Mathematical Theory of Communications, provided the mathematical means for describing the qualitative and quantitative behavior of communications channels in terms such as entropy, capacity, equivocation, bandwidth, and signal-to-noise ratios. The communication channel analogy, coupled with Shannon's theories, raised many questions about human behavior that are normally asked only when discussing physical communications channels: "How much information is provided by an input or an output?", "How much information is transmitted from the input to the output?", "Is it possible to characterize the amount of noise introduced into the process by the human operator?", and "If so, how can this noise be measured and what is it's impact on the capacity of channel?". These are questions which would naturally be extrapolated from information theory. (12:111)

In 1954, Dr. Paul Fitts felt it was indeed possible to answer these questions and stated:

> The information capacity of the motor system is specified by its ability to produce consistently one class of movement among several alternative movement classes. (3:382)

He further theorized that it was possible to measure various parameters when he wrote:

> ... Information capacity is limited only by the amount of statistical variability, or noise, that is characteristic of repeated efforts to produce the same response. The information capacity of the motor system, therefore, can be inferred from measures of the variability of successive responses that S (subject) attempts to make uniform. (3:383)

Essentially, Dr. Fitts had acknowledged that it is possible to use information theory to quantify human performance during an information processing task.

2.4 Previous Research

Since the work in this thesis centers around quantifying human performance in a continuous tracking task, this section will address some of the more significant research performed in that specific area.

In 1960 E.R.F.W. Crossman conducted one of the most definitive studies concerning information capacity of a human operator while performing a tracking task. This was one of the first studies accomplished which relied strictly on the theories developed by Shannon. In his experiment Crossman determined that a human operator has a trans-information rate (capacity) of 5 bits per second (2:15).

Questions persisted, however, about how to determine the amount of noise the human operator introduces during the processing of information. In information theory this is an extremely important issue because all noise introduced has a

detrimental effect on the capacity. Fitts recognized the significance of noise when he stated:

> It is possible to determine experimentally the noise associated with each category of response amplitude and rate, and to infer the average information capacity per response and maximum average rate of information transmission from the ratio of the magnitude of the noise to the magnitude of the possible range of responses. (3:382)

He further stated :

> An accepted method for estimating channel capacity in the case of a continuous signal requires a determination of the average power of the noise associated with the output signal. (3:383)

In a compensatory tracking task, the human operator attempts to track a signal that is continuously and randomly moving on a display. The objective for the human operator is to track the signal as closely as possible: that is, the operator is attempting to precisely follow the "signal track". The resulting error forms the basis for analysis of the noise. This error is described as the portion of the human operator's output that is not directly related to (not correlated with) the input (6:101). This is essentially the noise that the human operator injects into the process. In order to be consistent with previous research, this noise will hereafter be referred to as the remnant.

Human operator remnant (human injected noise) is contributed primarily by the following sources. (8:6-8)

1. Observation Remnant. This is usually a direct result of the design and location of the display. The display may be difficult to read (poorly focused) or poorly positioned (not directly in the subject's line of vision). The human operator is less sure of the input and therefore provides less precise (and more noisy) responses while tracking.
2. Scanning Remnant. This effect is most significant when multiple displays are used. The human operator must scan several displays, selecting the necessary information before making the appropriate response. In this case, the human operator has more information available, but now must sort through it to determine what the response should be.
3. Equalization Remnant. This is directly associated with the internal processing the human operator must provide. In the compensatory tracking task, it is the remnant generated as a result of the operator recognizing how far and how rapidly the signal is changing and then determining what the reaction (output) should be. In tracking tasks this should be the dominant source of remnant.
4. Motion-Cue Remnant. This remnant is caused by the physiological changes resulting from the effects

of motion on the operators equilibrium. This typically results from changes occuring in the middle ear.

5. Crosstalk Remnant. This remnant is most common in tracking tasks where a response can be multi-dimensional. In this case motion can be made by using a combination of a variety of muscular movements.
6. Neuromuscular Remnant. This is usually a direct result of the physiological interactions between the nerves and muscles that is required to provide motion. The effect becomes more pronounced when the amplitude of the required motion is larger and when the changes in direction are more frequent.

In practice it is impossible to differentiate among individual sources of remnant since none of the sources has any singular distinguishing waveform characteristics. Consequently, analyses conducted by Levison and others have modelled human operator remnant as a single, lumped (equivalent) noise process. This is predicated on the assumptions that the noise injected by each remnant source is a linearly independent white noise process and that these processes are independent of the input. The assumptions are tantamount to stating that the remnant is truly internal to

the human operator (6:102). Levison, in this reference, provided the model and theoretical foundation (using spectral analysis) for predicting human operator remnant and verified experimentally that the model was valid for a one-dimensional tracking task.

Sheridan and Ferrell, using the model provided by Levison, also performed an information theory analysis to quantify human performance. The results were consistent with those obtained by Crossman, Fitts, and Levison. (11:135-160)

Chapter III. Theory

3.1 Introduction

This chapter contains the theoretical analysis for determining the response equivocation of the human operator while performing a compensatory tracking task. It begins by specifying the compensatory tracking task model used in the study. A frequency analysis is then conducted, followed by an information theory analysis to determine the transinformation rate, response equivocation, and capacity of the human operator.

3.2 Model of the Compensatory Tracking Task

In this study we are essentially analyzing the performance of the human operator performing a tracking task under two conditions : passive stick operation and active stick operation. A simplified block diagram for a compensatory manual control system is shown in Figure 1.

In a compensatory tracking task, the overall objective is to have the human operator output follow the system input with little error. The system input is called the forcing function, a random function representing the movement of the target being tracked. This input is essentially the ideal (perfect) human operator response. It is significant to note that in a compensatory tracking task the human operator does not see the "movement" of the forcing function,but

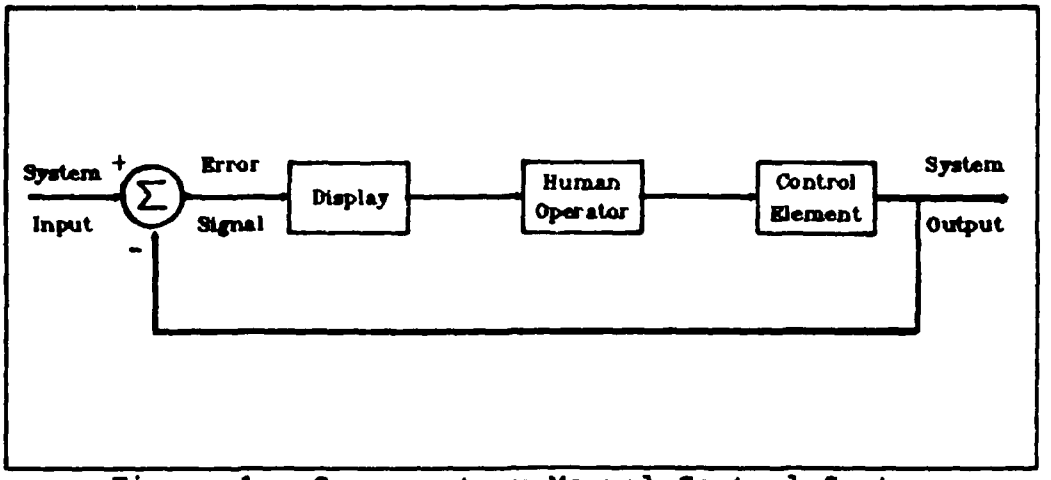

Figure 1 - Compensatory Manual Control System
(Adapted From 5:58)

rather the difference between his response and the forcing function. In this project there is only one class of forcing functions being used, a sum of sinusoids.

$$\Sigma A_n \mathrm{Sin}(n w_o + \theta_n)$$

where

all n's are relatively prime

A_n = Amplitude of sinusoid associated with specific n

θ_n = Uniformly distributed random phase

w_o = Fundamental frequency (radians/second)

A sum of sinusoids is being used to facilitate calculations of the human operator remnant (noise). This is explained in more detail later in this chapter.

The error signal in Figure 1 is the difference between the forcing function (target position) and the system output (position as a result of the human operator's response). It is this signal that appears on the display to the human operator. This error then is the input signal (stimulus) provided to the human operator.

The human operator block in Figure 1 can be represented by using two elements: a linear element (human operator describing function) and a non-linear element (human operator remnant). See Figure 2 below.

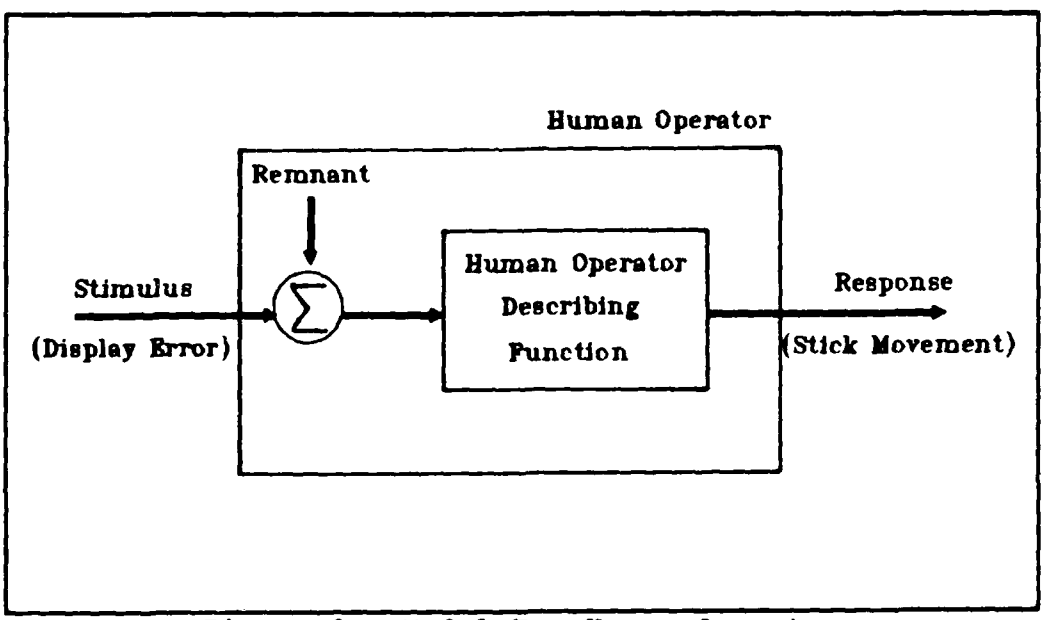

Figure 2 - Model For Human Operator

This model was used by Levison in his analysis of human operator remnant (6:102-103).

The human operator block in Figure 2 clearly represents a non-linear process. However, by restricting the input (forcing function) to a specific class of functions (random sinusoids), it is possible to exactly represent the human operator response by using a non-linear and linear element as shown in Figure 2. In control theory this is commonly referred to as a quasi-linear representation. (8:7-9) The linear element (human operator describing function) represents the linear portion of the human operator response to a specific input. The non-linear component (remnant or noise), however, represents the difference between the actual output (human operator response) and the linear response. As explained in the previous chapter, remnant actually results from many different sources. In order to adequately model the remnant, the following assumptions are needed:

1. Remnant from each source is a white gaussian noise process
2. Each noise process is independent of the other noise processes
3. Each noise process is independent of the forcing function

4. Each noise process is independent of all other system parameters

Using these assumptions, it is possible to incorporate all of the individual remnant noise processes into a single "lumped" additive white gaussian noise process. (6:102)

The control element block in Figure 1 is the entity the human operator's response is acting upon. In this scenario the human operator's response is the movement of a stick controller to a specific position. This controller would then typically act on an aircraft. So, the control element in this case would represent the dynamics of the aircraft's response to the stick movement. For this experiment we will assume the aircraft's response is instantaneous (a unity gain in the frequency domain). This essentially removes this block from the diagram in Figure 1, and the operator's response (stick position) to the display error becomes the output of the system.

Incorporating all of the elements discussed above into Figure 1 results in the block diagram shown in Figure 3 where

$r(t)$ = Forcing function

$e(t)$ = Display error

$n(t)$ = Noise or human operator remnant

$y_H(t)$ = Human operator describing function

$u(t)$ = Human operator response (stick position)

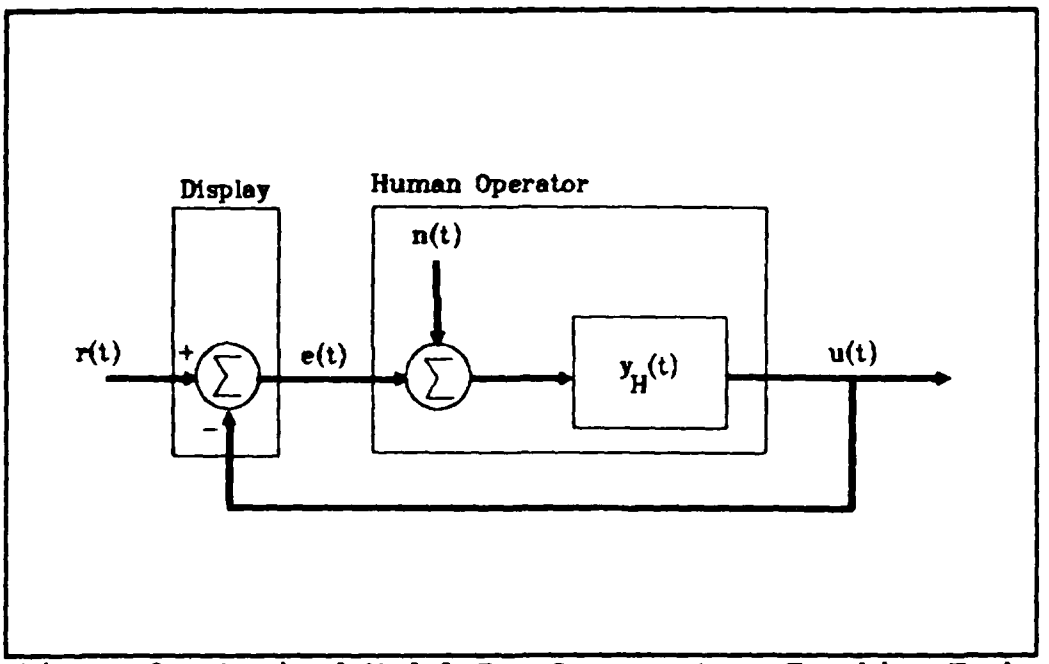

Figure 3 - Revised Model For Compensatory Tracking Task

3.3 Analysis of the Compensatory Control System

The analysis technique used in this section is essentially a combination of the techniques used by Sheridan and Ferrell (11:207-223) and Levison (6:102-104).

The forcing function used in this project consists of a sum of sinusoids whose frequencies are not harmonically related (all frequencies are relatively prime). Performing a Fourier transform of this forcing function yields a frequency domain representation consisting of discrete spectral lines. Because of this, the analysis will be accomplished in the frequency domain and involves

determining the spectral characteristics of the forcing function, display error, remnant, human operator response (output), and the human operator describing function shown in Figure 4 below, where:

R(w) = the Fourier transform of r(t)

E(w) = the Fourier transform of e(t)

N(w) = the Fourier transform of n(t)

$Y_H(w)$ = the Fourier transform of $y_H(t)$

U(w) = the Fourier transform of u(t)

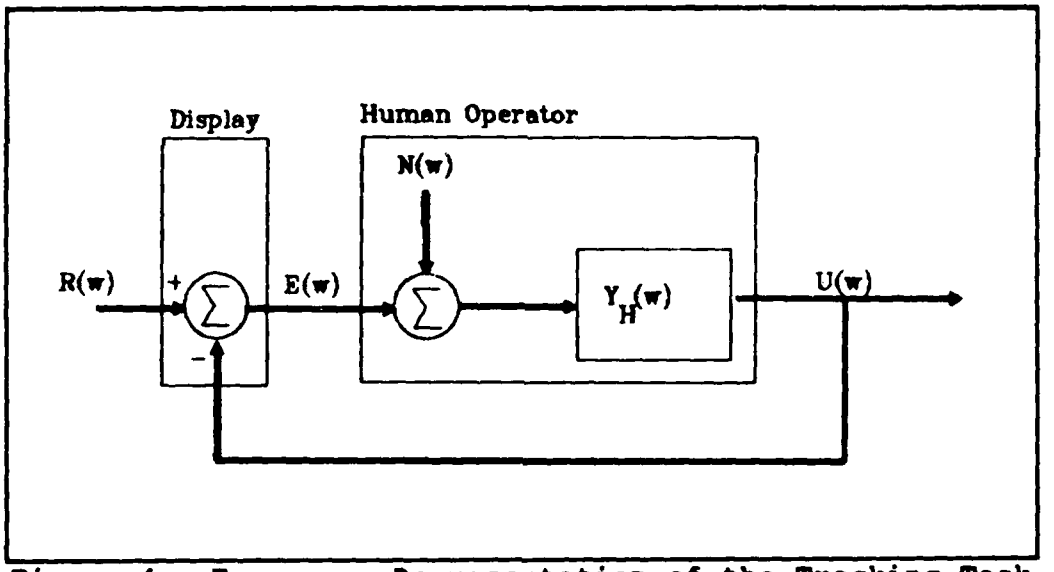

Figure 4 - Frequency Representation of the Tracking Task

The analysis will move from the input (forcing function) to the output (human operator response) as shown in Figure 4. The power spectral density (PSD) of the

forcing function, $\Phi_{rr}(w)$, is defined as the Fourier transform of the autocorrelation of the forcing function.

$$\Phi_{rr}(w) = \lim_{T\to\infty} \frac{1}{2T} \int_{-\infty}^{\infty} R(w)\cdot R(-w)\ dw \qquad (1)$$

However, if we restrict this integral to a small frequency band, dw, (an infinitesimally small bandwidth about each spectral line) then this expression becomes

$$\Phi_{rr}(w) = \lim_{T\to\infty} \frac{1}{2T} [R(w)\cdot R(-w)] \qquad (2)$$

It is significant to note that to be completely accurate, the above expression should be written as

$$\Phi_{rr}(nw_o) = \sum \lim_{T_n\to\infty} \frac{1}{2T_n} [R(nw_o)\cdot R(-nw_o)] \qquad (3)$$

From this point on, we will use the notation used in Equation 2.

At this stage, the PSD of the remnant will just be defined as the Fourier transform of the autocorrelation of the noise.

$$\Phi_{nn}(w) = \lim_{T\to\infty} \frac{1}{2T} [N(w)\cdot N(-w)] \qquad (4)$$

The noise power will be dealt with in more detail later.

The PSD of the error signal, $\Phi_{ee}(w)$, is found using the same approach.

$$\Phi_{ee}(w) = \lim_{T\to\infty} \frac{1}{2T} [E(w)\cdot E(-w)] \qquad (5)$$

But, from Figure 4, we also have

$$E(w) = R(w) - U(w) \qquad (6)$$

and

$$U(w) = [E(w) + N(w)]\cdot Y_H(w)$$

So, substituting into Eq (6) yields

$$E(w) = \frac{1}{1 + Y_H(w)}[R(w) - Y_H(w)\cdot N(w)] \qquad (7)$$

Using this expression for E(w) and the assumption that the noise is independent of (not correlated with) the forcing function, the PSD for the display error then becomes

$$\Phi_{ee}(w) = \left|\frac{1}{1 + Y_H(w)}\right|^2 \Phi_{rr}(w) + \left|\frac{Y_H(w)}{1 + Y_H(w)}\right|^2 \Phi_{nn}(w) \qquad (8)$$

Notice that Eq (8) contains two terms. The first term represents the display error power correlated with the forcing function. The second term then, represents the display error power not correlated with the forcing function.

Using these terms then permits us to write the expression for the display error power PSD as follows:

$$\Phi_{ee}(w) = \Phi_{eer}(w) + \Phi_{een}(w) \tag{9}$$

where

$$\Phi_{eer}(w) = \left| \frac{1}{1 + Y_H(w)} \right|^2 \Phi_{rr}(w) \tag{10}$$

and

$$\Phi_{een}(w) = \left| \frac{Y_H(w)}{1 + Y_H(w)} \right|^2 \Phi_{nn}(w) \tag{11}$$

Using the same technique to determine the PSD of the human operator response, $\Phi_{uu}(w)$, yields the following

$$\Phi_{uu}(w) = \left| \frac{Y_H(w)}{1 + Y_H(w)} \right|^2 \Phi_{rr}(w) + \left| \frac{Y_H(w)}{1 + Y_H(w)} \right|^2 \Phi_{nn}(w) \tag{12}$$

As with Eq (8), Eq (9) also contains two terms -- one term representing that portion of the output (response) signal that is correlated with the forcing function, and the other term representing the portion of the output (response) signal not correlated with the forcing function. The latter portion represents the amount of remnant or noise power contained in the PSD.

Using Equation 12, it is now possible to more precisely define the PSD of the noise (remnant), $\Phi_{nn}(w)$.

First, rewrite Equation 12 as

$$\Phi_{uu}(w) = \Phi_{uur}(w) + \Phi_{uun}(w) \tag{13}$$

where

$$\Phi_{uur}(w) = \left| \frac{Y_H(w)}{1 + Y_H(w)} \right|^2 \cdot \Phi_{rr}(w) \tag{14}$$

and

$$\Phi_{uun}(w) = \left| \frac{Y_H(w)}{1 + Y_H(w)} \right|^2 \cdot \Phi_{nn}(w) \tag{15}$$

This is merely a restatement of the fact that the human operator response consists of signal power (power correlated with the forcing function) and noise (operator remnant). Now, dividing Eq (15) by Eq (14) and solving for $\Phi_{nn}(w)$ yields

$$\Phi_{nn}(w) = \frac{\Phi_{uun}(w)}{\Phi_{uur}(w)} \cdot \Phi_{rr}(w) \tag{16}$$

Notice that in Eq (16) $\Phi_{uun}(w)/\Phi_{uur}(w)$ is the ratio of the remnant (noise) in the human operator response that is correlated to the input spectrum. This is essentially a noise to signal ratio for the human operator response with respect to the forcing function, r(t). This is significant because, as will be seen in Chapters IV and V, all three terms on the right side of Eq (16) are either pre-determined or can be measured directly. So, it will be possible to directly calculate a specific value for $\Phi_{nn}(w)$, the noise power spectrum.

The only component that remains to be defined is $Y_H(w)$, the human operator describing function. This has previously been defined as the linear portion of the human operator response. Therefore, $Y_H(w)$ can be expressed as the following ratio:

$$Y_H(w) = \frac{\text{Human response correlated with the forcing function}}{\text{Display error correlated with the forcing function}}$$

This can also be written as

$$Y_H(w) = \frac{\Phi_{uur}(w)}{\Phi_{eer}(w)}$$

Each of these terms can also be determined experimentally. So, again, a specific value can be calculated for $Y_H(w)$.

3.4 Information Theory

Up to this point the analysis has been very much in line with "classical" control theory analysis. Now we will diverge from the control theory and, using the derived results obtained thus far, move into the realm of information theory. That is, we will now view the human operator from the perspective of being an information channel -- " a transmitter and receiver of information".

As discussed in Chapter II, the analogy of the human operator and the information channel is appropriate since the human operator is continuously receiving information (in the form of stimuli), processing the information, and responding to the specific stimuli. However, the response is not always the desired response; such as a batter missing the baseball. The basic objective is to characterize or quantify the relationship between the stimulus and response using information theory. Characterizing this relationship will begin with some basic information theory definitions and then move on to analysis of the specific compensatory tracking task.

The most common representation of an information channel is illustrated in Figure 5.

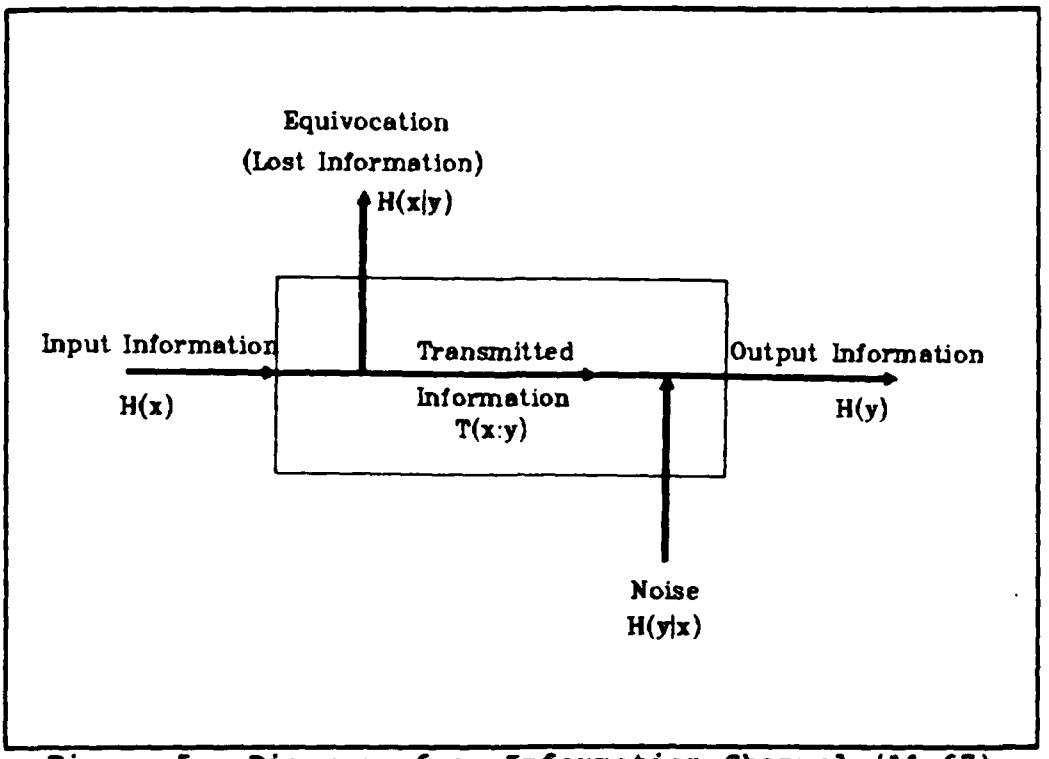

Figure 5 - Diagram of an Information Channel (11:67)

The basic operation of the channel is straightforward. Information received at the input is transferred to the output. If the information is not transmitted exactly, then only two things could have occurred: some of the information could have been lost and/or noise could have been introduced during the transfer process.

Defining the five components shown in Figure 5 will essentially provide the entire framework for the information theory needed in this analysis. Information theory measurements have their basis in entropy calculations. In information theory, entropy is defined as the amount of

information contained in a signal. These signals, however, are actually random waveforms. As a consequence, the entropy can be viewed as the predictibility or uncertainty of the waveform. If an output is deterministic, it is totally predictable and therefore contains no useful information. However, the entropy is related to the probability density function of the random waveform.

Let the input signal be a random variable X. Then the input information is the entropy of the input, X. In this study the human operator is considered to be a continuous channel. So the entropy of the input, H(X), in bits per second is the differential entropy

$$H(X) = \int f(x) \cdot \text{Log}_2 \frac{1}{f(x)} dx \qquad (17)$$

where f(x) is the probability density function of the input waveform. Similarly, the output information is defined as the entropy of the output waveform, Y, and can be determined by

$$H(Y) = \int f(y) \cdot \text{Log}_2 \frac{1}{f(y)} dy \qquad (18)$$

where f(y) is the probability density function of the random output waveform. From Figure 5 it is obvious that if the human operator is considered as a perfect channel (no noise and no equivocation), then H(X) = H(Y).

Equivocation and noise (often called prevarification) are conditional entropies. Equivocation, $H(X|Y)$, represents the entropy in the input from the perspective of the receiver (channel output). It is the uncertainty concerning what was actually transmitted given that a specific response was received. For this reason equivocation is sometimes referred to as the amount of information that is lost between the input and output. Equivocation can be determined as follows:

$$H(X|Y) = \int f(x|y) \cdot \text{Log}_2 \frac{1}{f(x|y)} \, dx \qquad (19)$$

where $f(x|y)$ is the conditional probability density function of x conditioned only. (1:58)

In similar fashion, noise, $H(Y|X)$, represents the entropy in the output from the perspective of the transmitter (channel input). It is the uncertainty of what was actually received given that a specific stimulus was transmitted. Noise can be determined as follows (1:58)

$$H(Y|X) = \int f(y|x) \cdot \text{Log}_2 \frac{1}{f(y|x)} \, dy \qquad (20)$$

The transinformation (often called mutual information), $T(X;Y)$, represents the entropy (uncertainty) difference between the channel input before the input was sent and

after it was received. Therefore, it is often referred to as the information gain and is represented as

$$T(X;Y) = H(X) - H(X|Y) \tag{21}$$

Notice this can also be written as

$$H(X|Y) = H(X) - T(X;Y) \tag{22}$$

It is also significant to note that transinformation is symmetric. (1:149-150) That is

$$T(X;Y) = T(Y;X) \tag{23}$$

and

$$T(Y;X) = H(Y) - H(Y|X) \tag{24}$$

With these information theory terms defined, we now move to the specific analysis of the compensatory tracking task shown in Figure 3. Recall in the model for this task that it is the display which provides the input (stimulus) for the human operator and it is the human operator who acts as the information channel.

The analysis is greatly simplified primarily by the assumption that the remnant process, n(t), is an additive white gaussian noise (AWGN) process. Also, recall that the forcing function, r(t), is a sum of sinusoids with random phases. The random phases are selected prior to each tracking task trial and are primarily used to ensure the

task cannot be learned (see Chapter IV). These random phases, however, are not changed during the course of a tracking trial. Therefore, the forcing function is actually deterministic for each trial. Also, the human operator describing function defined as a linear function and ,as such, can add no nonlinearities (noise) to the process. As a result, not only is n(t) an AWGN process, but so is the display error, e(t), and the operator response, u(t).

The entropy of the input to the human operator is actually the entropy of the output of the display, e(t). This particular entropy, however, can also be viewed as the transinformation of the display or

$$T[e(t);d(t)] = H[e(t)] - H[e(t)|d(t)] \tag{25}$$

where

e(t) = display error (display output)

d(t) = r(t)-u(t) = input to the display

Because e(t) is an AWGN process, its entropy can be determined from its PSD (1:247).

$$H[e(t)] = \text{Log}_2 2\pi[S_e(w) + N_e(w)] \tag{26}$$

where $S_e(w)$ = Portion of $\Phi_{ee}(w)$ correlated with the forcing function

$N_e(w)$ = Portion of $\Phi_{ee}(w)$ not correlated with the forcing function

Also, the equivocation of the display becomes (1:246)

$$H[e(t)|d(t)] = \text{Log}_2[2\pi N_e(w)] \tag{27}$$

Substituting Equations 23 and 24 into Equation 22 yields a transinformation of

$$T[e(t);d(t)] = \text{Log}_2 \frac{S_e(w) + N_e(w)}{N_e(w)} \tag{28}$$

$S_e(w)$ and $N_e(w)$ are actually the correlated and uncorrelated components of the display error PSD as illustrated in Equations 9,10, and 11. Using those expressions, we can write the expression for the transinformation of the display as following:

$$T[e(t);d(t)] = \text{Log}_2 \frac{\Phi_{eer}(w) + \Phi_{een}(w)}{\Phi_{een}(w)} \tag{29}$$

Substituting the expressions for $\Phi_{eer}(w)$ and $\Phi_{een}(w)$ and simplifying yields

$$T[e(t);d(t)] = \text{Log}_2 \left[1 + \frac{\Phi_{rr}(w)}{|Y_H(w)|^2 \Phi_{nn}(w)} \right] \tag{30}$$

Since u(t) is also an AWGN process, the same technique is used to find the equivocation of the channel (operator).

$$H[e(t)|u(t)] = H[e(t)] - T[e(t);u(t)] \tag{31}$$

First, recall that the transinformation of the display, Equation 28, is the input entropy, H[e(t)], for the channel. So, the only remaining task is to find the transinformation of the channel. Using the same rationale as used for the transinformation of the display yields

$$T[e(t);u(t)] = \text{Log}_2 \frac{S_u(w) + N_u(w)}{N_u(w)} \qquad (32)$$

where $S_u(w)$ = Portion of $\Phi_{uu}(w)$ that is correlated with the forcing function

$N_u(w)$ = Portion of $\Phi_{uu}(w)$ that is not correlated with the forcing function

Referring back to Figure 3 and Equations 9, 10, 11, we can rewrite Equation 32 in terms of $Y_H(w)$, $\Phi_{eer}(w)$, $\Phi_{een}(w)$, and $\Phi_{nn}(w)$ as follows:

$$T[e(t);u(t)] =$$

$$\text{Log}_2 \left[\frac{|Y_H(w)|^2 [\Phi_{eer}(w) + \Phi_{een}(w) + \Phi_{nn}(w)]}{|Y_H(w)|^2 [\Phi_{een}(w) + \Phi_{nn}(w)]} \right] \qquad (33)$$

Substituting the expressions for $\Phi_{eer}(w)$ and $\Phi_{een}(w)$ and simplifying yields

$$T[e(t);u(t)] = \text{Log}_2\left[1 + \frac{\Phi_{rr}(w)}{\left[\left|1+Y_H(w)\right|^2 + \left|Y_H(w)\right|^2\right]\Phi_{nn}(w)}\right] \quad (34)$$

Thus, recalling that for this project the input entropy to the human operator is actually the transinformation of the display, the equivocation then becomes the difference between the transinformation of the display and the transinformation of the human operator, and can be determined as follows:

$$H[e(t)|u(t)] = T[e(t);d(t)] - T[e(t);u(t)] \quad (35)$$

Chapter IV. Method of Testing

4.1 Introduction

This chapter describes the experimental apparatus and data gathering techniques used throughout the experiment. Additional details relating to the stick under test are provided in Reference 9.

Experiments were conducted to determine the capacity of the human operator using the stick in both the passive and active mode. The subjects were provided with a single axis lateral (side to side) compensating tracking task. The input forcing function minus the plant output was displayed on a video monitor. The plant was unity gain and its input was the subject's stick output.

4.2 Experimental Hardware

4.2.1 Computers. An Electronic Associate, Inc. 680 analog computer was used to drive the display unit and compute the root mean squared system errors. An SEL 32/77 digital computer was used to generate the forcing functions and convert analog data to digital formats for storage on a 9-track, 800 bpi magnetic tape recorder. A DEC PDP-1134 computer generated the data projections that were displayed on the monitor.

4.2.2 Chair. The subject's chair was an F-4 fighter aircraft ejection seat located in room 104 of the Armstrong Aerospace Medical Research Laboratory, Wright- Patterson AFB, OH. The chair was equipped with an arm rest so as not to put undue strain on the subject's arm. The stick could be accurately manipulated using only hand and wrist motion.

4.2.3 Display. The subject was provided with a Panasonic Model TR-930U video display placed approximately 50 inches away. Display brightness and contrast levels were adjusted for maximum viewing comfort, and a constant level of room lighting was maintained throughout the data collection period.

The image produced on the display unit, and illustrated in Figure 6, was that of an aft view of a maneuvering aircraft. The aircraft only moved in the horizontal direction. The movement was controlled by the difference signal between the forcing function and the operator's output. The subject's task was to minimize the distance of the maneuvering aircraft from an image of a gun sight.

4.2.4 Control. The control stick was the primary device through which the subject interfaced with the information displayed on the video monitor. The stick was used in both the passive and the active mode. In the

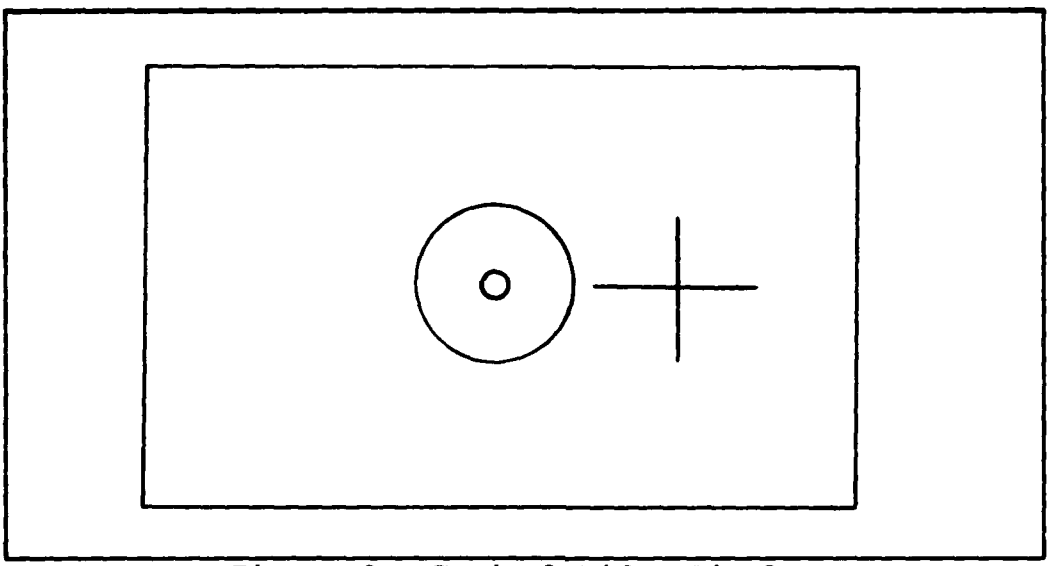

Figure 6 - Typical Video Display

passive mode the stick behaved as any normal stick controller where the force was provided entirely by the operator. In this mode, the stick moves with negligible force and is called a displacement stick. In the active mode, the stick produced resistive forces on the subject's hand which were a function of the operator output. In the active mode, the stick requires substantially more force and is referred to as a force stick. The stick was allowed to move freely only in the horizontal axis for all data runs.

A transducer provided electrical outputs proportional to the horizontal displacements as measured by the rotational potentiometer located in the base of the stick. The outputs were sampled and recorded on magnetic tape and were the basis for the calculations.

Additional information about the stick design and control can be obtained from Reference 9.

4.3 Forcing Functions

Three forcing functions were used during this experiment. To insure stationarity in the experiment, the class of forcing functions used was restricted to functions which exhibited stationary characteristics (8:12). Moreover, the forcing functions had to appear random to the subjects, otherwise the subjects could detect and learn to anticipate the deterministic nature of the forcing function.

Both stationarity and randomness requirements were satisfied by using forcing functions consisting of sums of sinusoids. It was determined that a forcing function of at least five sinusoids was sufficient to cause the subjects to view the forcing functions as random processes (11:62).

In this experiment each forcing function was a sum of fifteen sinusoids, each with a random initial phase which provided for random appearing signals. Forcing Function #1 (FF1) was generated by processing this sum of sinusoids through a second-order Butterworth filter with a cutoff frequency of 1 Hz. Forcing Function #2 (FF2) was generated by processing the same sinusoids through a second-order Butterworth filter with a cutoff frequency of 2 Hz. The third forcing function (FF3) was generated by processing the

sum of sinusoids through a Gaussian filter with a 1 Hz cutoff frequency.

To insure orthogonality among the fifteen component frequencies, the measurement time interval of 81.96 seconds contained an integral number of cycles of each component. Thus, each component was a harmonic of the fundamental frequency w_o

$$w_o = 2\pi/T = .07667 \tag{36}$$

Therefore each forcing function was of the form

$$f(t) = \Sigma A_i \sin(w_i t + \theta_i) \tag{37}$$

where

$w_i = k_i w_o$

k_i is an integer from a set of relatively prime numbers

A_i is the amplitude for each component

θ_i is the initial phase for each component

Figure 7 shows the frequency response of three forcing functions used for this experiment. Frequencies in Figure 7 are in radians per second.

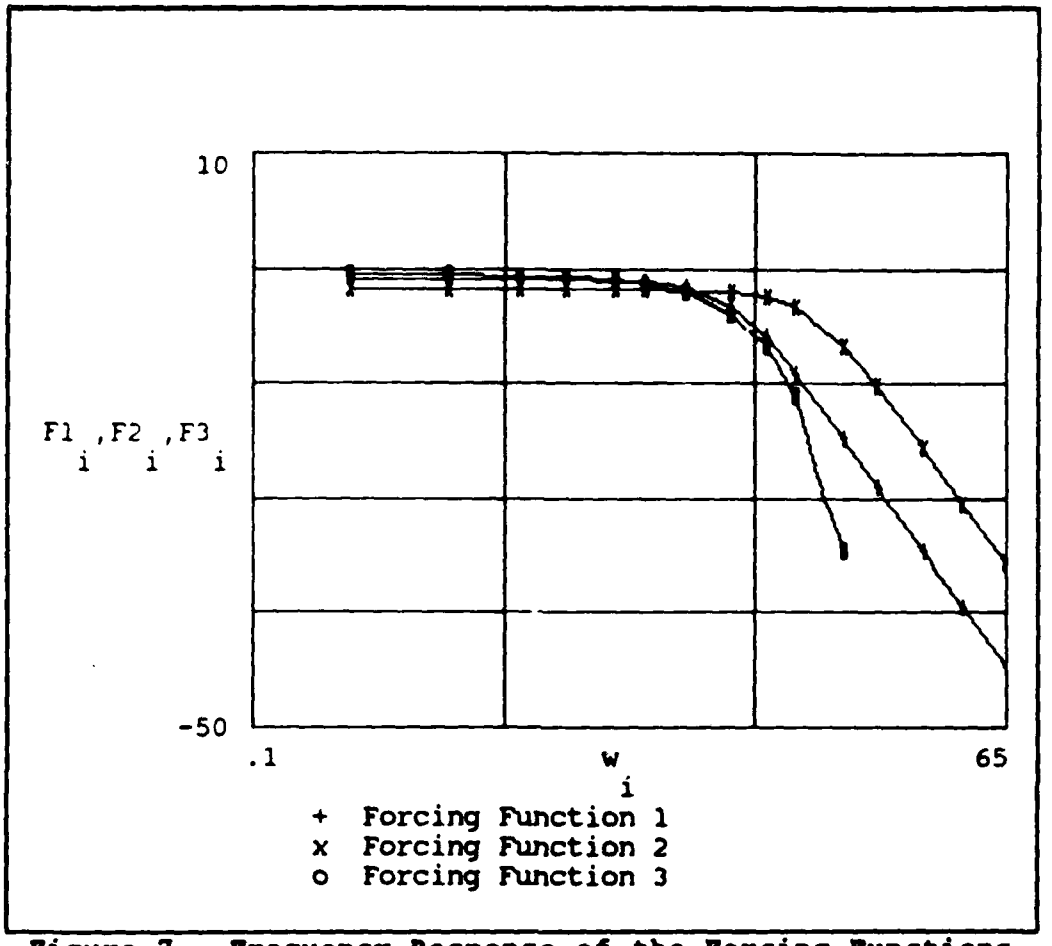

Figure 7 - Frequency Response of the Forcing Functions

The initial phase shifts associated with each component were randomly selected from a uniform distribution between 0 and 2π to insure the subjects could not predict the tracking tasks. The randomness of the phases associated with each frequency also prevented large positive or negative swings. As previously stated, the individual frequencies of the forcing functions were made up of relatively prime numbers

insuring that there could never be any periodicity which the subjects could recognize and learn to anticipate.

The amplitudes of each of the forcing functions were scaled so that all three forcing functions had equal power and produced the same maximum displacement on the display. The total input power for each forcing function was approximately 3.7 watts. Table 1 shows the approximate frequencies in radians per second, the number of harmonics, and amplitudes for each forcing function.

Table 4.1 - Forcing Function Design

Sinusoid Number	Harmonic	Frequency (rad/sec)	Amplitude (volts) FF1	FF2	FF3
1	3	0.230	0.979	0.867	1.035
2	7	0.537	0.979	0.867	1.032
3	13	0.997	0.979	0.867	1.022
4	19	1.457	0.978	0.867	1.008
5	29	2.224	0.971	0.867	0.973
6	37	2.838	0.959	0.866	0.935
7	53	4.065	0.903	0.863	0.840
8	79	6.059	0.717	0.845	0.650
9	107	8.207	0.495	0.798	0.441
10	139	10.661	0.321	0.704	0.245
11	211	16.184	0.146	0.448	0.038
12	283	21.706	0.082	0.276	0.003
13	419	32.137	0.037	0.131	0.001
14	587	45.022	0.019	0.067	0.001
15	839	64.351	0.009	0.033	0.000

4.4 Training and Experimental Procedures

4.4.1 Subjects. Six subjects participated in this study. All, by virtue of their profession, were assumed to possess good eyesight and a fairly reasonable ability for manual control. Three of the subjects had participated in similar experiments and had prior experience with the stick control characteristics. The remaining three subjects were novices with regard to the stick control. None of the subjects had prior experiences with the forcing functions used in this experiment.

4.4.2 Instructions. The subjects were instructed to minimize the distance of the maneuvering aircraft from the center of the gun sight displayed on the screen. This, in turn, minimized mean-squared errors. After each run their score was posted on the CRT display.

4.4.3 Run Length. All training and testing runs lasted 81.96 seconds with a 2 minute rest period between each run. Each session consisted of 9 runs (3 for each forcing function) and lasted approximately 40 minutes each day.

4.4.4 Training. To minimize variability due to practice effects, each subject was trained to a stable level of performance. This meant that each subject participated in at least four sessions. Two subjects required one additional session to insure that their scores had leveled

off, indicating they were not still in the learning mode. After each session the scores were analyzed to determine if the subjects had reached the trained level. If the subjects were not showing substantial changes in error scores over the last three days, they were considered trained. The data was recorded during every session. However, the subjects were unaware of which day's data was to be used for analysis. This prevented additional strain which might have affected their performance. Figure 8 shows a typical proficiency curve.

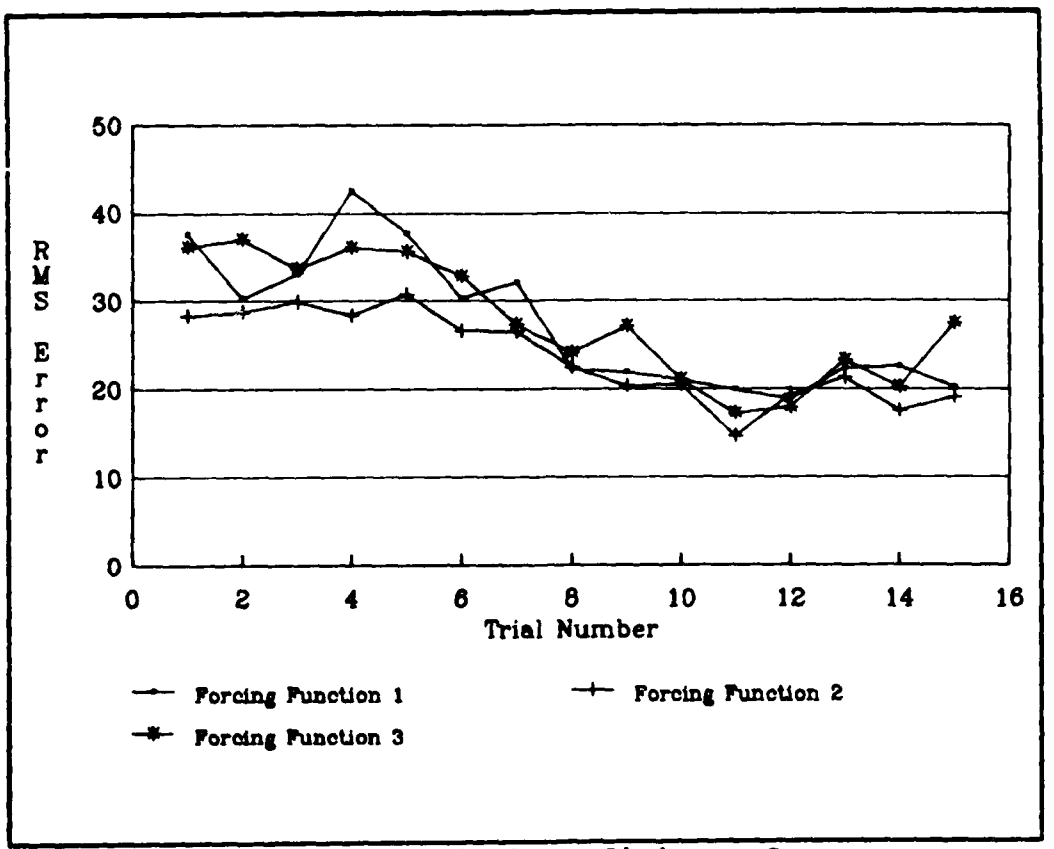

Figure 8 - Typical Proficiency Curve

Chapter V. Experimental Results

5.1 Introduction

This chapter contains the analysis performed on the data obtained from the experiment outlined in Chapter IV. Data for one subject (using the same forcing function) is analyzed for both the passive and active setups to validate the calculation methods used in this study. Next, having justified these methods, the various performance measures (noise remnant, input entropy, transinformation, and equivocation) for the remaining subjects are summarized.

Throughout the experiment a program based on the Cooley-Tukey Fast Fourier Transform (FFT) algorithm was used to produce the power spectral densities from the data sampled during each experimental run. These power spectral densities were then used to calculate the various performance parameters.

5.2 Method of Analysis

To insure that the FFT algorithm used was a good approximation to the continuous Fourier transform, three parameters, controllable by the experimenter, had to be considered. These were the sampling rate (which had to satisfy the Nyquist criteria of at least twice the highest frequency present in the waveform), the length of time record (which determined the lowest recoverable frequency),

and the total number of sample points (which determine the frequency resolution). The maximum frequency containing any appreciable power was 10.242 Hz (see Table 1). The length of the time record was set to 81.96 seconds, and the number of samples was set at 2048. These values set the minimum sampling frequency at 25 Hz a maximum frequency of 12.5 Hz and a frequency resolution of .012201 Hz.

5.3 Key Parameters

One of the key quantities needed to calculate the necessary parameters was the noise remnant introduced by the subject. As reported in Chapter IV, a sum of shaped sinusoids were used as forcing functions. This class of forcing functions was used to simplify the calculation of signal and noise power. As reported by Levison, the noise cannot be easily separated from the signal power at the input frequencies. However, by concentrating the input power at selected frequencies through the use of sinusoidal forcing functions, the separation of noise power from the linear response to the forcing function is facilitated. Power measured at any frequency other than the original input frequencies must be, with the exception of system noise and "noisy" generation of forcing function, remnant injected by the operator. (6:104-105;7:7) In this experiment the forcing functions were generated with a

minimum of 30dB signal to noise ratio at each of the fifteen frequencies.

The other measurements necessary to compute the required parameters were the power spectrum of the stick roll, $\Phi_{uu}(w)$, and the power spectrum of the display error, $\Phi_{ee}(w)$. From these two measurements the subject's transfer function can be determined. The correlated and uncorrelated portions of stick roll power spectral density (PSD) and display error PSD were determined as shown in Chapter III.

Table 2 tabulates data for one run for Subject #2 with the stick in the passive mode and forcing function #1 as the input.

Table 2 - Typical Data Run (Subject #2, Passive Mode)

w	$\Phi_{rr}(w)$	$\Phi_{eer}(w)$	$\Phi_{een}(w)$	$\Phi_{uur}(w)$	$\Phi_{uun}(w)$
0.230	-3.2	-9.7	-29.6	-8.5	-31.5
0.537	-3.2	-8.4	-32.3	-9.7	-32.1
0.997	-3.3	-7.2	-32.9	-8.7	-34.9
1.457	-3.3	-7.3	-36.1	-10.3	-38.6
2.224	-3.2	-5.0	-27.6	-9.9	-27.1
2.838	-3.4	-5.3	-33.9	-9.6	-33.7
4.065	-4.0	-3.8	-29.0	-10.9	-28.6
6.059	-5.9	-4.0	-30.1	-11.7	-30.0
8.207	-9.2	-5.0	-29.5	-13.2	-29.7
10.661	-13.1	-10.0	-31.8	-19.0	-32.5
16.184	-20.0	-24.0	-39.2	-30.0	-40.2
21.706	-25.0	-25.4	-41.2	-99.0	-42.6
32.137	-31.6	-33.1	-48.2	-99.0	-53.9
45.022	-38.1	-44.6	-50.6	-99.0	-59.4
64.351	-43.8	-65.7	-51.3	-65.7	-61.1

Note 1: w in radians/second.
Note 2: All other values are in decibels.

Table 3 shows similar data obtained with the stick operating in the active mode.

Table 3 - Typical Data Run (Subject #2, Active Mode)

w	$\Phi_{rr}(w)$	$\Phi_{eer}(w)$	$\Phi_{een}(w)$	$\Phi_{uur}(w)$	$\Phi_{uun}(w)$
0.230	-3.3	-11.0	-32.0	-7.5	-34.8
0.537	-3.1	-9.0	-30.8	-8.8	-32.8
0.997	-3.2	-7.4	-29.0	-8.8	-28.2
1.457	-3.2	-7.9	-31.6	-8.8	-31.3
2.224	-3.2	-6.0	-29.8	-8.4	-30.5
2.838	-3.5	-5.8	-31.2	-9.3	-32.9
4.065	-4.1	-3.7	-30.1	-10.2	-31.4
6.059	-6.0	-4.4	-30.6	-13.6	-32.0
8.207	-9.2	-6.4	-32.3	-15.9	-33.2
10.661	-12.9	-9.8	-33.3	-19.7	-34.0
16.184	-19.8	-22.5	-39.5	-27.6	-40.5
21.706	-24.8	-27.0	-42.9	-38.8	-45.0
32.137	-31.8	-32.5	-47.9	-99.0	-54.9
45.022	-38.3	-45.5	-50.1	-66.2	-63.5
64.351	-43.6	-45.8	-50.5	-70.6	-65.9

Note 1: w in radians/second.
Note 2: All other values are in decibels.

5.4 Analysis

The noise PSD injected by the subject is calculated using Equation 16. The human operator describing function, defined as the ratio of the correlated portion of the stick roll PSD and the correlated portion of the display error PSD, can be calculated as

$$Y_H(w) = \Phi_{uur}(w)/\Phi_{eer}(w) \qquad (38)$$

Also, the display entropy, transinformation, and equivocation can be calculated by using Equations (28), (30), and (31), respectively. Tables 4 and 5 contain tabulated results for Subject #2 using the stick in the passive and active mode, respectively. It is significant to note that not all values of the stick roll PSD were used. If the ratio of correlated to uncorrelated power at each input frequency was not greater than, or equal to unity, the estimate was deemed unreliable and not used in the calculations.

Table 4 - Calculated Results (Subject #2, Passive Mode)

w	$Y_H(w)$	$\Phi_{nn}(w)$	Entropy	Transinfo	Equiv
0.230	1.2	-26.2	6.65	5.49	1.14
0.537	-1.3	-25.6	7.95	5.72	2.23
0.997	-1.5	-29.5	8.54	7.41	1.13
1.457	-3.0	-31.6	9.57	8.07	1.40
2.224	-4.8	-20.4	7.52	5.11	2.41
2.838	-4.3	-27.5	9.50	7.38	2.12
4.065	-7.0	-21.7	8.38	5.94	2.44
6.059	-7.6	-24.2	8.67	6.70	1.97
8.207	-8.1	-25.7	8.14	6.88	1.26
10.661	-8.8	-26.6	7.25	5.51	1.74
16.184	-5.7	-30.2	5.09	2.09	3.00

Note 1: w in radians/second.
Note 2: $Y_H(w)$ and $\Phi_{nn}(w)$ in decibels.
Note 3: Entropy, transinformation, and equivocation are in bit-radians/second.

Table 5 - Calculated Results (Subject #2, Active Mode)

w	$Y_H(w)$	$\Phi_{nn}(w)$	Entropy	Transinfo	Equiv
0.230	3.4	-30.6	6.99	6.55	0.44
0.537	0.2	-27.1	7.25	6.02	1.23
0.997	-1.4	-22.6	7.19	5.07	2.08
1.457	-0.9	-25.7	7.88	5.92	2.96
2.224	-2.4	-25.3	7.91	6.42	1.49
2.838	-3.5	-27.1	8.44	7.08	1.36
4.065	-6.4	-25.3	8.77	7.15	1.62
6.059	-9.1	-24.4	8.71	6.63	2.08
8.207	-9.5	-26.5	8.61	6.70	1.89
10.661	-9.8	-27.2	7.81	5.80	2.01
16.184	-5.0	-32.7	5.68	3.43	2.25
21.706	-11.0	-31.0	5.32	1.37	3.95

Note 1: w in radians/second.
Note 2: $Y_H(w)$ and $\Phi_{nn}(w)$ in decibels.
Note 3: Entropy, transinformation, and equivocation are in bit-radians/second.

5.5 Average Results

To obtain a reliable measure of noise power introduced by each subject and a good estimate of the human capacity while performing the tasks in this experiment, we averaged across trials for each forcing function and for each subject. As outlined in Chapter IV, each subject was tested twice. First using the stick in the passive mode and, subsequently, using the stick in the active mode. Therefore two data sessions were taken each consisting of 9 runs (3 for each forcing function). In the next few pages, averages for each of the three forcing functions are shown. Because of the differences in the forcing functions, an

average across the three inputs was not performed since we want to show human noise and capacity as a function of task difficulty. Similarly, as Levison reported, averaging across subjects using the same forcing function would not give an accurate measure of the noise injected. Each subject has a different transfer function and these variations would result in an increase in remnant. (7:5)

Therefore, averaging only across the same forcing function and the same experimental setup for each subject allows us to interpret noise and information theory parameters for a typical subject as a function of task difficulty and stick mode.

The following tables show the average results for Subject #2 for all three forcing functions in both the average and passive modes of operation. Table 6 shows the averaged results for the human operator describing function. Table 7 contains the averaged results for the human operator remnant. Table 8 provides the averaged results for the display error entropy. Table 9 shows the averaged results for transinformation. Table 10 contains the averaged results for the response equivocation.

Table 6 - Human Operator Describing Function (Subject #2)

	FF #1		FF #2		FF #3	
Freq	Passive	Active	Passive	Active	Passive	Active
0.230	1.44	1.85	-0.40	-3.69	4.34	1.98
0.537	0.25	-0.05	-3.78	-4.06	1.53	0.91
0.997	-1.37	-2.76	-3.37	-4.17	-0.73	-1.16
1.457	-2.37	-1.69	-6.42	-5.57	-0.80	-1.88
2.224	-5.00	-4.52	-7.31	-7.18	-3.78	-4.08
2.838	-4.45	-4.85	-7.40	-8.26	-5.21	-4.92
4.065	-5.63	-7.38	-8.36	-9.30	-5.65	-5.97
6.057	-7.35	-9.78	-8.70	-11.86	-8.19	-8.57
8.207	-7.87	-10.94	-10.97	-13.77	-9.28	-9.57
10.661	-8.21	-10.28	-12.30	-13.84	-8.99	-8.57
16.184	-3.23	-6.04	-14.39	-12.72	---	---
21.706	---	-9.53	---	-18.31	---	---
32.137	---	---	---	---	---	---
45.022	---	---	---	---	---	---
64.351	---	---	---	---	---	---

Note 1: Frequency values are in radians/second.
Note 2: All other values are in units of decibels.

Table 7 - Human Operator Remnant (Subject #2)

	FF #1		FF #2		FF #3	
Freq	Passive	Active	Passive	Active	Passive	Active
0.230	-25.33	-30.00	-18.59	-19.03	-26.58	-27.29
0.537	-24.73	-24.13	-17.58	-23.84	-24.86	-27.37
0.997	-25.74	-22.08	-25.18	-31.55	-28.54	-26.64
1.457	-25.23	-27.06	-13.20	-25.96	-24.73	-25.63
2.224	-20.35	-24.40	-20.38	-23.19	-23.13	-24.36
2.838	-24.60	-23.70	-19.76	-23.10	-25.18	-22.92
4.065	-22.79	-24.24	-21.43	-22.43	-23.07	-23.04
6.057	-22.84	-24.95	-21.49	-22.84	-23.01	-24.82
8.207	-25.18	-26.14	-17.35	-22.62	-24.16	-26.14
10.661	-26.45	-28.14	-18.59	-24.28	-26.92	-31.15
16.184	-30.97	-32.22	-21.33	-26.20	---	---
21.706	---	-32.47	---	-23.77	---	---
32.137	---	---	---	---	---	---
45.022	---	---	---	---	---	---
64.351	---	---	---	---	---	---

Note 1: Frequency values are in radians/second.
Note 2: All other values are in units of decibels.

Table 8 - Display Error Entropy (Subject #2)

	FF #1		FF #2		FF #3	
Freq	Passive	Active	Passive	Active	Passive	Active
0.230	6.58	6.67	5.09	6.20	6.63	7.99
0.537	7.58	7.77	6.31	7.77	7.56	7.56
0.997	8.30	7.89	7.65	9.50	8.21	8.81
1.457	7.68	8.76	6.84	8.24	7.86	9.59
2.224	7.19	8.09	8.81	8.61	7.89	8.01
2.838	8.48	8.01	7.36	8.79	8.66	7.74
4.065	8.49	8.82	8.22	8.49	7.96	7.87
6.057	8.10	9.08	7.92	9.28	8.20	8.45
8.207	7.86	8.83	7.73	9.65	7.65	8.50
10.661	7.11	8.07	8.07	9.57	6.96	7.85
16.184	4.94	5.88	7.69	8.53	---	---
21.706	---	5.21	---	8.18	---	---
32.137	---	---	---	---	---	---
45.022	---	---	---	---	---	---
64.351	---	---	---	---	---	---

Note 1: Frequency values are in radians.
Note 2: All other values are in units of bit-radians/sec.

Table 9 - Transinformation (Subject #2)

	FF #1		FF #2		FF #3	
Freq	Passive	Active	Passive	Active	Passive	Active
0.230	5.15	6.68	3.20	3.70	5.78	6.72
0.537	5.24	5.34	3.46	5.70	5.40	6.97
0.997	6.65	5.30	5.69	8.33	7.71	6.48
1.457	6.28	7.14	4.16	7.68	6.21	6.29
2.224	5.02	6.28	5.43	6.01	6.07	6.37
2.838	6.64	6.32	5.14	6.10	6.74	5.95
4.065	6.45	6.79	5.85	6.10	6.40	6.11
6.057	6.50	6.90	6.25	6.70	6.10	6.50
8.207	6.78	6.44	4.87	6.51	5.75	6.49
10.661	5.51	6.02	4.50	6.58	5.13	6.55
16.184	2.24	3.28	3.05	4.74	---	---
21.706	---	1.77	---	3.13	---	---
32.137	---	---	---	---	---	---
45.022	---	---	---	---	---	---
64.351	---	---	---	---	---	---

Note 1: Frequency values are in radians.
Note 2: All other values are in bit-radians/sec.

Table 10 - Equivocation (Subject #2)

	FF #1		FF #2		FF #3	
Freq	Passive	Active	Passive	Active	Passive	Active
0.230	1.43	0.00	1.89	2.50	0.85	1.27
0.537	2.35	2.43	2.85	2.07	2.16	0.59
0.997	1.65	2.59	1.96	1.17	0.50	2.32
1.457	1.41	1.63	2.68	0.56	1.65	3.31
2.224	2.16	1.81	3.38	2.60	1.82	1.64
2.838	1.83	1.70	2.23	2.70	1.92	1.78
4.065	2.03	2.03	2.37	2.38	1.56	1.76
6.057	1.60	2.19	1.68	2.58	2.10	1.95
8.207	1.08	2.39	2.86	3.13	1.88	2.01
10.661	1.60	2.04	3.57	2.99	1.83	1.30
16.184	2.70	2.60	4.64	3.79	---	---
21.706	---	3.44	---	5.04	---	---
32.137	---	---	---	---	---	---
45.022	---	---	---	---	---	---
64.351	---	---	---	---	---	---

Note 1: Frequency values are in radians.
Note 2: All other values are in bit-radians/sec.

Graphical representations of Table 6 through 10 can be found in Appendix B. Similar graphical representations for the remaining five subjects can be found in Appendices A, C, D, E, and F.

As a final measure of comparison, the individual entropy and equivocation for forcing functions 1, 2, and 3 (in both the passive and active modes) are tabulated in Tables 11, 12, and 13, respectively.

Table 11 - Summary Chart for Forcing Function #1

	Entropy		Equivocation	
Subject	Passive	Active	Passive	Active
1	13.91	12.12	6.51	4.52
2	13.10	14.81	3.16	3.95
3	12.65	14.87	3.30	4.20
4	15.19	14.39	6.26	5.98
5	14.33	14.43	4.47	3.58
6	16.58	17.48	6.33	8.89

Note: All values are in bits/sec.

Table 12 - Summary Chart for Forcing Function #2

	Entropy		Equivocation	
Subject	Passive	Active	Passive	Active
1	12.66	13.91	6.88	6.27
2	13.00	16.36	4.79	5.02
3	14.03	15.64	4.37	4.32
4	12.28	15.17	4.89	7.60
5	14.27	15.27	5.07	4.37
6	12.79	17.63	5.71	9.40

Note: All value in bits/sec.

Table 13 - Summary Chart for Forcing Function #3

	Entropy		Equivocation	
Subject	Passive	Active	Passive	Active
1	11.26	10.88	4.42	3.23
2	12.34	13.11	2.59	2.85
3	11.22	12.68	2.14	2.99
4	15.11	14.18	7.10	5.75
5	13.57	12.41	4.10	2.61
6	12.66	16.65	3.94	7.36

Note: All values in bits/second.

Chapter VI. Conclusions/Recommendations

6.1 Conclusions

As stated earlier in this report, no attempt is made to draw comparisons of performance between subjects. This is primarily a result of the fact that each individual subject develops his or her own internal strategy for performing the tracking task function. For example, in discussions with subjects after the testing was completed, one subject stated that he was trying to track as much movement on the display as possible. Another subject, however, stated that he recognized that he was not able to track all movements on the display, so he resorted to a strategy of ignoring the faster (higher frequency) display movements and concentrated on tracking the trends (lower frequency components) of the display. The two strategies are obviously different, but also extremely difficult to compare and contrast.

The overall objective of this thesis was to analyze the changes in response equivocation (lost information) as the subjects track a target under passive and active stick operation. As can be seen by viewing Tables 11, 12, and 13, as well as the graphs in Appendices A-F, no conclusions can immediately be drawn from observing only the equivocation results. In some cases equivocation increases and in other cases it decreases, with no apparent pattern or trend.

However, in performing the analysis for equivocation, data was obtained that permits other conclusions.

From the data contained in Appendices A-F, it is possible to confidently state that changes in performance definitely occur when operating the stick in the active mode. This change in performance, however, may manifest itself in a different manner for each subject. For example, Subject #5's data under forcing function #2 (see Appendix E, Figures E.5 - E.8) shows a slight increase in the gain of the human operator describing function and a significant decrease in the human operator induced remnant (noise). There is also a corresponding increase in transinformation (more information being transmitted), a decrease in equivocation (less information being lost), and virtually no change in the display error entropy. However, Subject #6's data under forcing function #2 (see Appendix F, Figures F.5 - F.8) shows a significant decrease in gain for the human operator describing function, but only a slight decrease in human operator remnant. There is a corresponding increase in transinformation (only at lower frequencies), but significant increases in display error entropy (amount of information available to the subject) and equivocation. Although the changes in performance are not the same, there is no doubt that a change in performance has occurred.

These changes in performance cannot be attributed specifically to a corresponding change in any specific parameter ($Y_H(w)$, $\Phi_{nn}(w)$, display error entropy, transinformation, or equivocation). By again observing Equations (8), (12), and (16), it is easy to see that the relationships between the input and output power spectral densities, $Y_H(w)$, and $\Phi_{nn}(w)$ are all intertwined. Also, these power spectral densities were used to determine the entropy, transinformation, and equivocation results. There does appear to be a strong relationship between $\Phi_{nn}(w)$, the transinformation rate, and the equivocation. In those cases where $\Phi_{nn}(w)$ changed significantly, as with the situation discussed above with Subject #5, there appears to be a corresponding significant change in transinformation and display error entropy.

In conclusion, characterizing a subject's performance merely by determining the response equivocation does not seem appropriate. However, by viewing the subject's performance in terms of the five parameters used throughout this study, it may indeed be possible to quantify the change in performance. Characterizing that change in performance, however, is a much more difficult task.

6.2 Recommendations

This section contains recommendations for continuing study in the area of the smart stick controller.

One of the initial assumptions made early in this project was the assumption that the control element was unity gain (i.e. an aircraft with an instantaneous response). Although this may not be a realistic or practical scenario, it was indeed convenient for laying down the initial theoretical analysis. This effort should be repeated using a control element which more closely resembles the response of an actual aircraft to stick movement.

The results obtained in this study indicated that maximum transinformation rates for a particular subject can vary by as much as 50 per cent depending on whether forcing function #1, #2, or #3 is used. Further work should be conducted with various higher order forcing functions (shapes, amplitudes, bandwidths, etc) to try to determine if there exists one or more forcing functions that will effectively measure the upper limit for transinformation and the lower limit for equivocation.

An underlying characteristic of the compensatory tracking task evaluated in this study was that it was a single axis tracking task (the target moved horizontally only). This analysis should be repeated for a two-

dimensional tracking task. This would undoubtedly complicate the theoretical derivations and calculations required, particularly in the area of determining "cross-axis" parameters such as noise. However, this would, perhaps, move the research into a more application-oriented environment.

Finally, as stated in the conclusions, the impact of $Y_H(w)$ and $\Phi_{nn}(w)$ on performance is thoroughly intertwined and as yet uncertain. We suspect that a change in $\Phi_{nn}(w)$ will have a much more significant effect than a corresponding change in $Y_H(w)$. A sensitivity analysis on the impact of these two quantities may resolve the issue concerning which is the more dominant parameter.

Appendix A: Graphical Results For Subject #1

This appendix contains graphical representations of the results obtained by testing Subject #1. Each graph consists of a visual comparison of the active and passive modes of operation for a specific parameter under a specific forcing function.

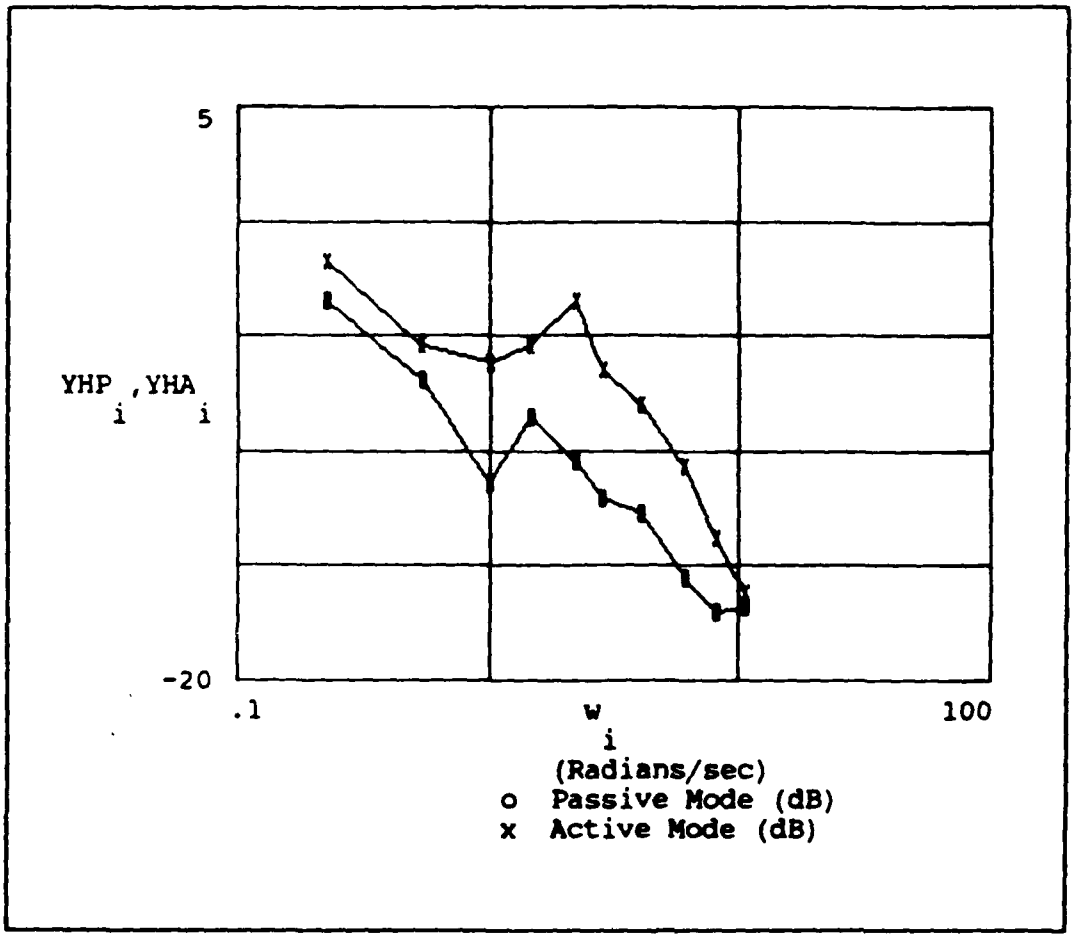

Figure A.1 - Human Operator Describing Function (FF #1)

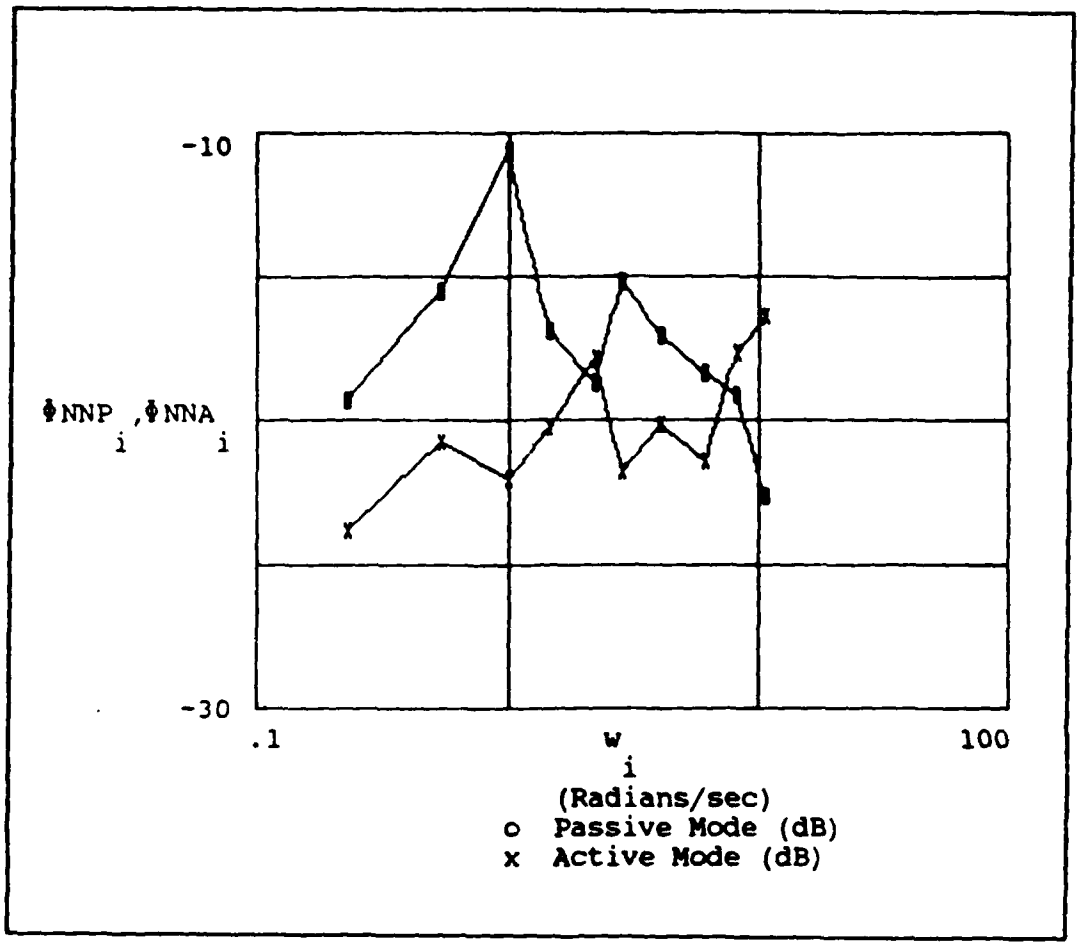

Figure A.2 - Operator Remnant/Noise (FF #1)

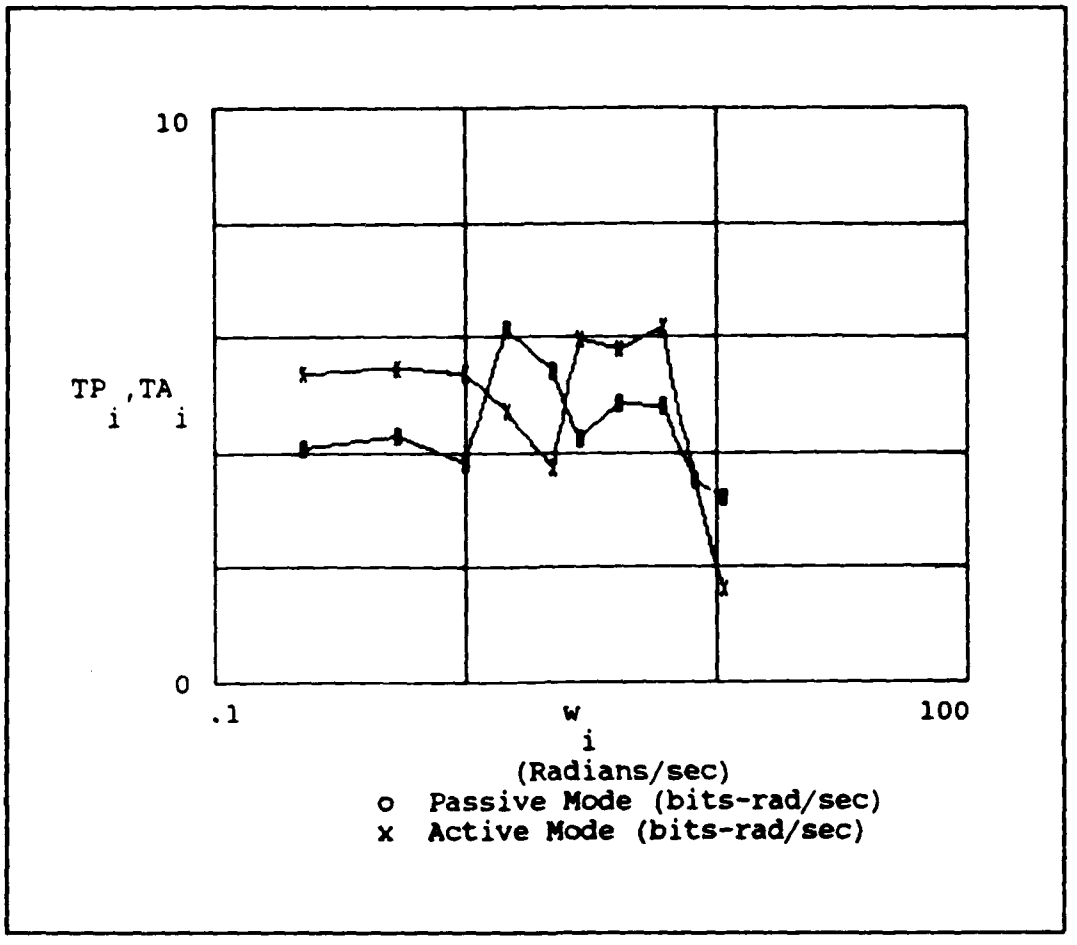

Figure A.3 - Transinformation Rate (FF #1)

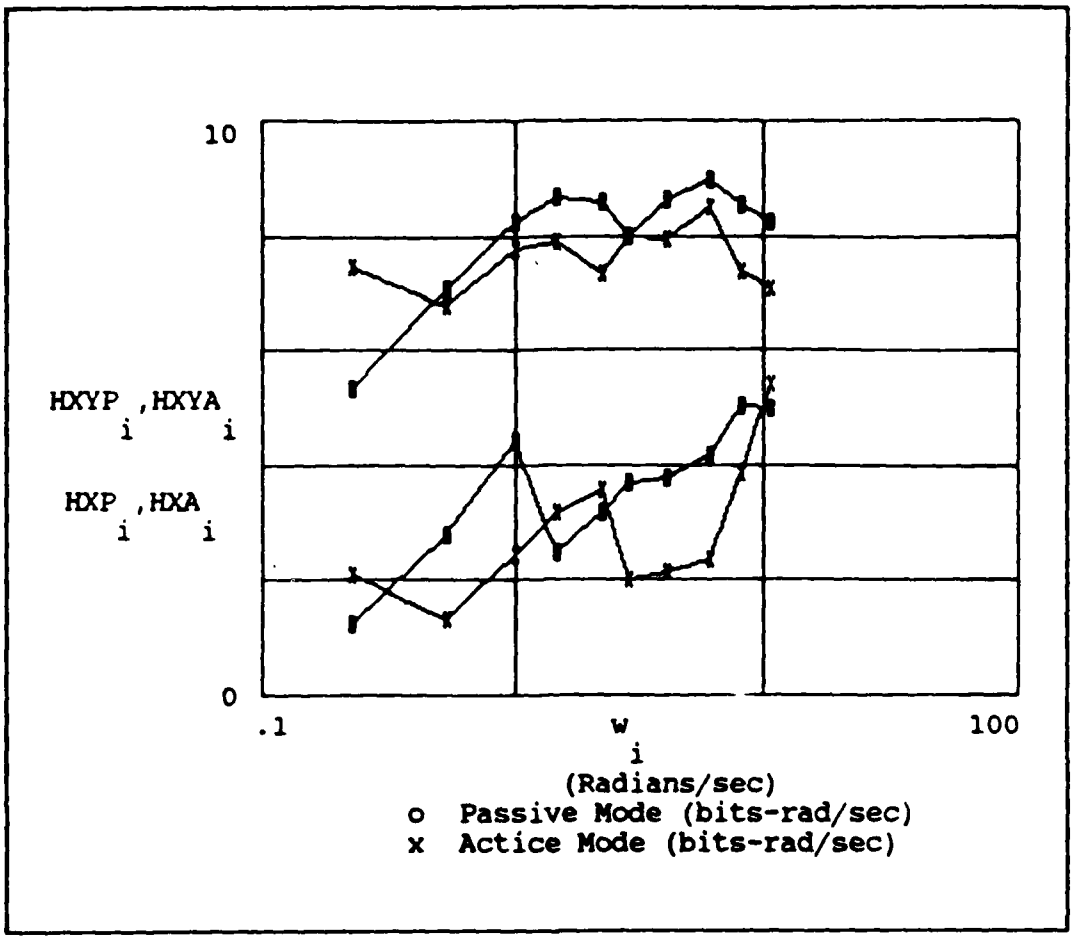

Figure A.4 - Display Error Entropy and Equivocation (FF #1)

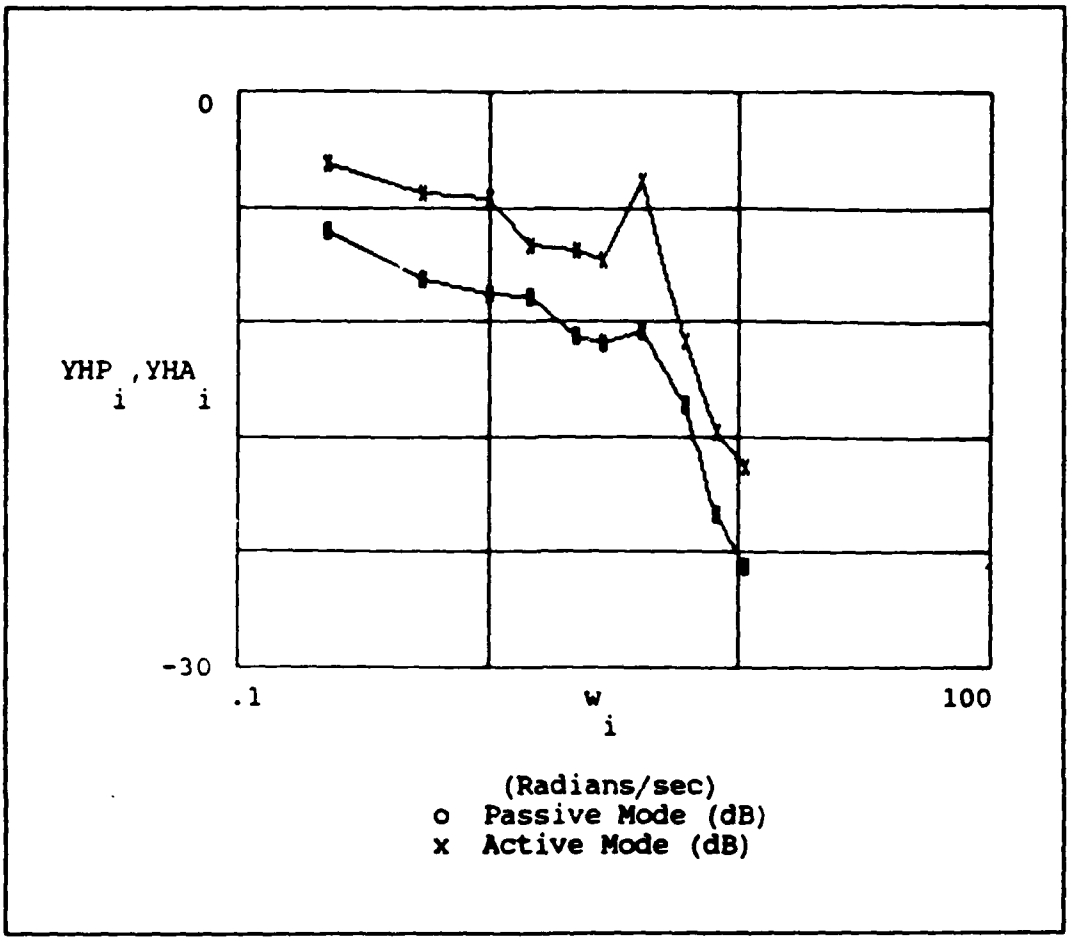

Figure A.5 - Human Operator Describing Function (FF #2)

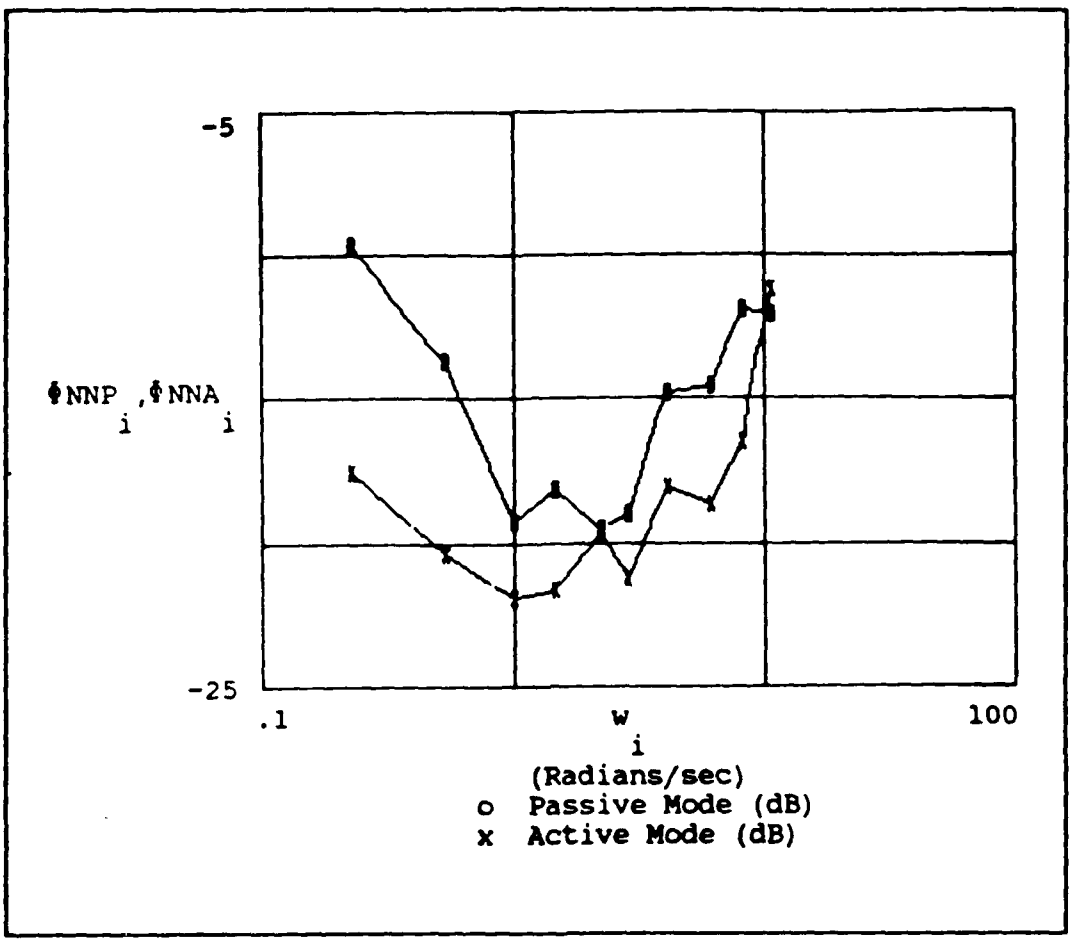

Figure A.6 - Operator Remnant/Noise (FF #2)

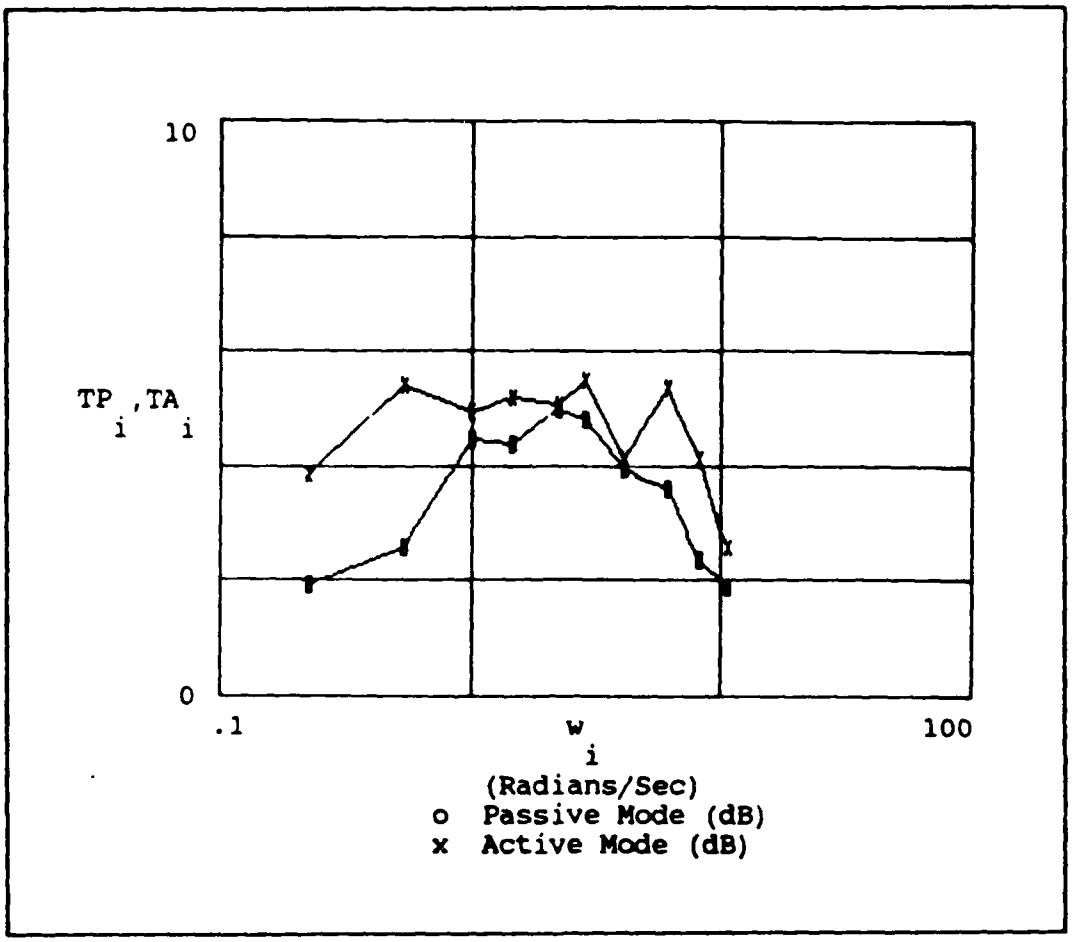

Figure A.7 - Transinformation Rate (FF #2)

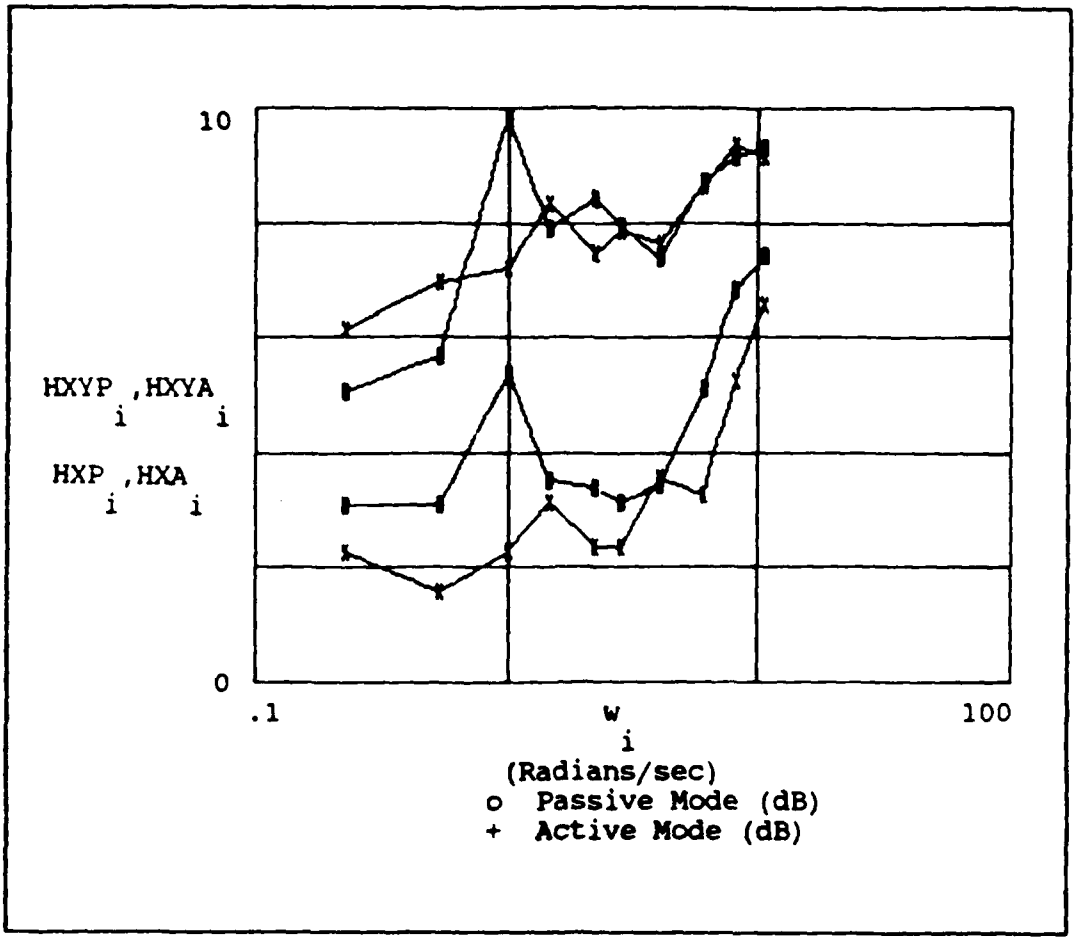

Figure A.8 - Display Error Entropy and Equivocation (FF #2)

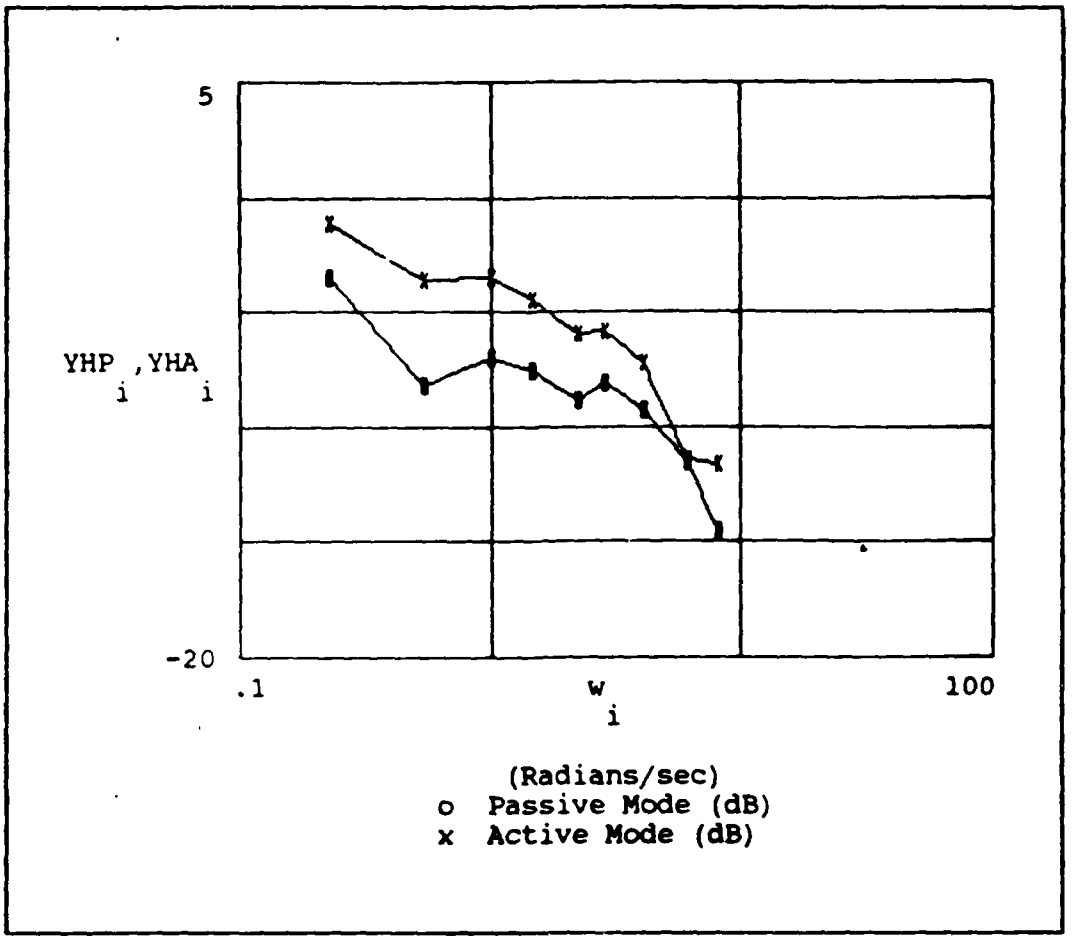

Figure A.9 - Human Operator Describing Function (FF #3)

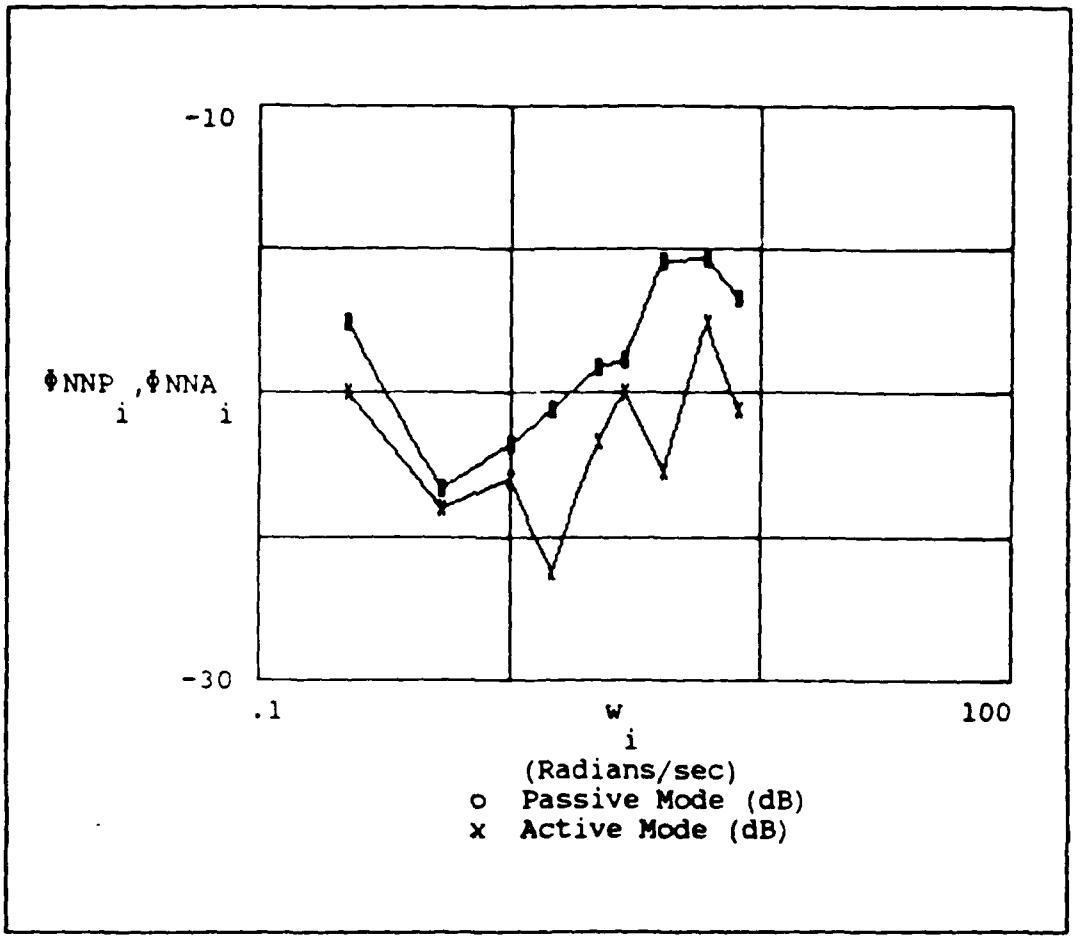

Figure A.10 - Operator Remnant/Noise (FF #3)

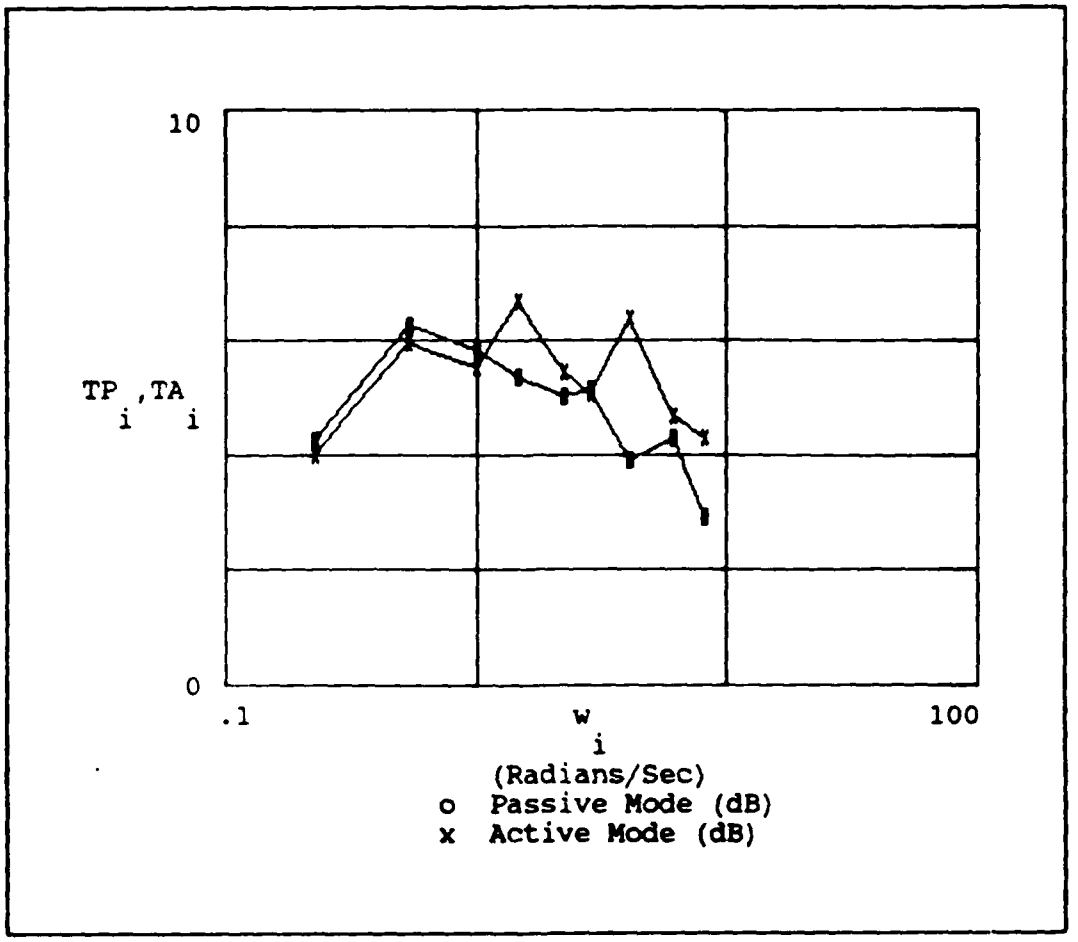

Figure A.11 - Transinformation Rate (FF #3)

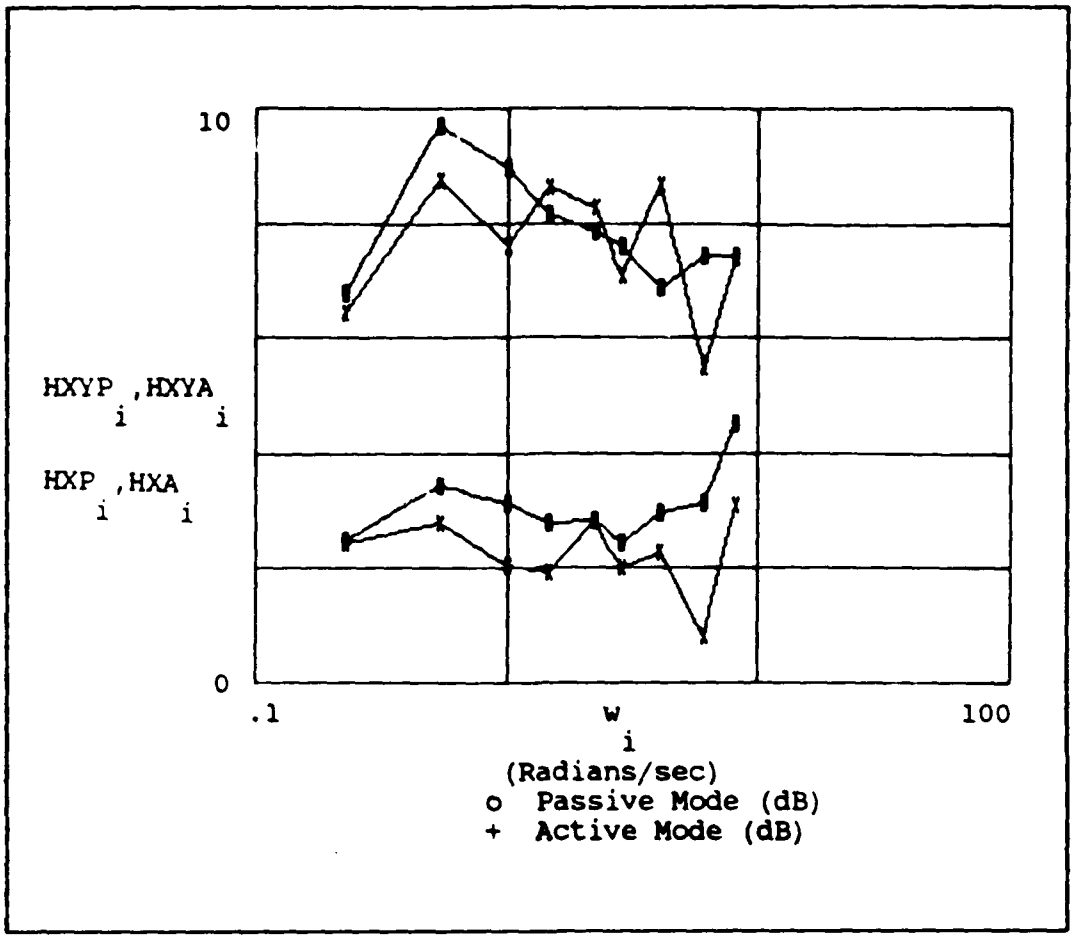

Figure A.12 - Display Error Entropy and Equivocation (FF #3)

Appendix B: Graphical Results For Subject #2

This appendix contains graphical representations of the results obtained by testing Subject #2. Each graph consists of a visual comparison of the active and passive modes of operation for a specific parameter under a specific forcing function.

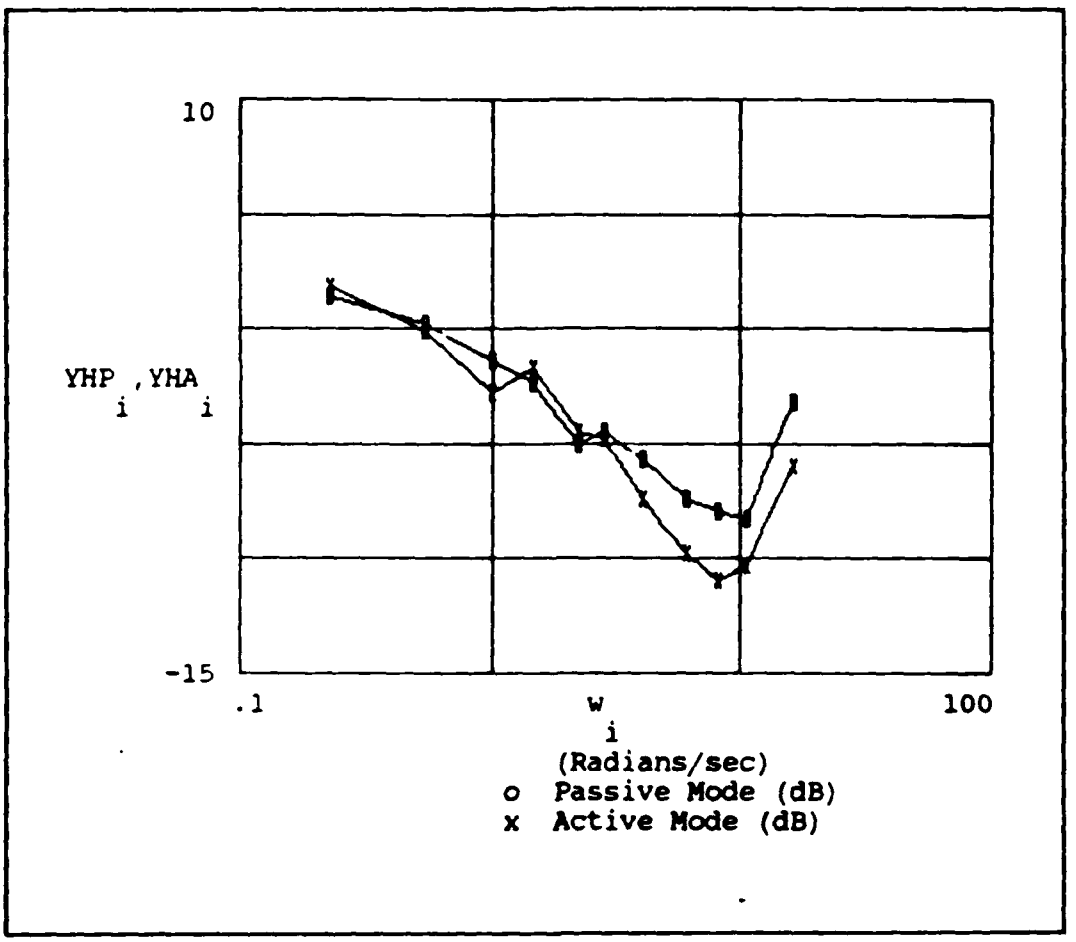

Figure B.1 - Human Operator Describing Function (FF #1)

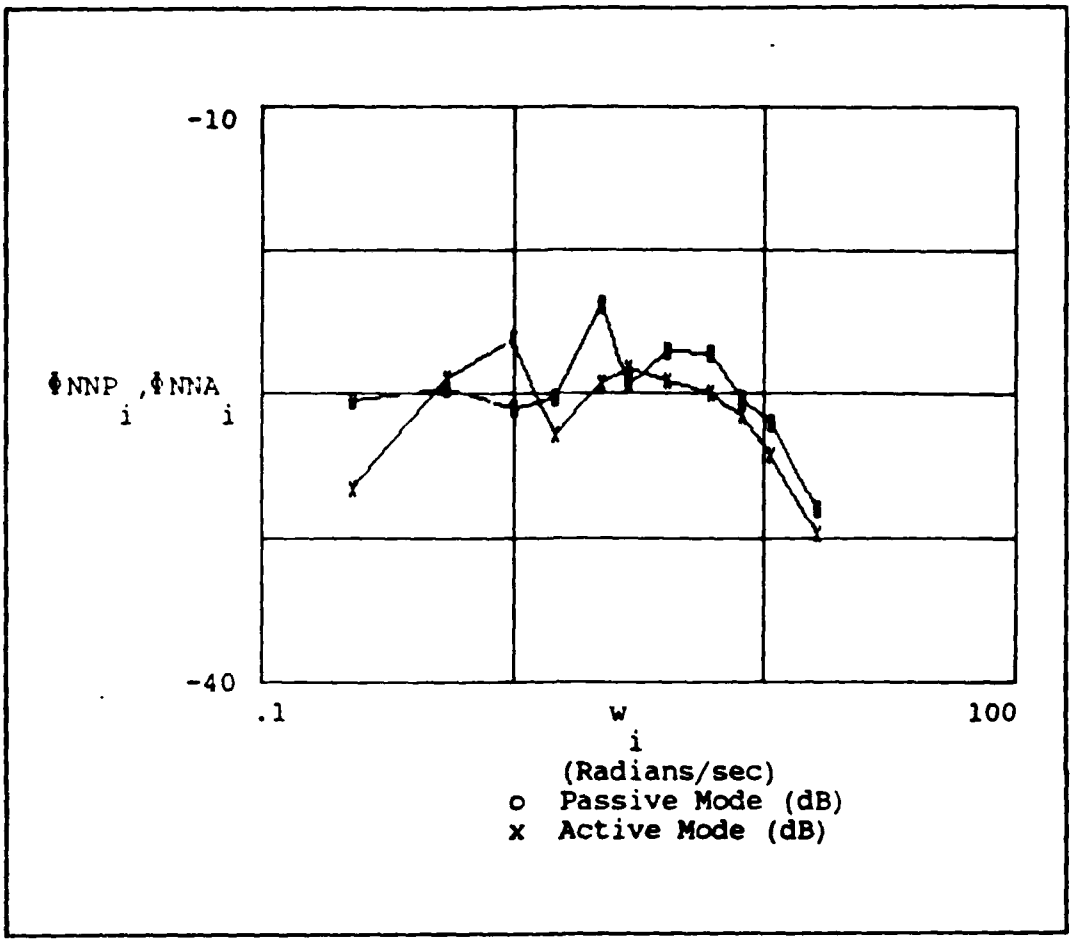

Figure B.2 - Operator Remnant/Noise (FF #1)

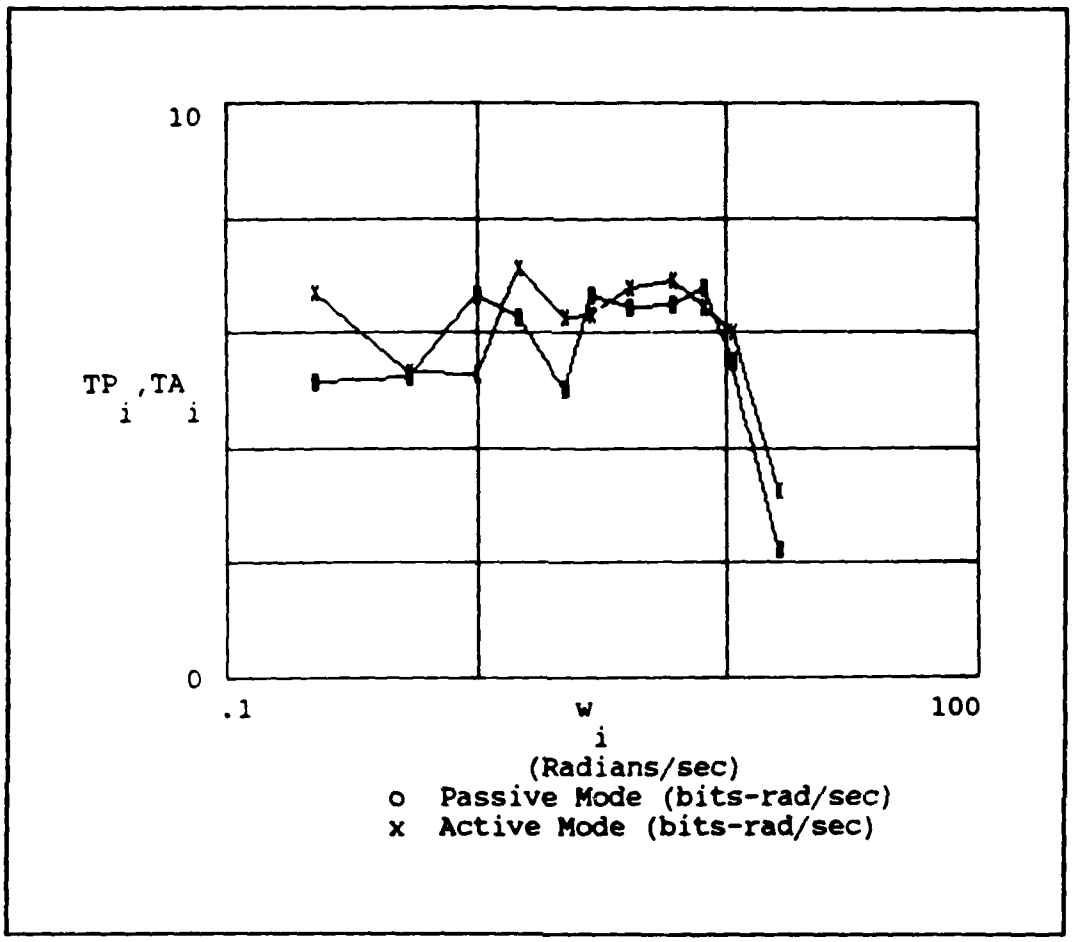

Figure B.3 ~ Transinformation Rate (FF #1)

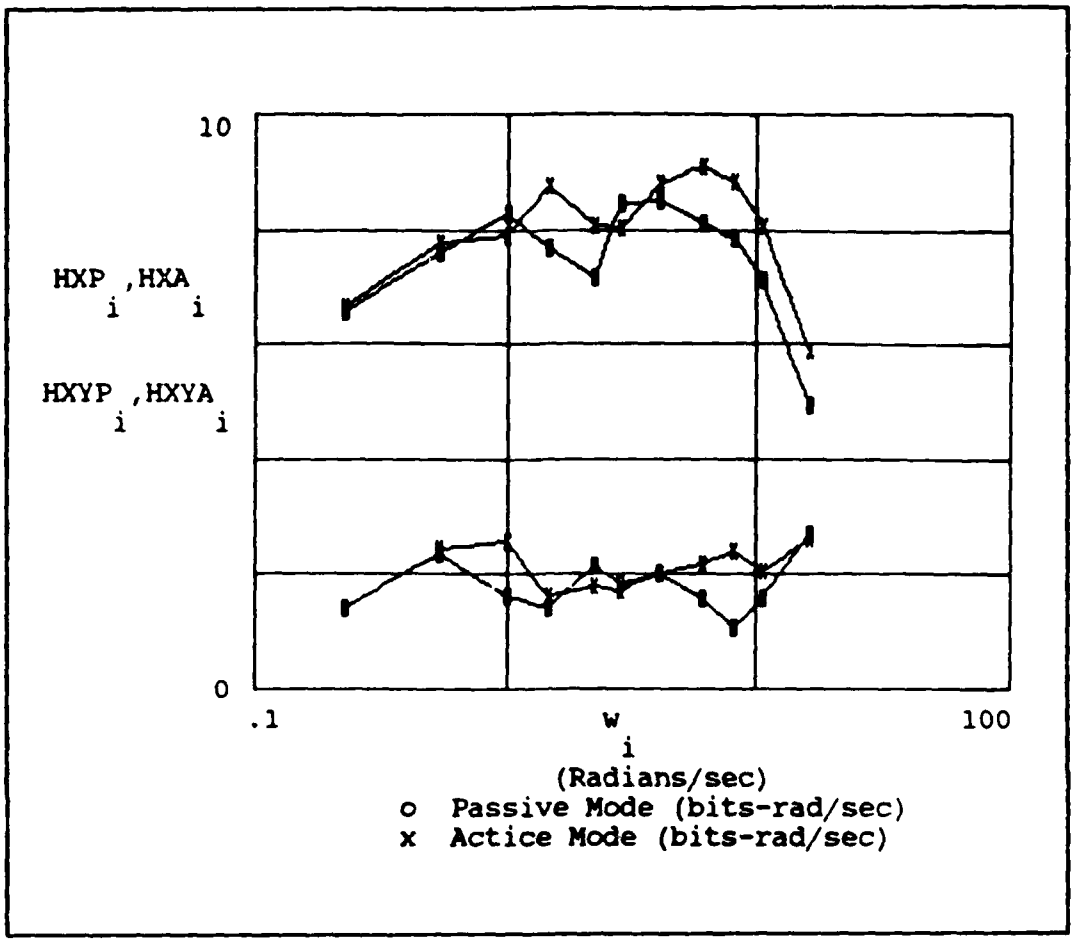

Figure B.4 - Display Error Entropy and Equivocation (FF #1)

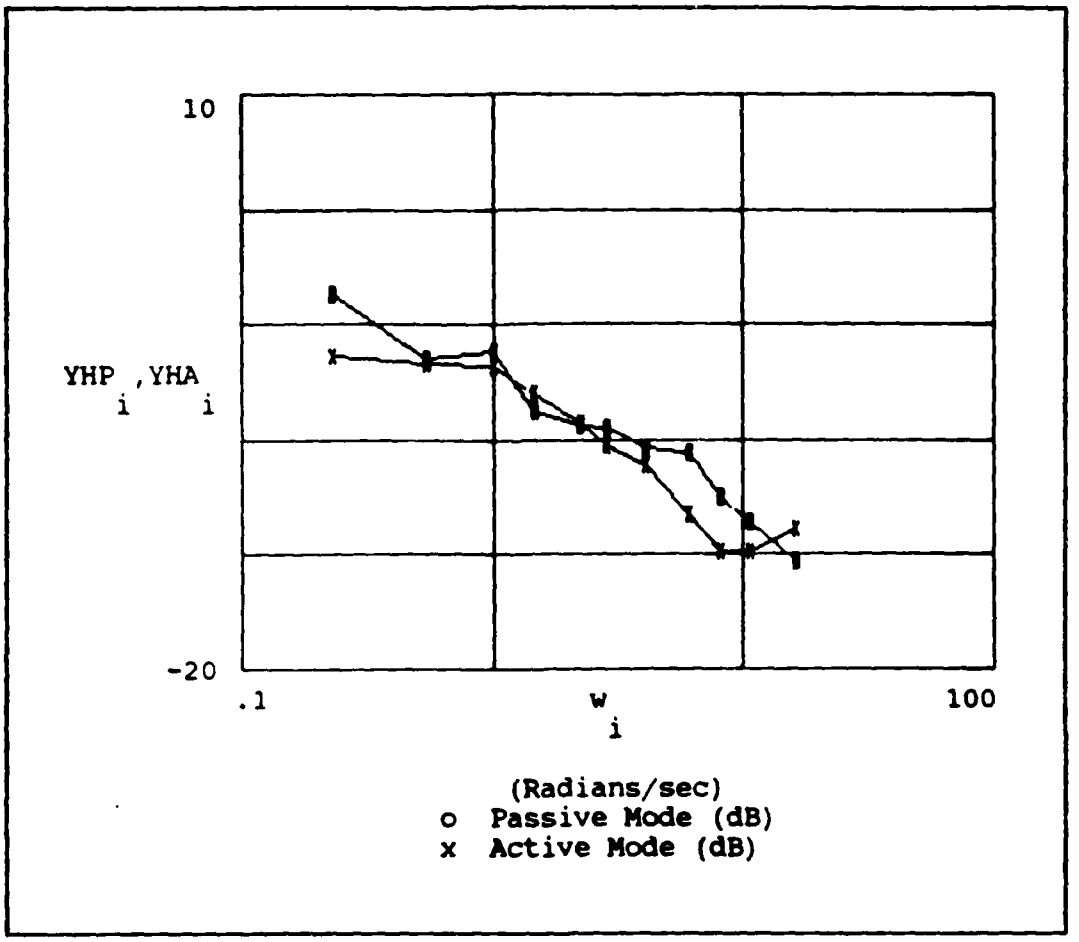

Figure B.5 - Human Operator Describing Function (FF #2)

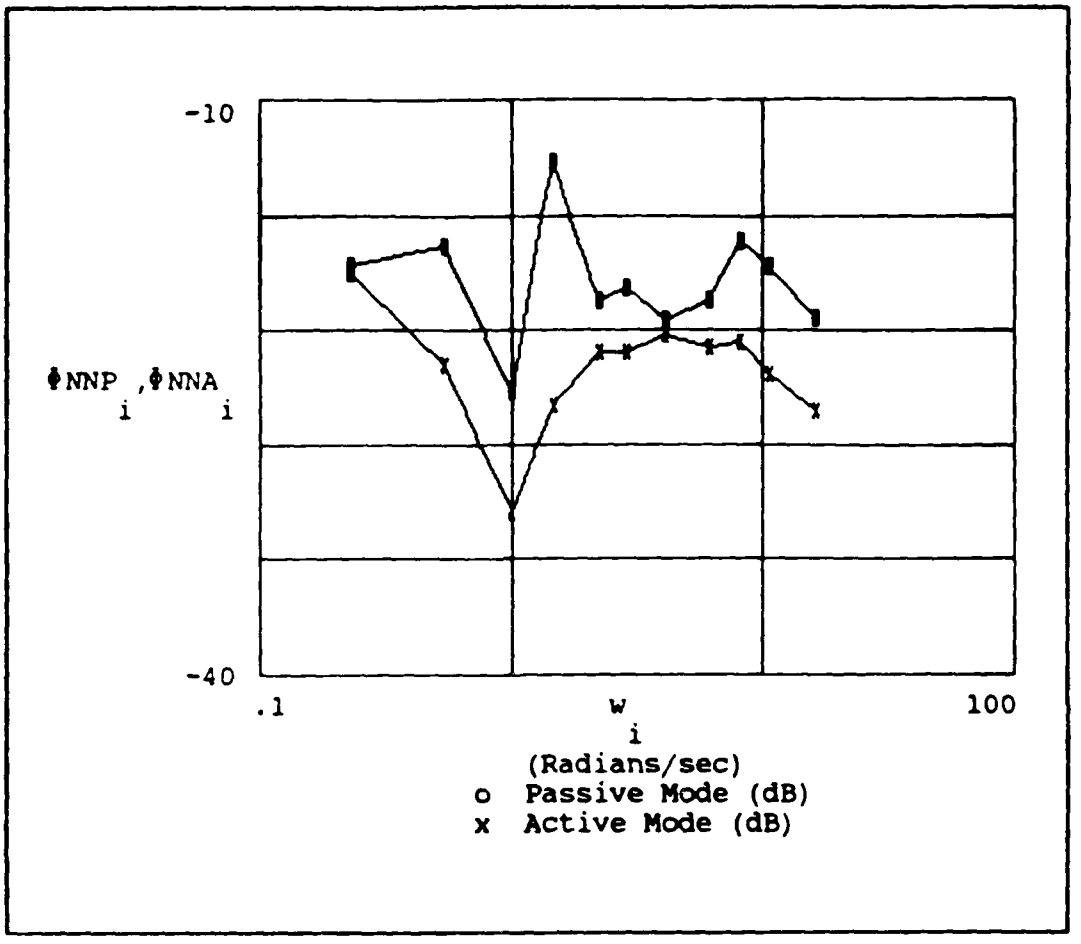

Figure B.6 - Operator Remnant/Noise (FF #2)

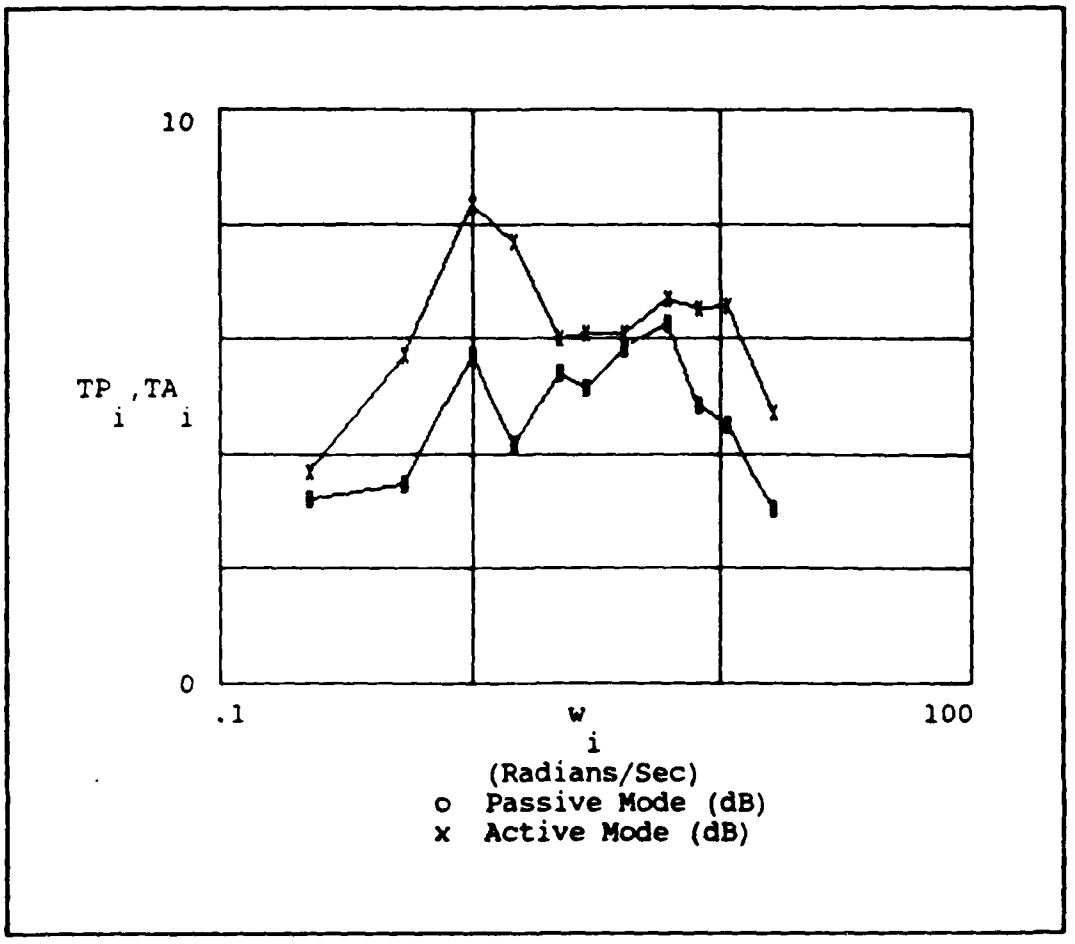

Figure B.7 - Transinformation Rate (FF #2)

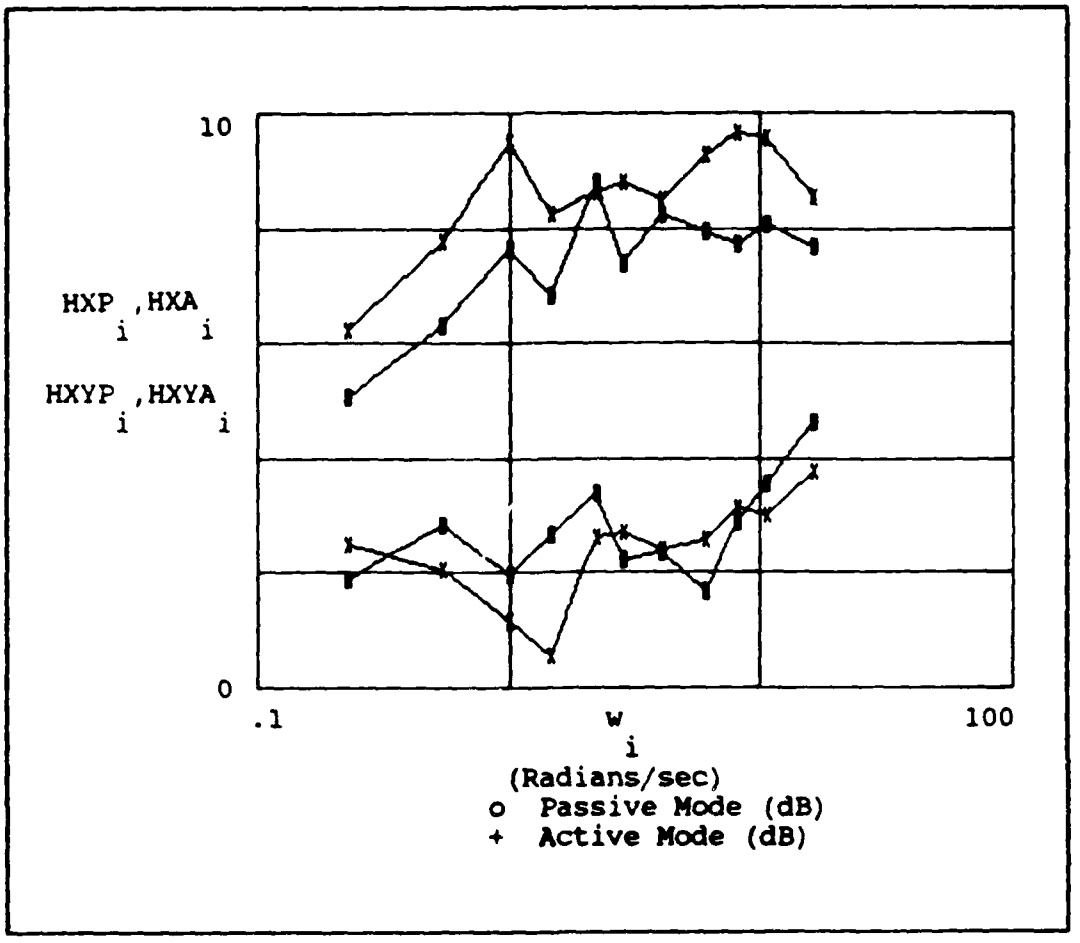

Figure B.8 - Display Error Entropy and Equivocation (FF #2)

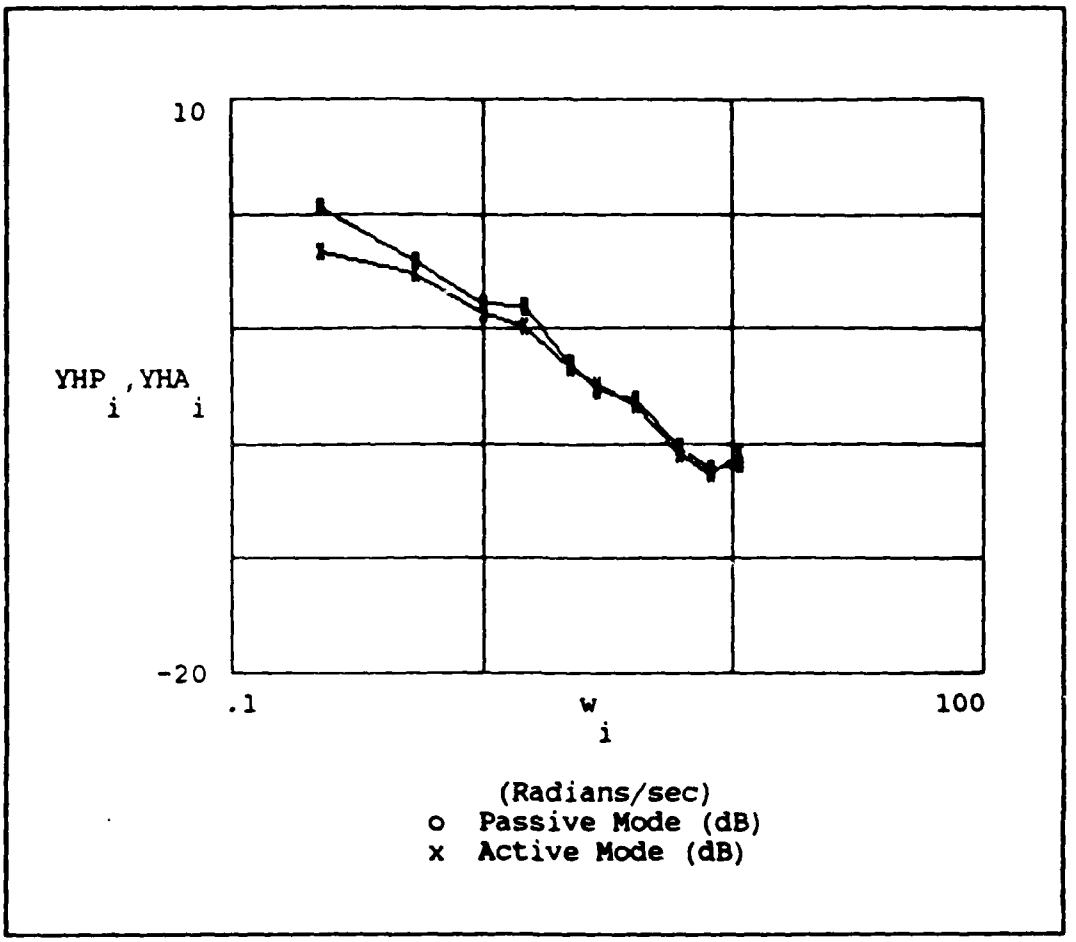

Figure B.9 - Human Operator Describing Function (FF #3)

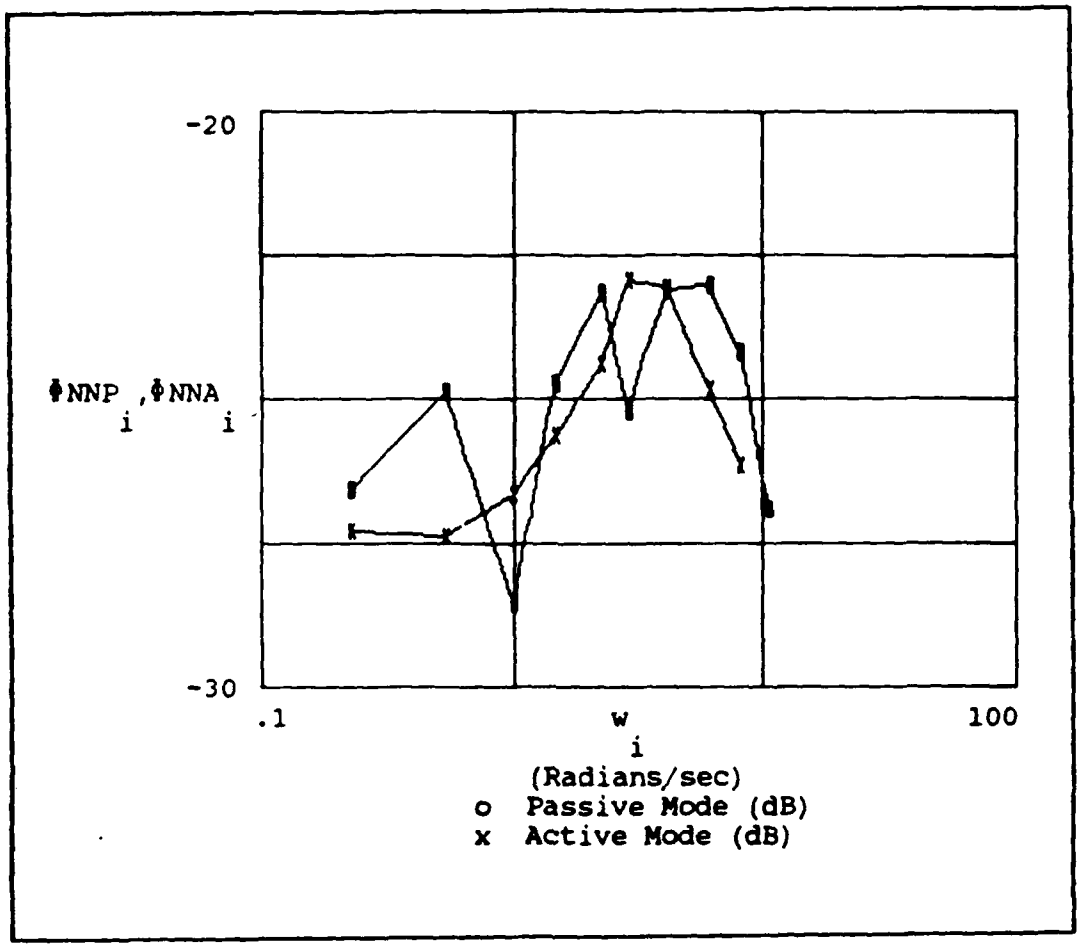

Figure B.10 - Operator Remnant/Noise (FF #3)

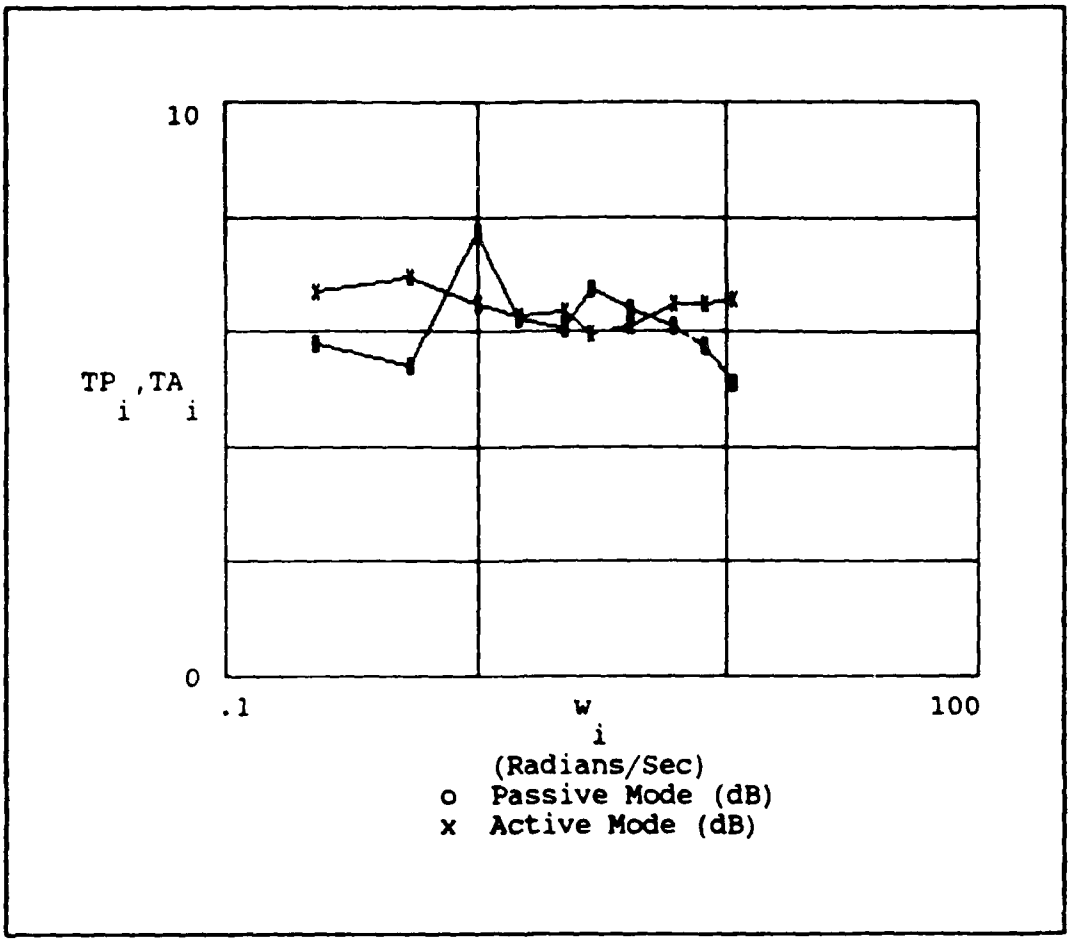

Figure B.11 - Transinformation Rate (FF #3)

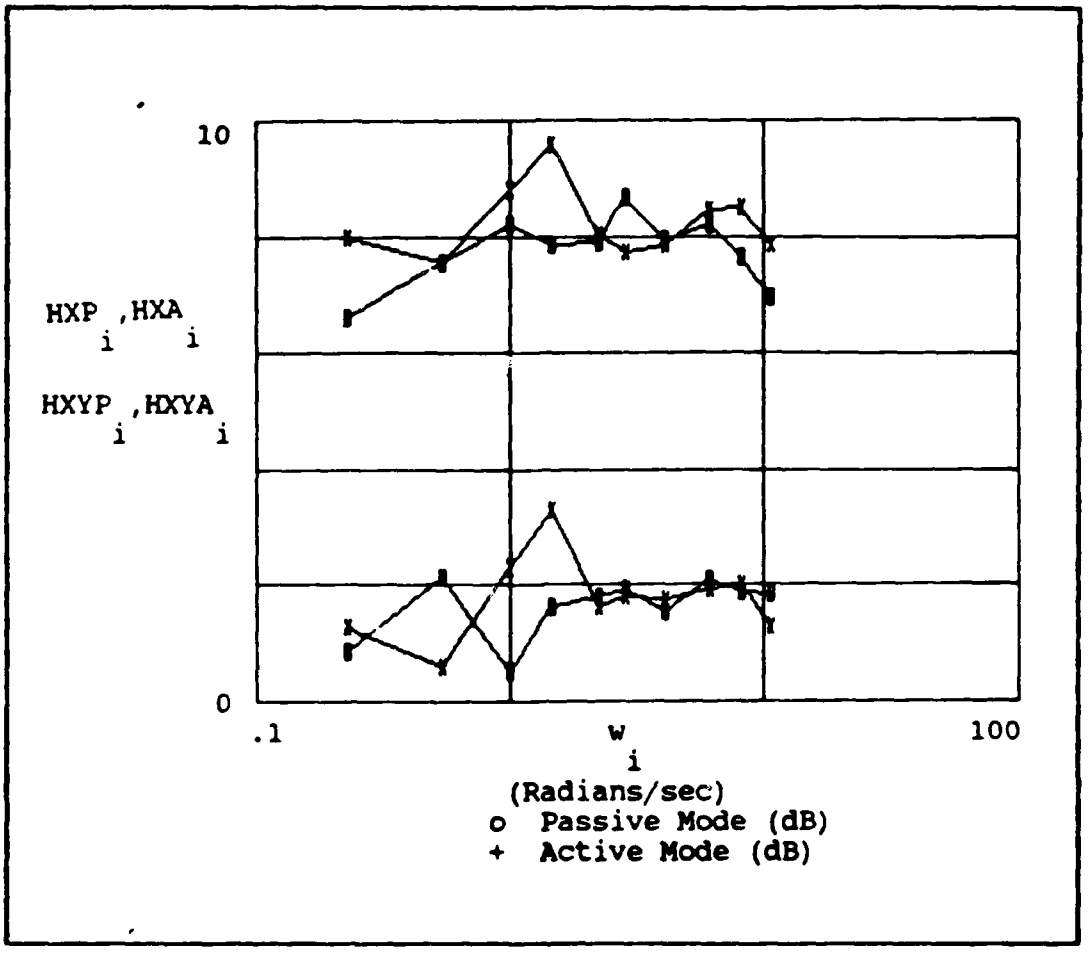

Figure B.12 - Display Error Entropy and Equivocation (FF #3)

Appendix C: Graphical Results For Subject #3

This appendix contains graphical representations of the results obtained by testing Subject #3. Each graph consists of a visual comparison of the active and passive modes of operation for a specific parameter under a specific forcing function.

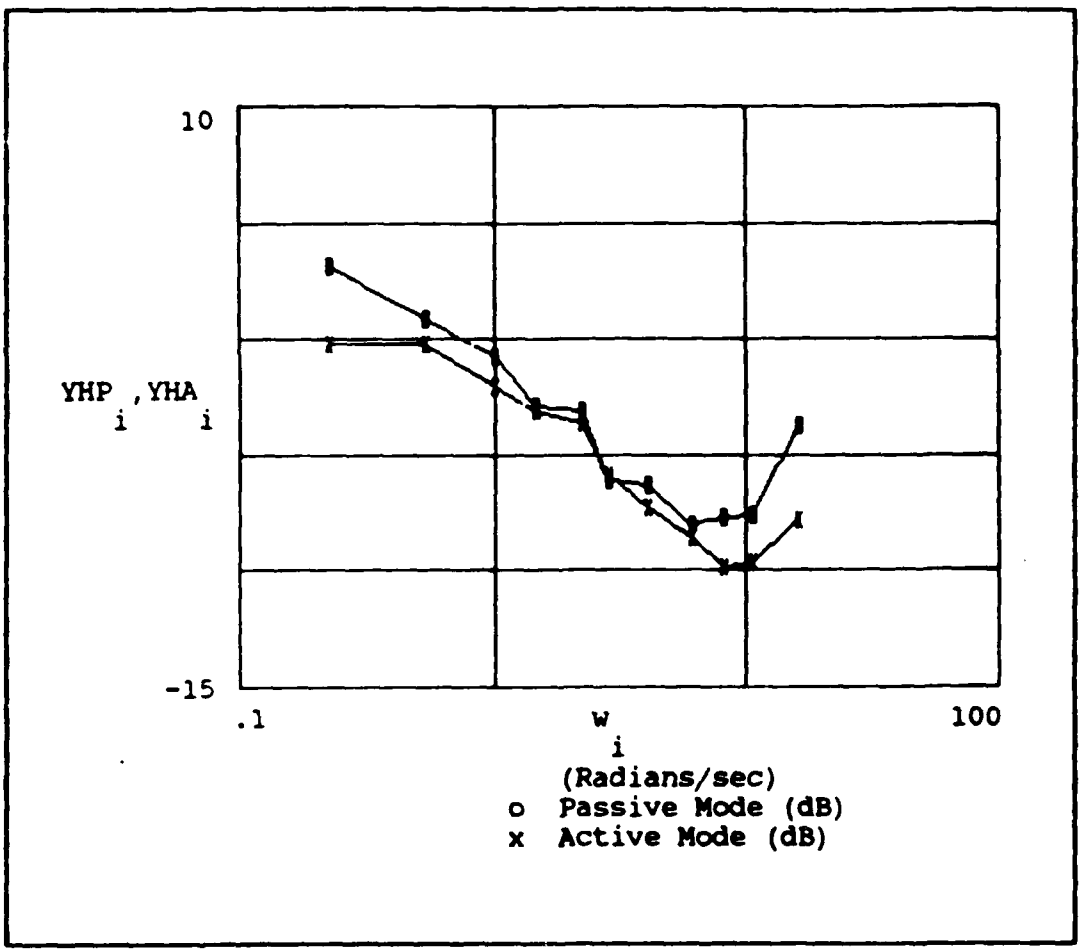

Figure C.1 - Human Operator Describing Function (FF #1)

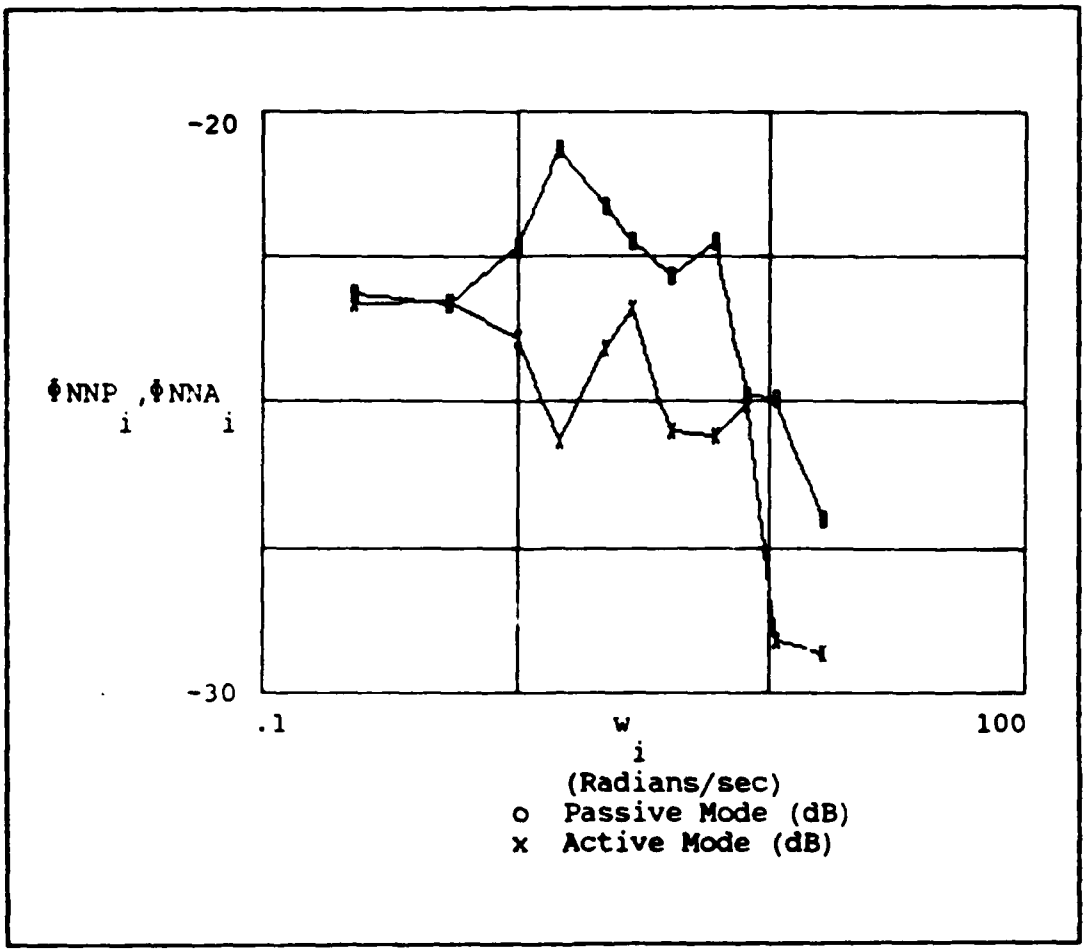

Figure C.2 - Operator Remnant/Noise (FF #1)

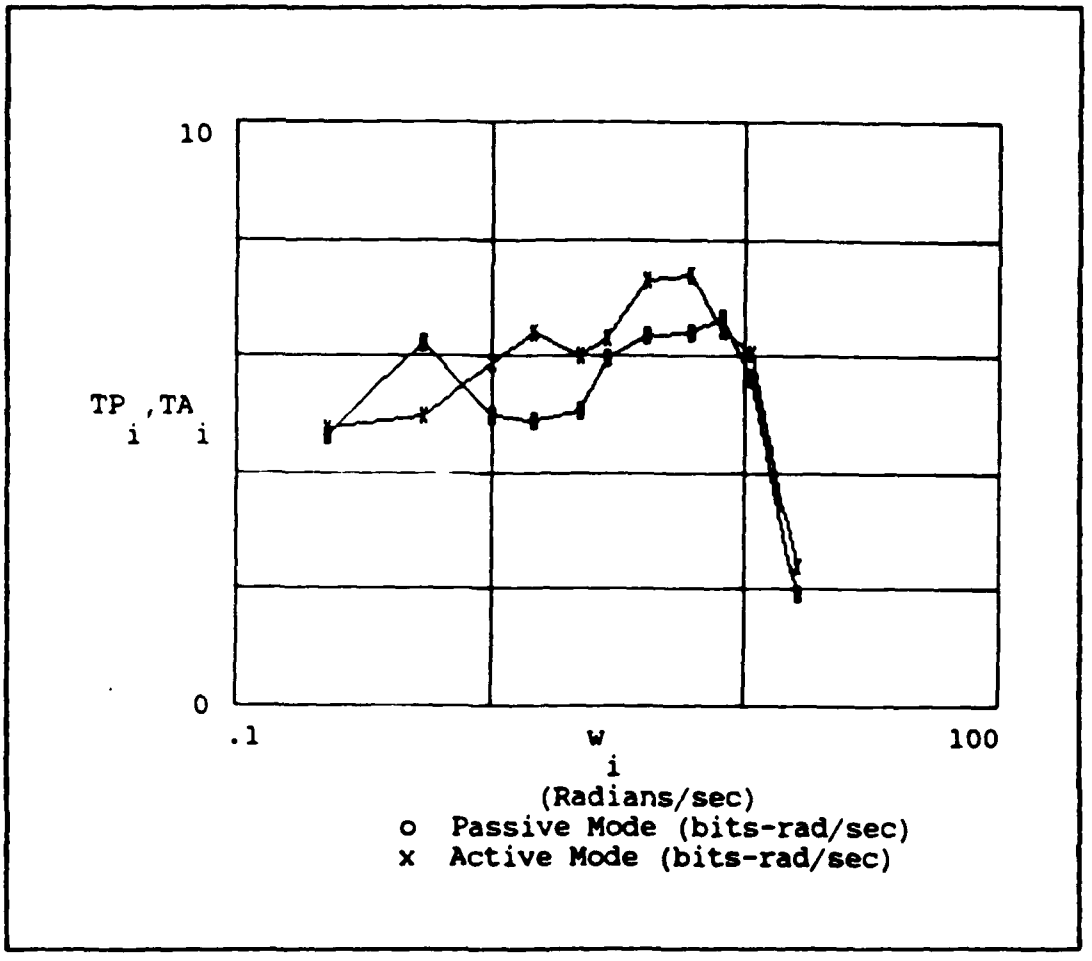

Figure C.3 - Transinformation Rate (FF #1)

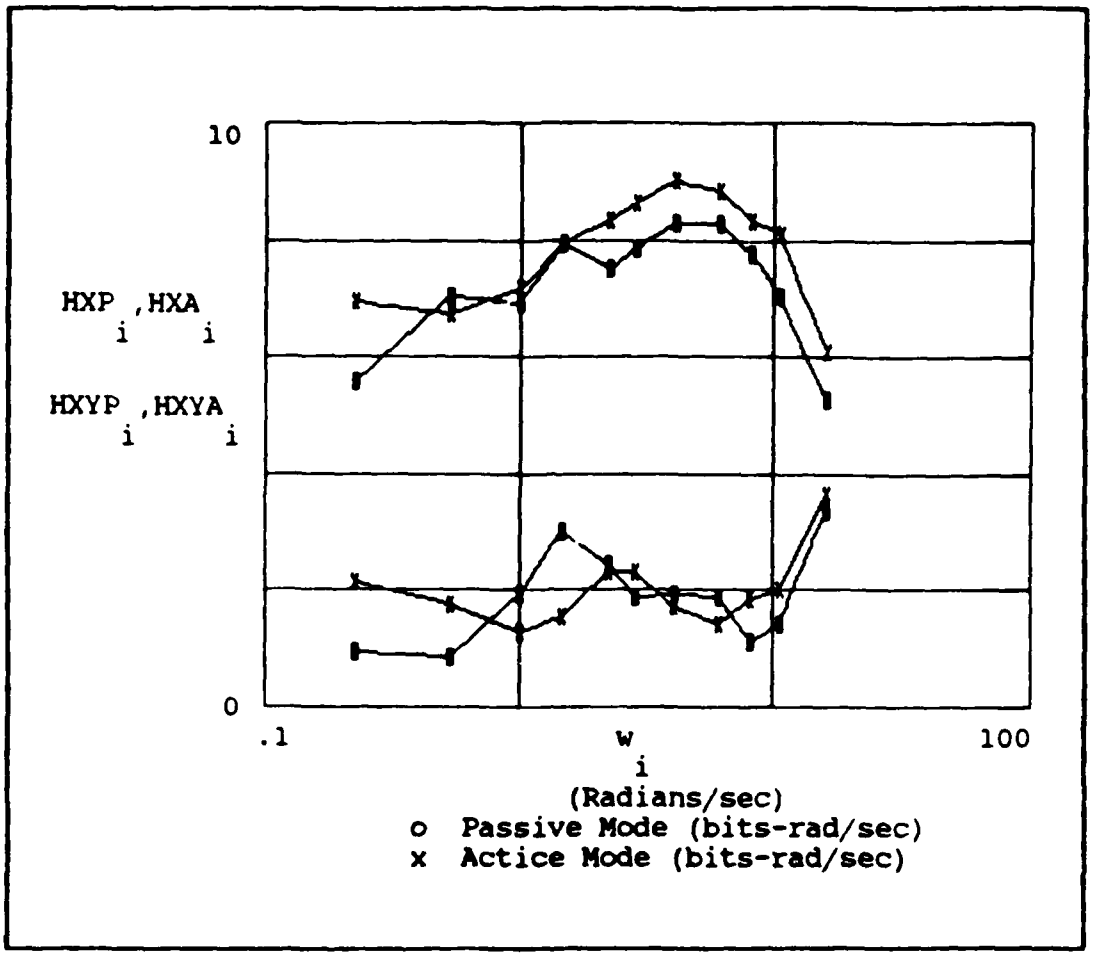

Figure C.4 - Display Error Entropy and Equivocation (FF #1)

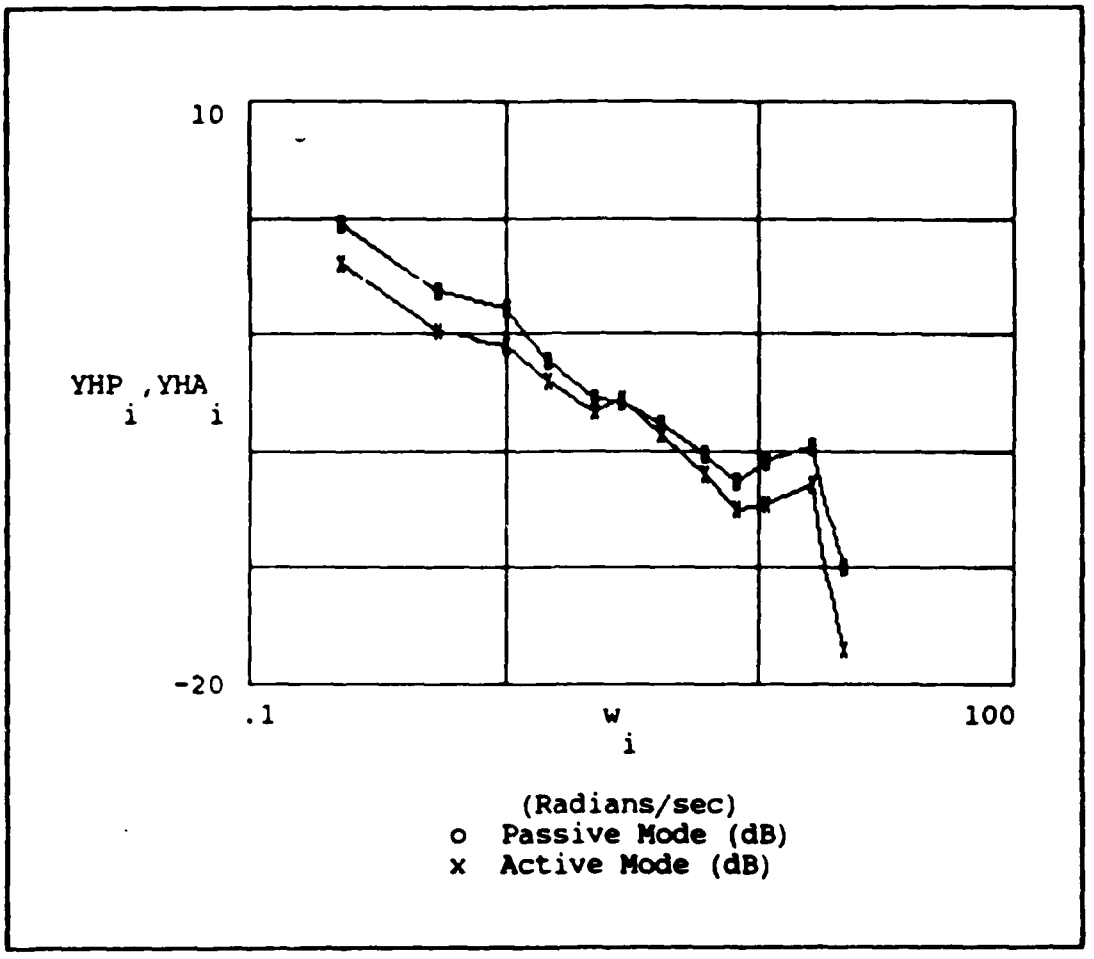

Figure C.5 - Human Operator Describing Function (FF #2)

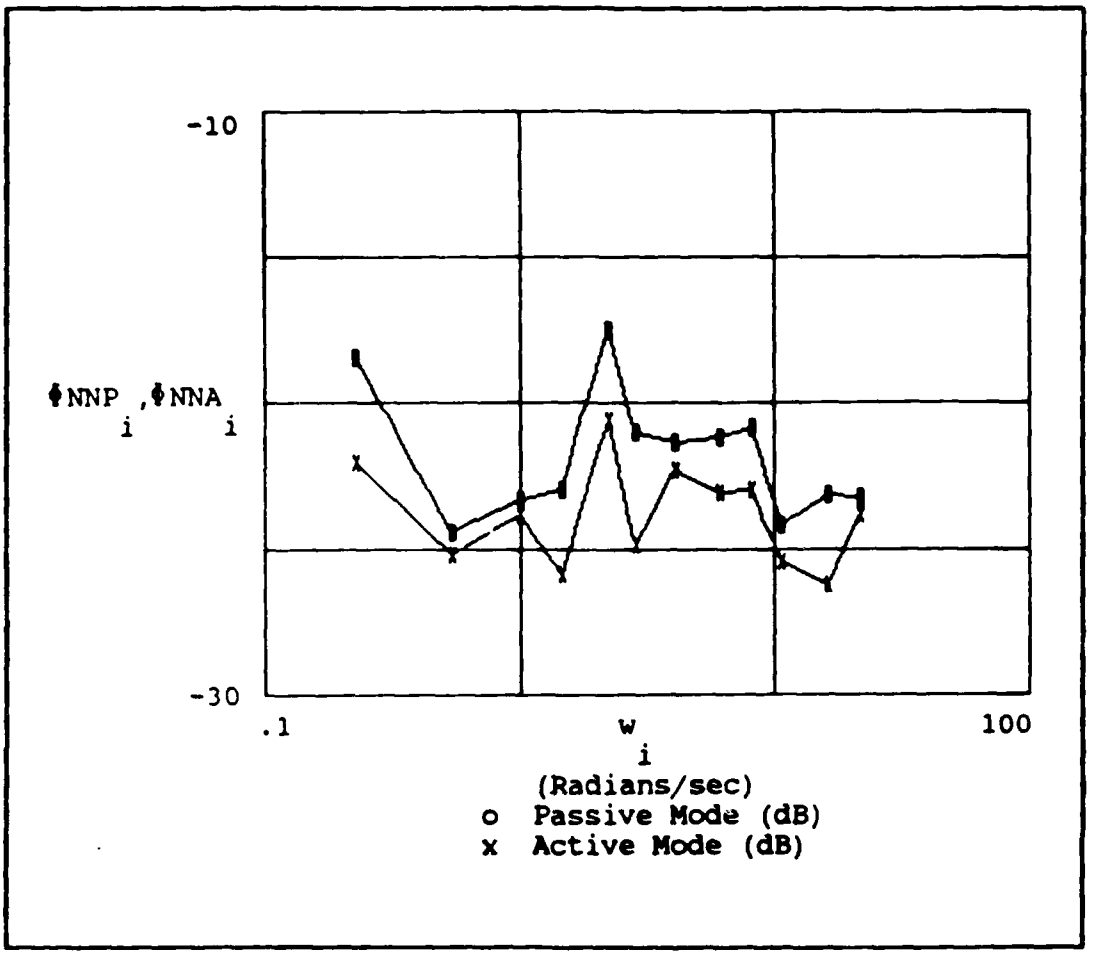

Figure C.6 - Operator Remnant/Noise (FF #2)

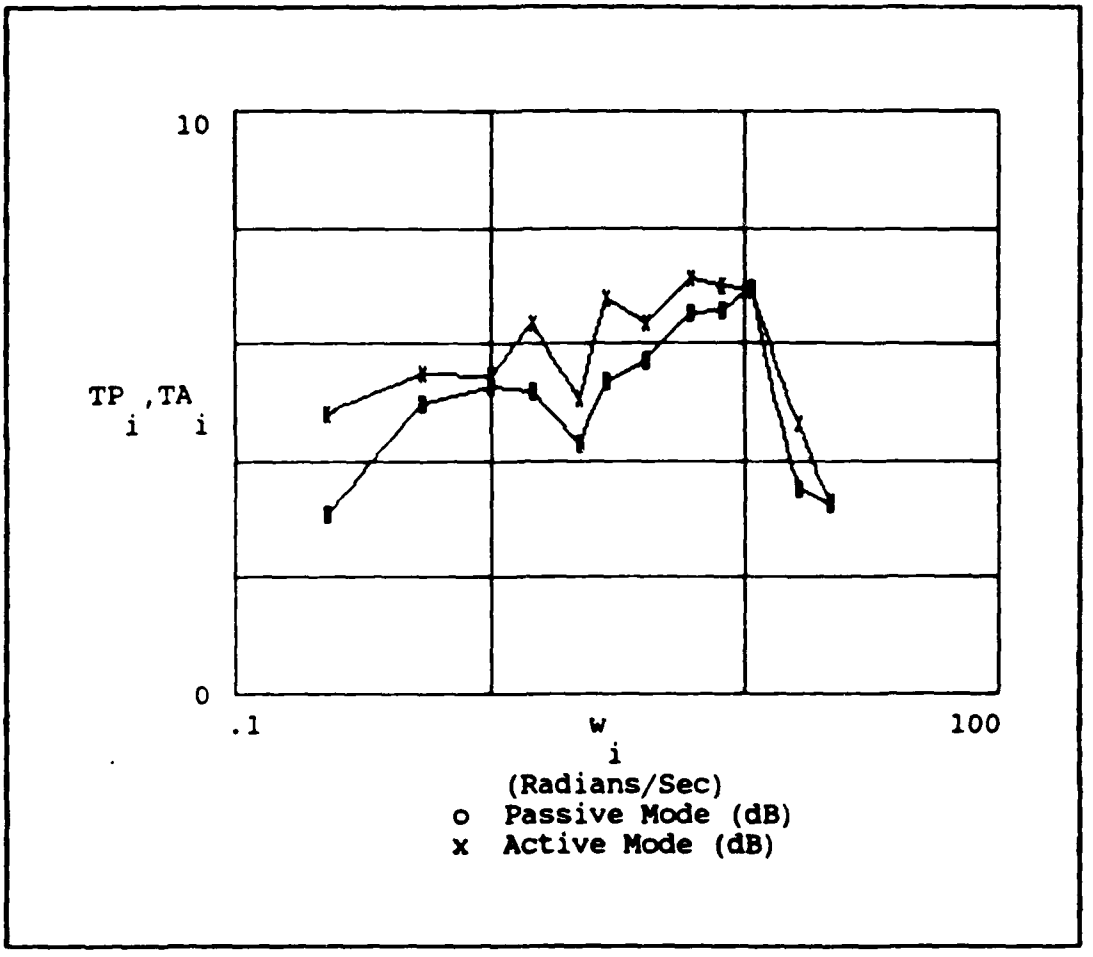

Figure C.7 - Transinformation Rate (FF #2)

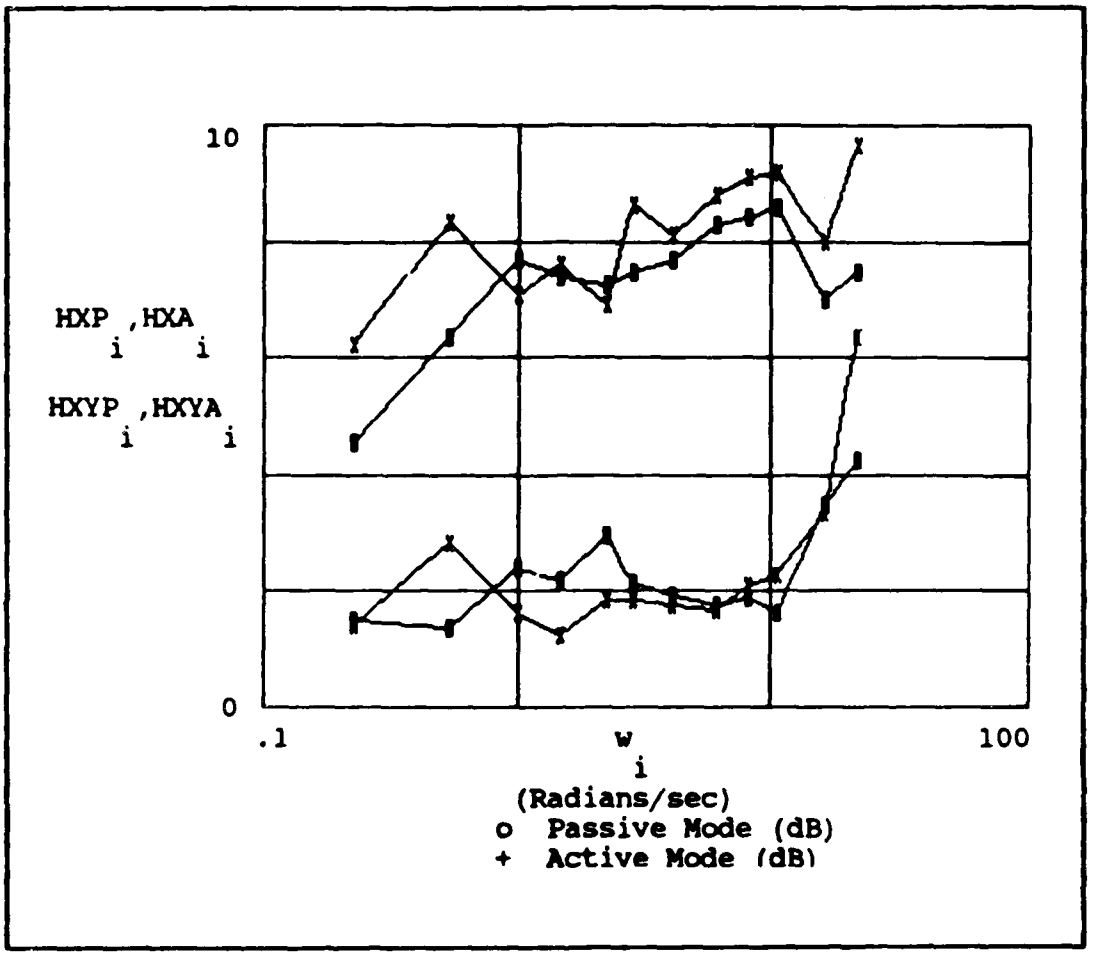

Figure C.8 - Display Error Entropy and Equivocation (FF #2)

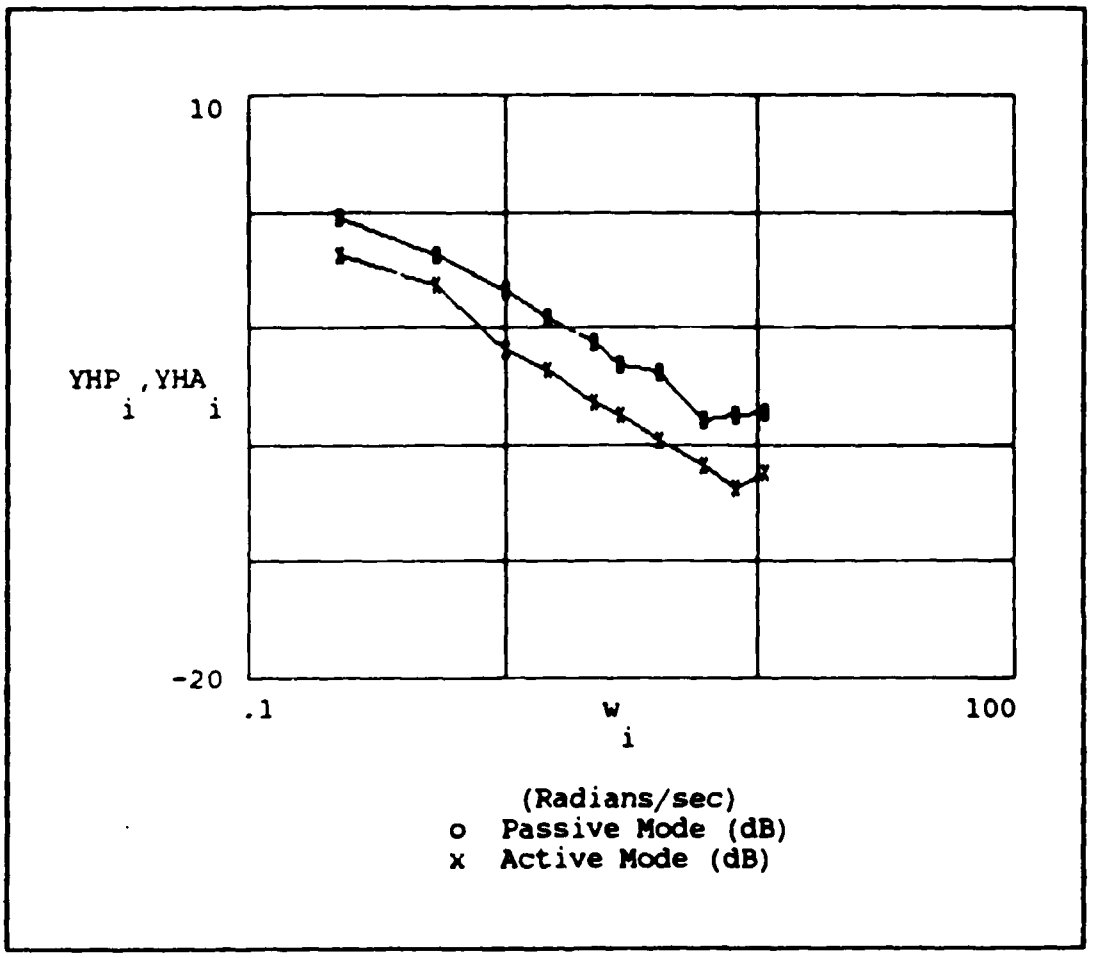

Figure C.9 - Human Operator Describing Function (FF #3)

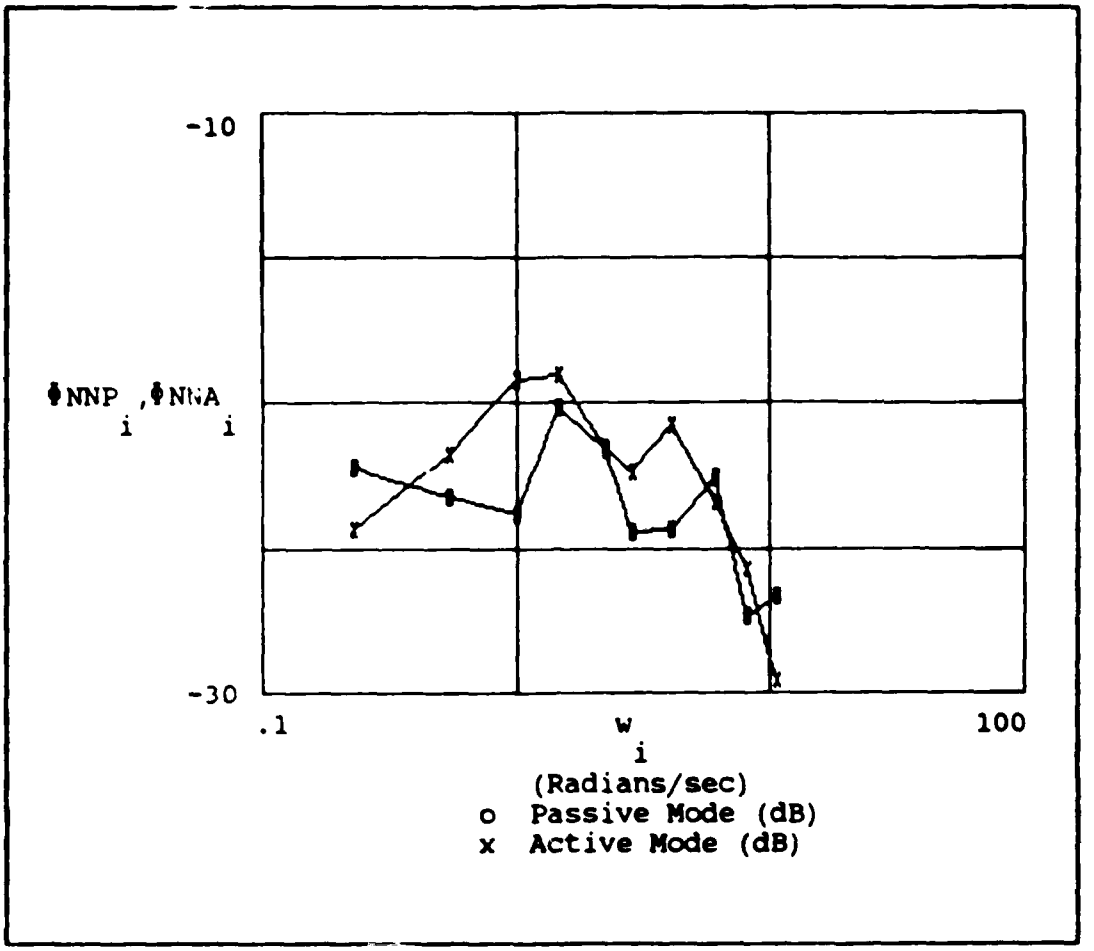

Figure C.10 - Operator Remnant/Noise (FF #3)

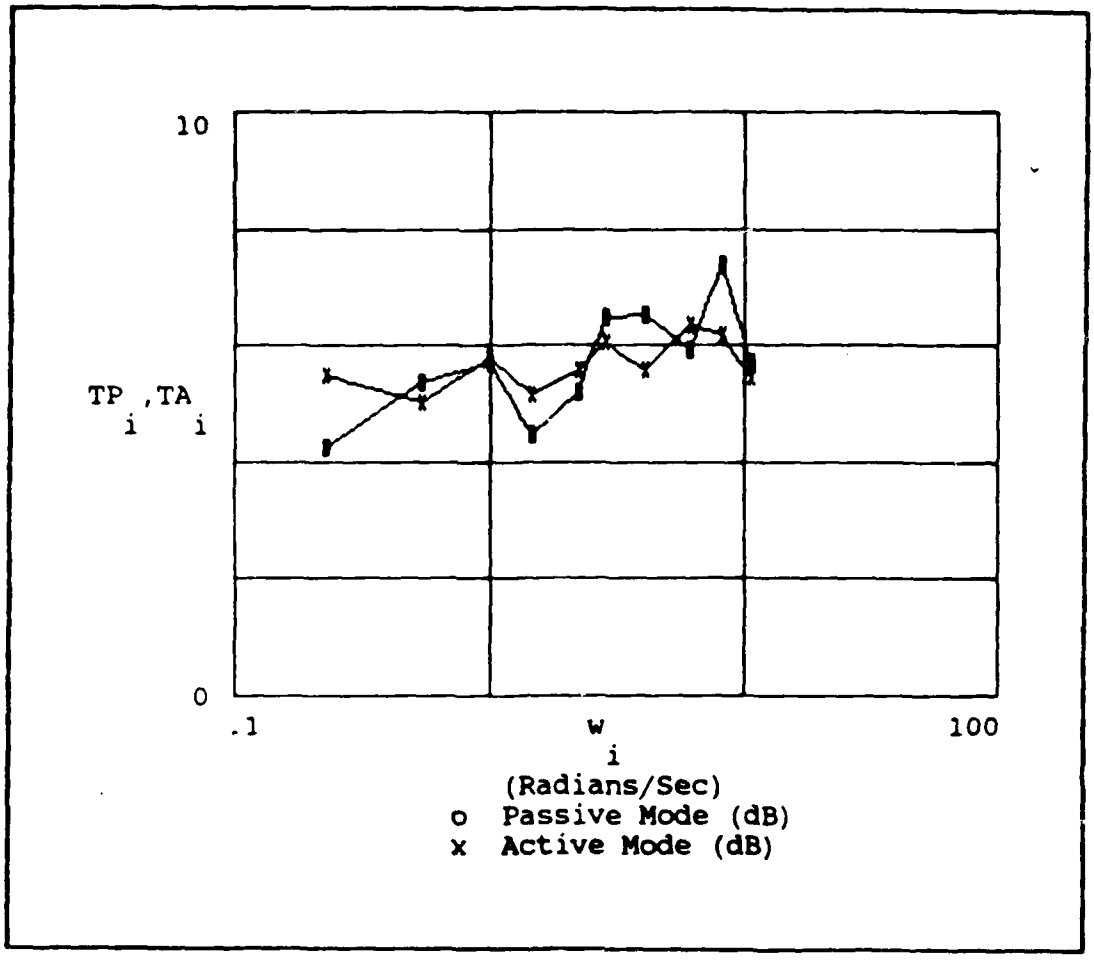

Figure C.11 - Transinformation Rate (FF #3)

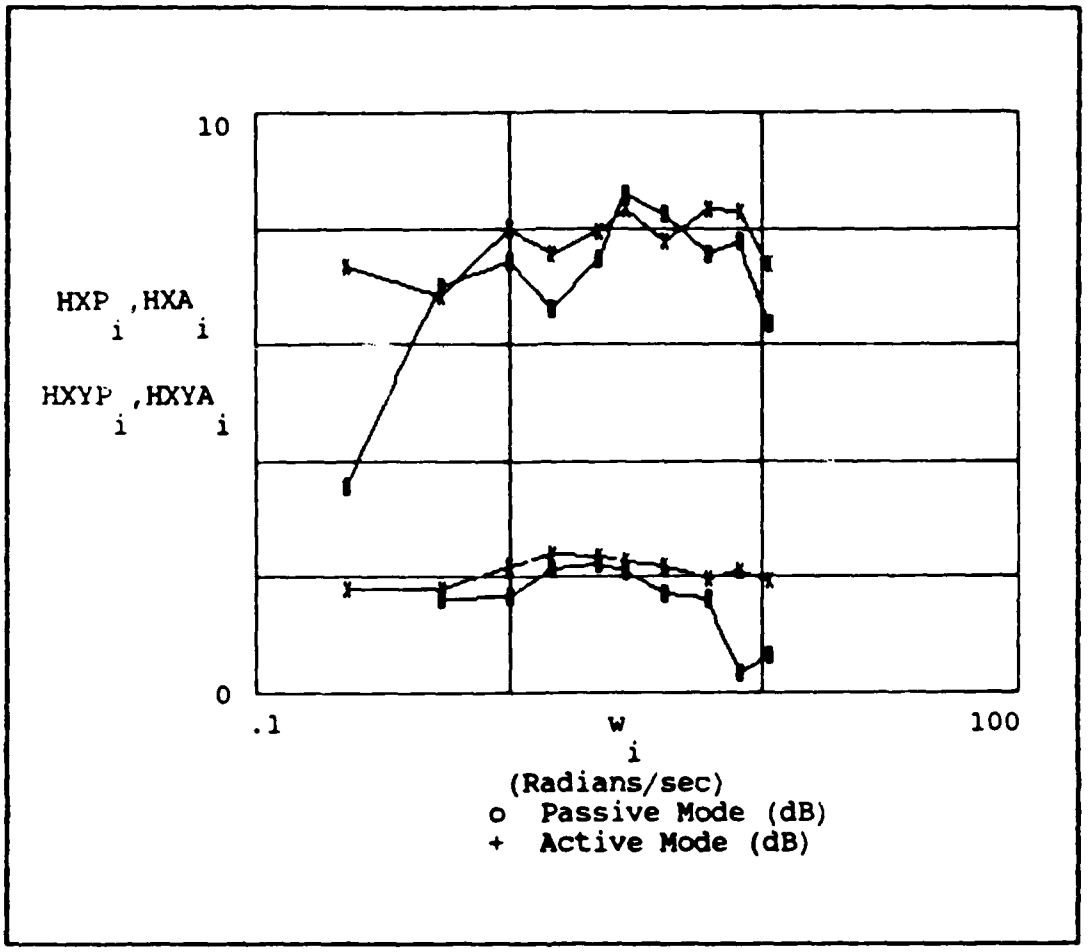

Figure C.12 - Display Error Entropy and Equivocation (FF #3)

Appendix D: Graphical Results For Subject #4

This appendix contains graphical representations of the results obtained by testing Subject #4. Each graph consists of a visual comparison of the active and passive modes of operation for a specific parameter under a specific forcing function.

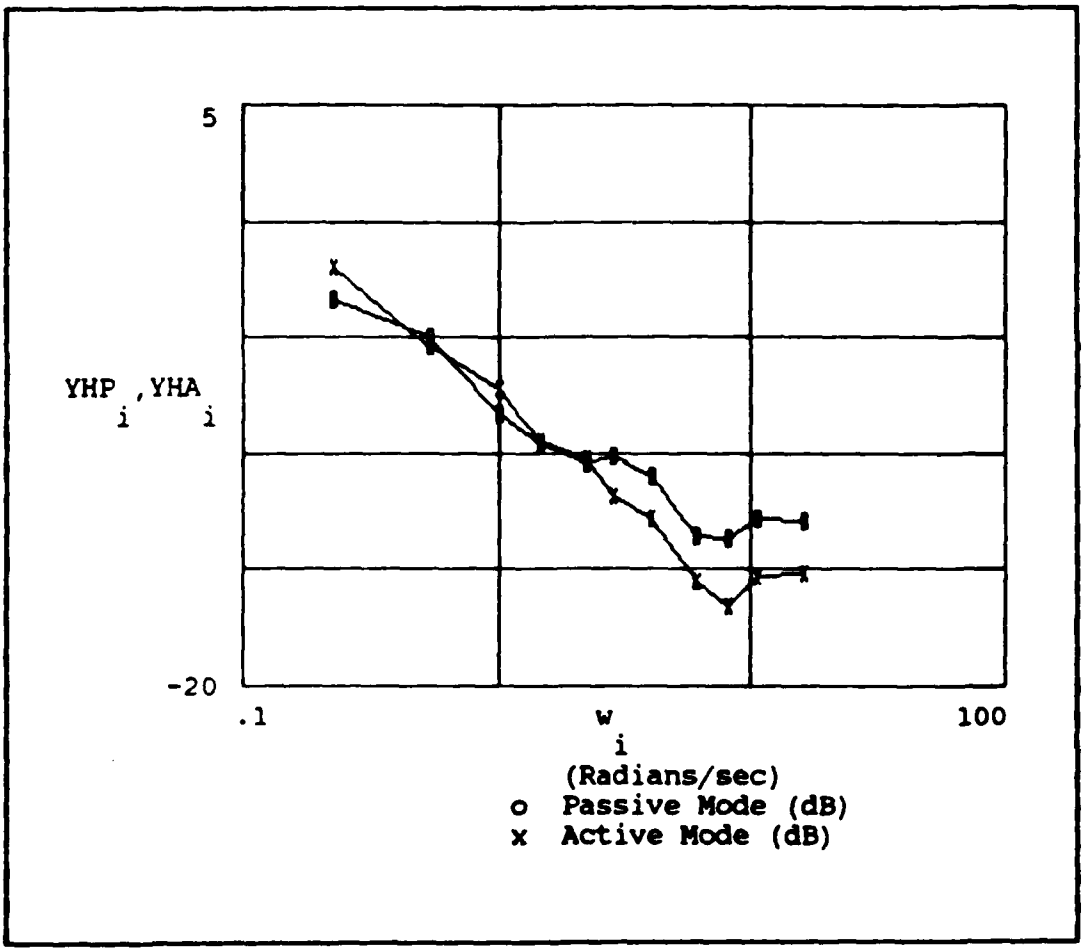

Figure D.1 - Human Operator Describing Function (FF #1)

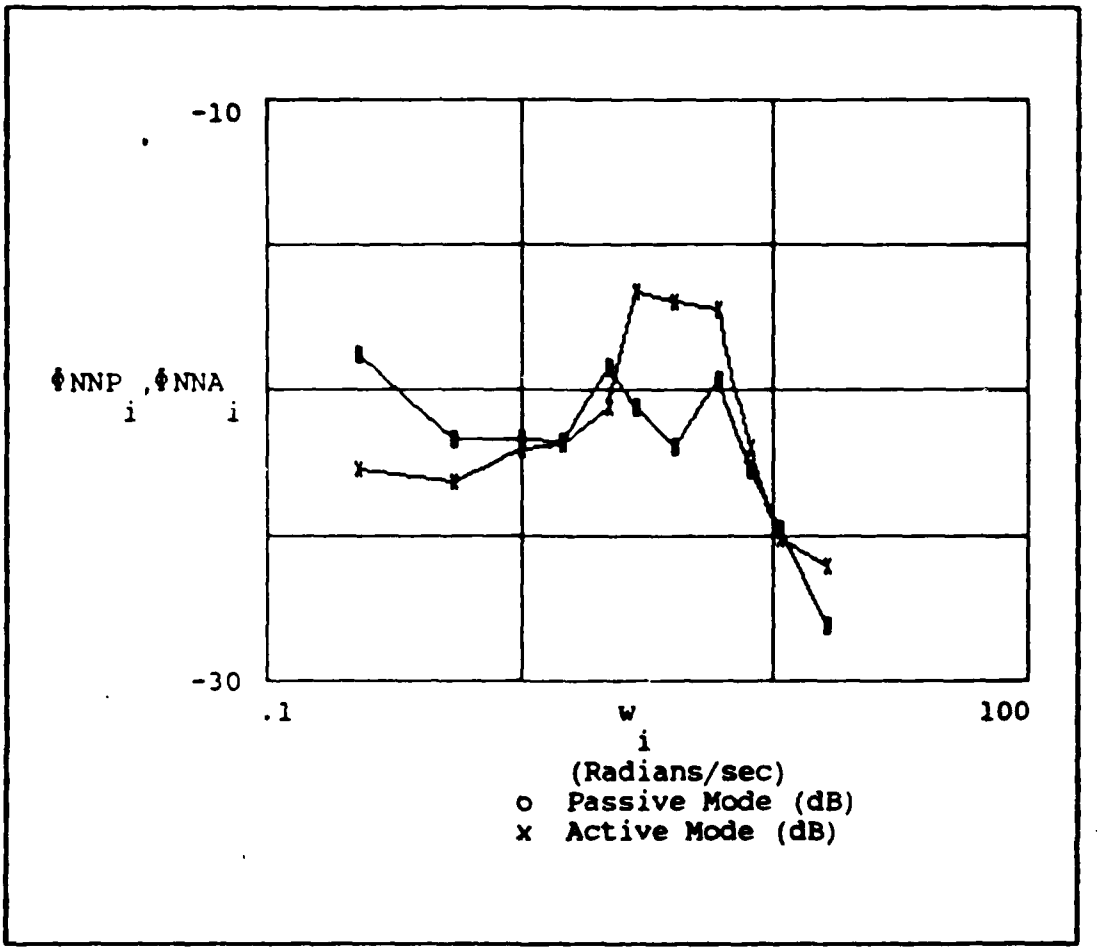

Figure D.2 - Operator Remnant/Noise (FF #1)

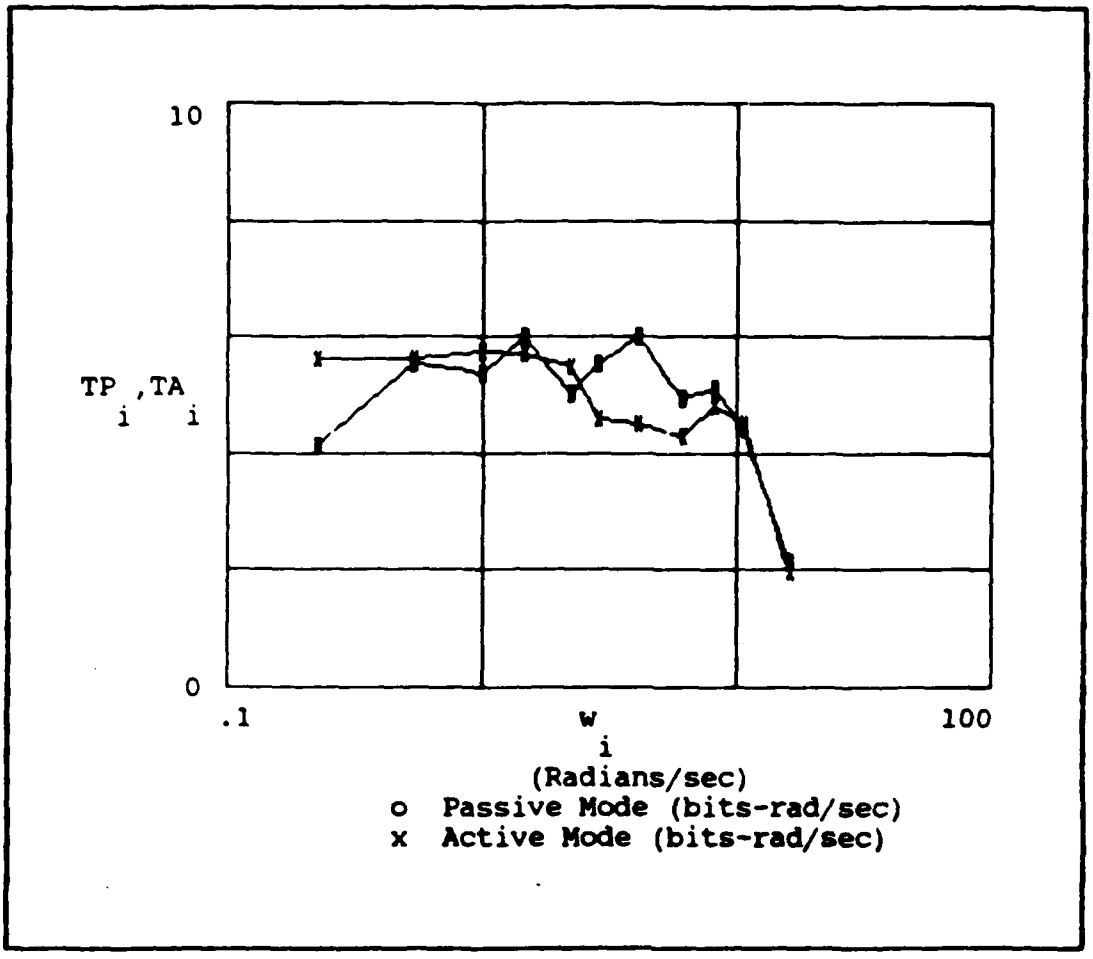

Figure D.3 - Transinformation Rate (FF #1)

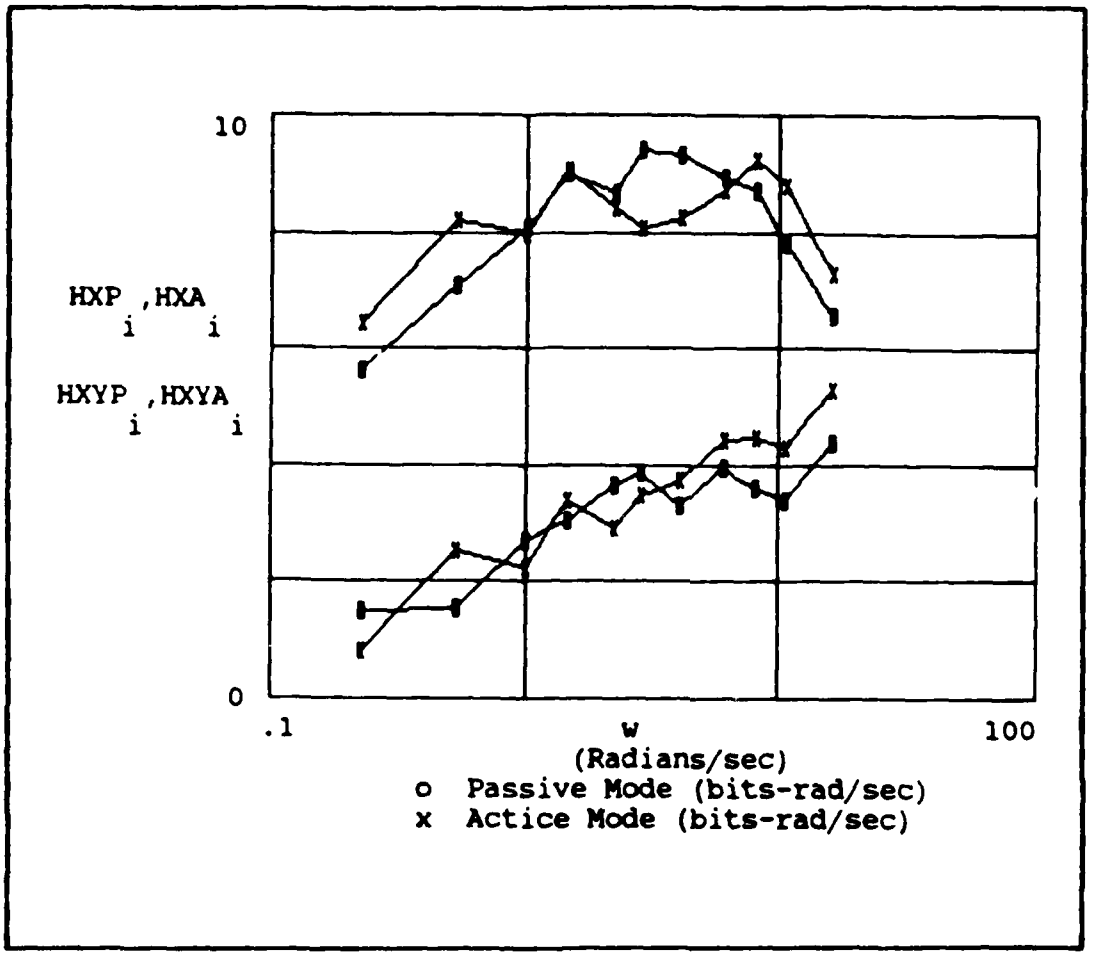

Figure D.4 - Display Error Entropy and Equivocation (FF #1)

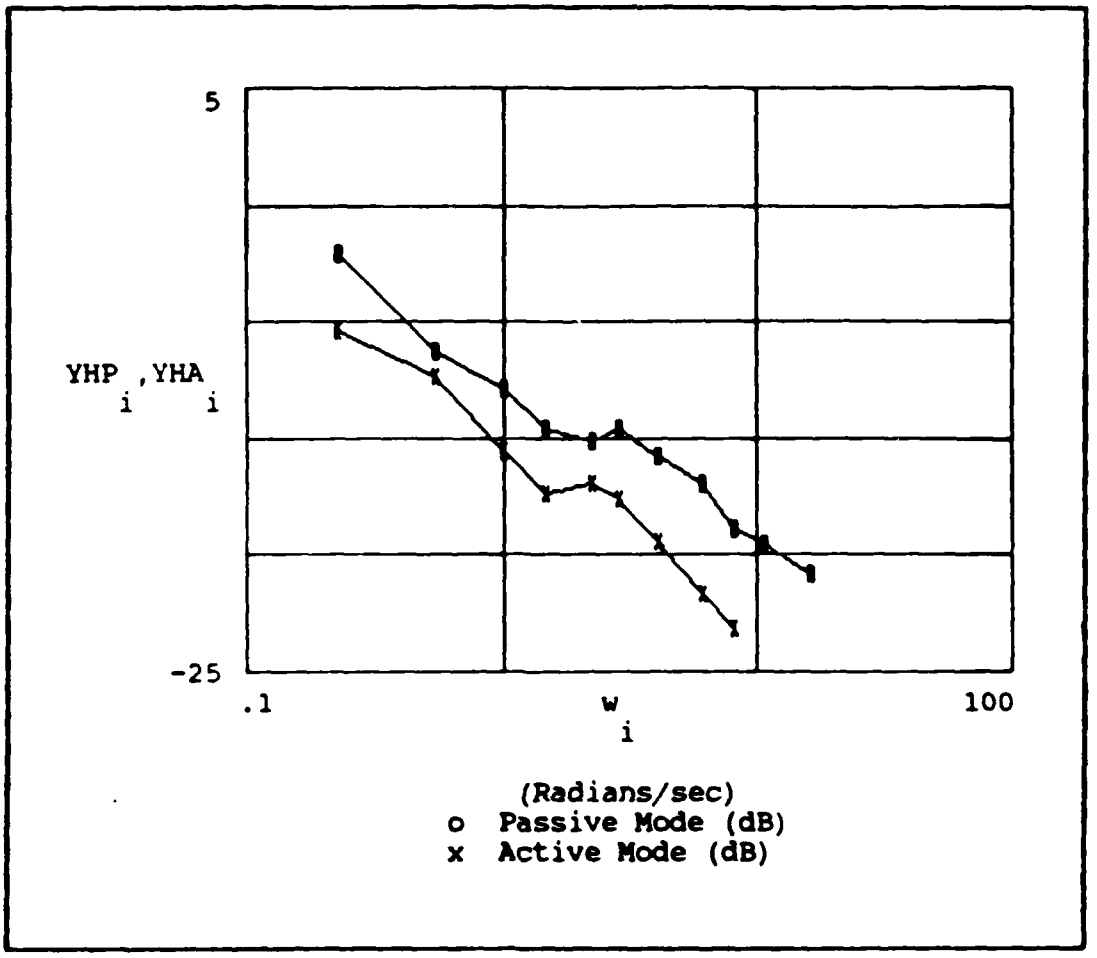

Figure D.5 - Human Operator Describing Function (FF #2)

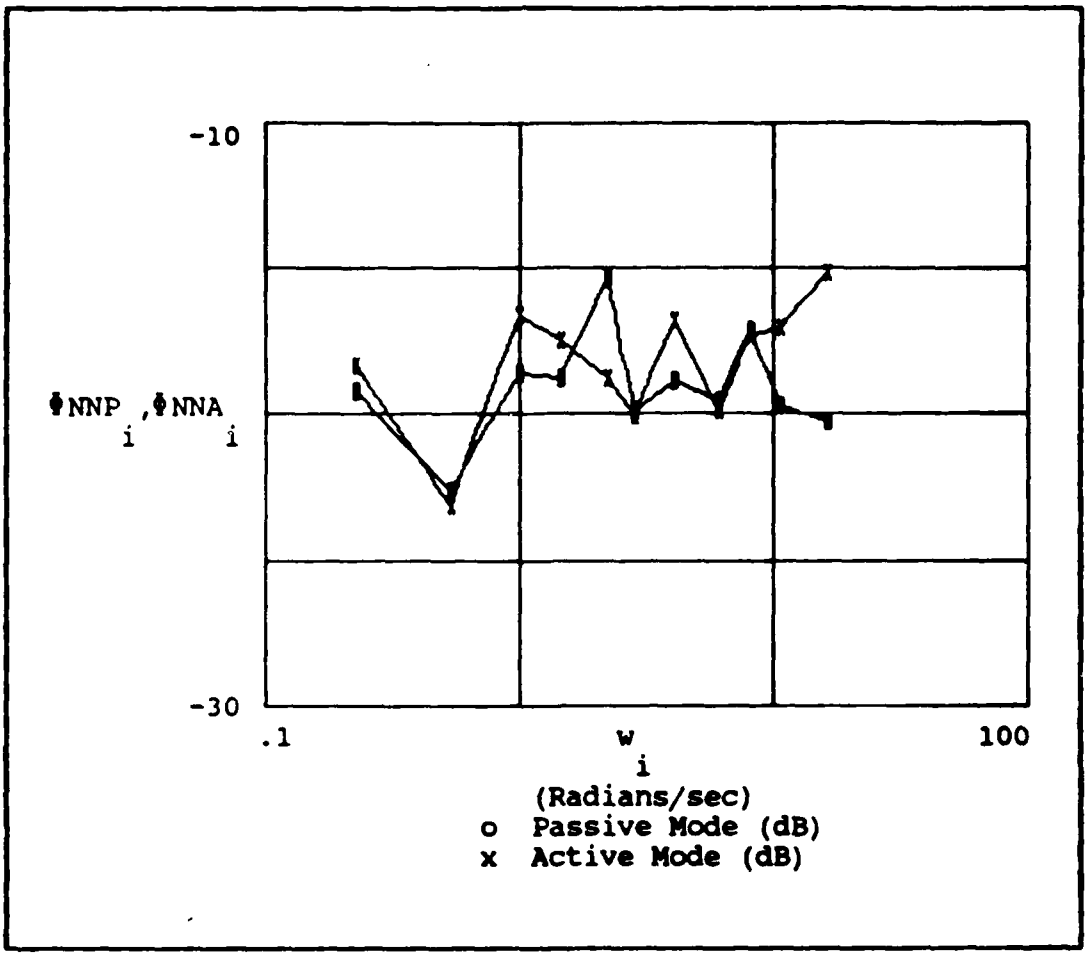

Figure D.6 - Operator Remnant/Noise (FF #2)

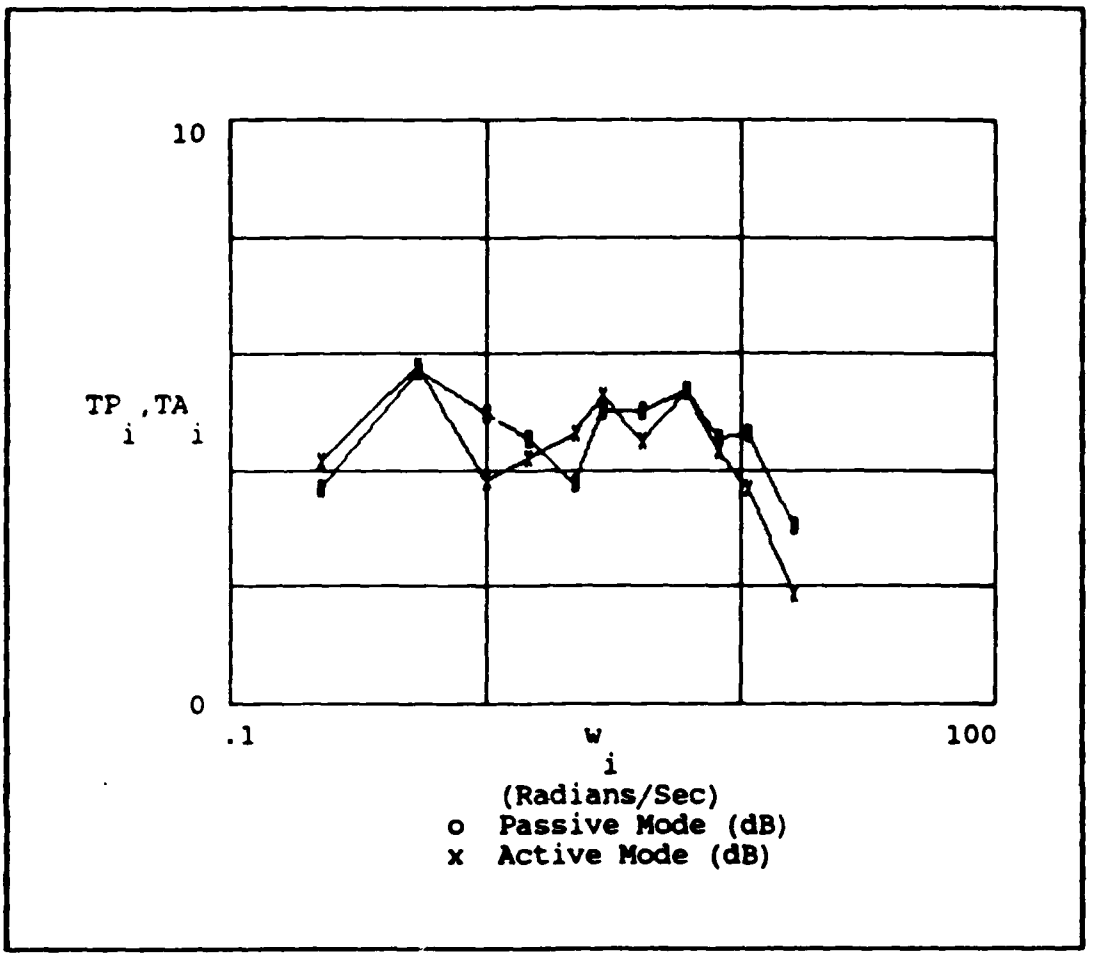

Figure D.7 - Transinformation Rate (FF #2)

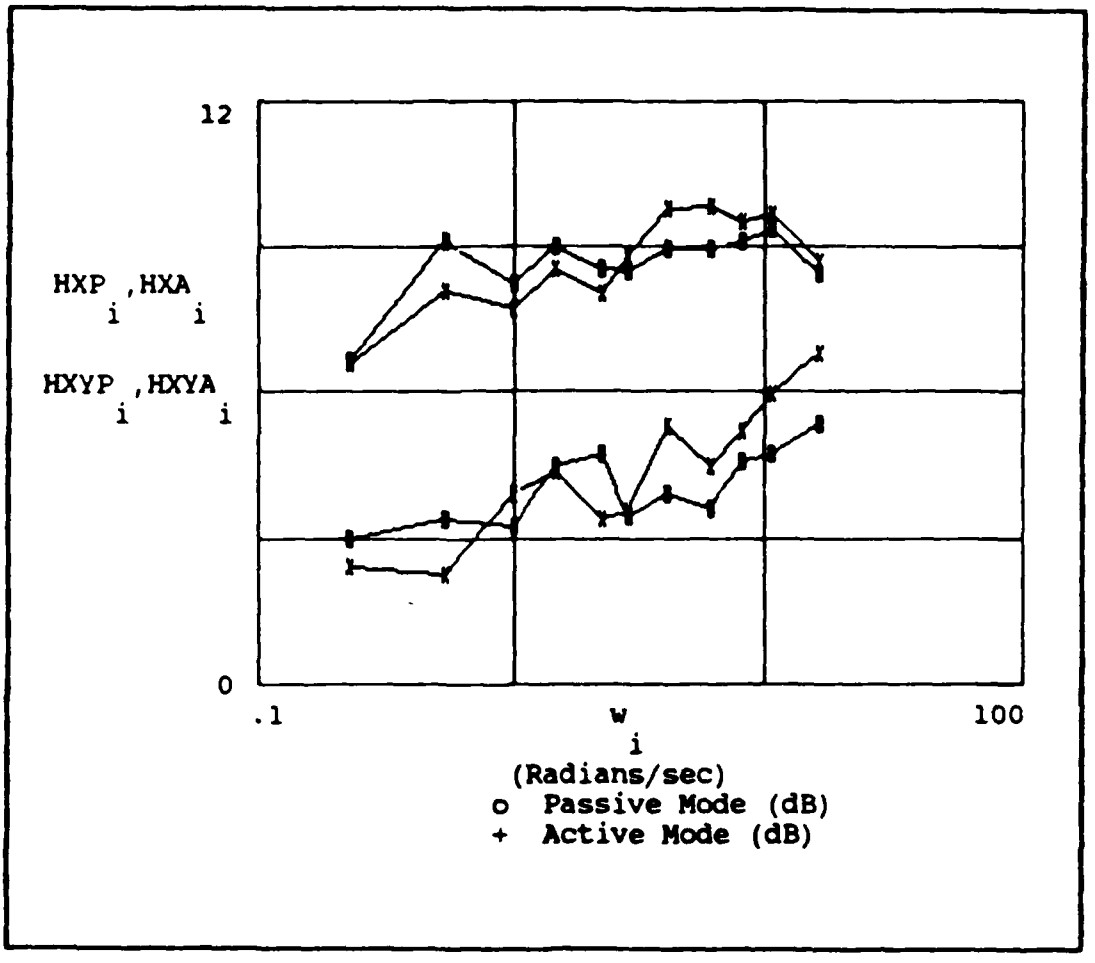

Figure D.8 - Display Error Entropy and Equivocation (FF #2)

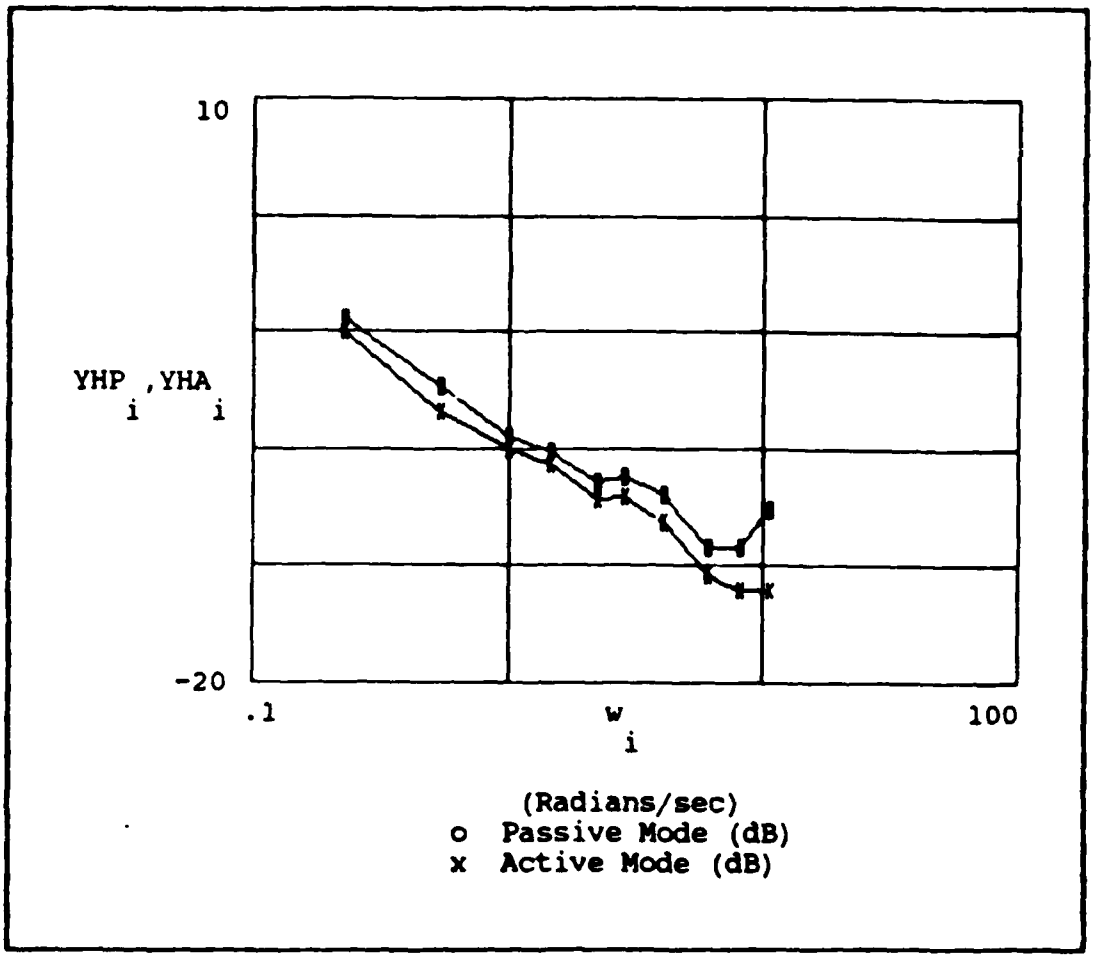

Figure D.9 - Human Operator Describing Function (FF #3)

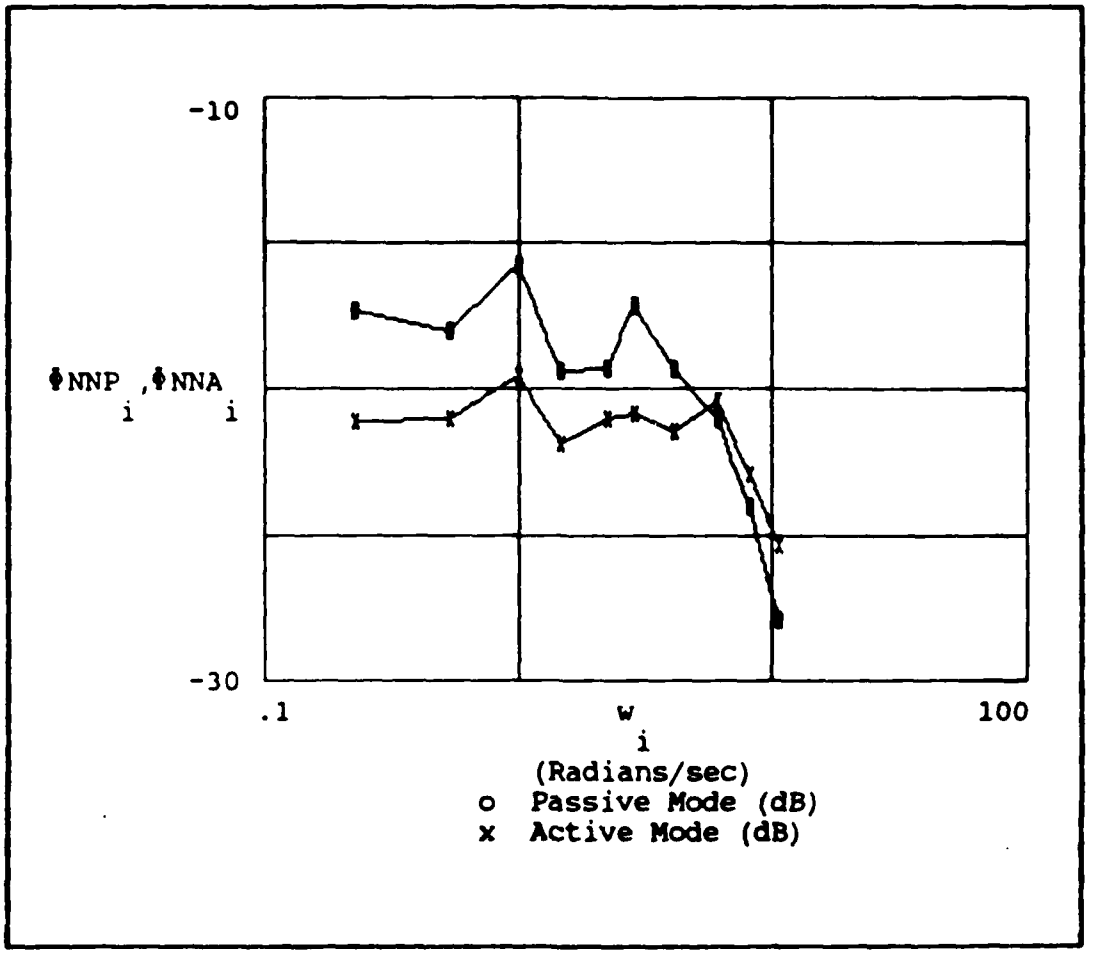

Figure D.10 - Operator Remnant/Noise (FF #3)

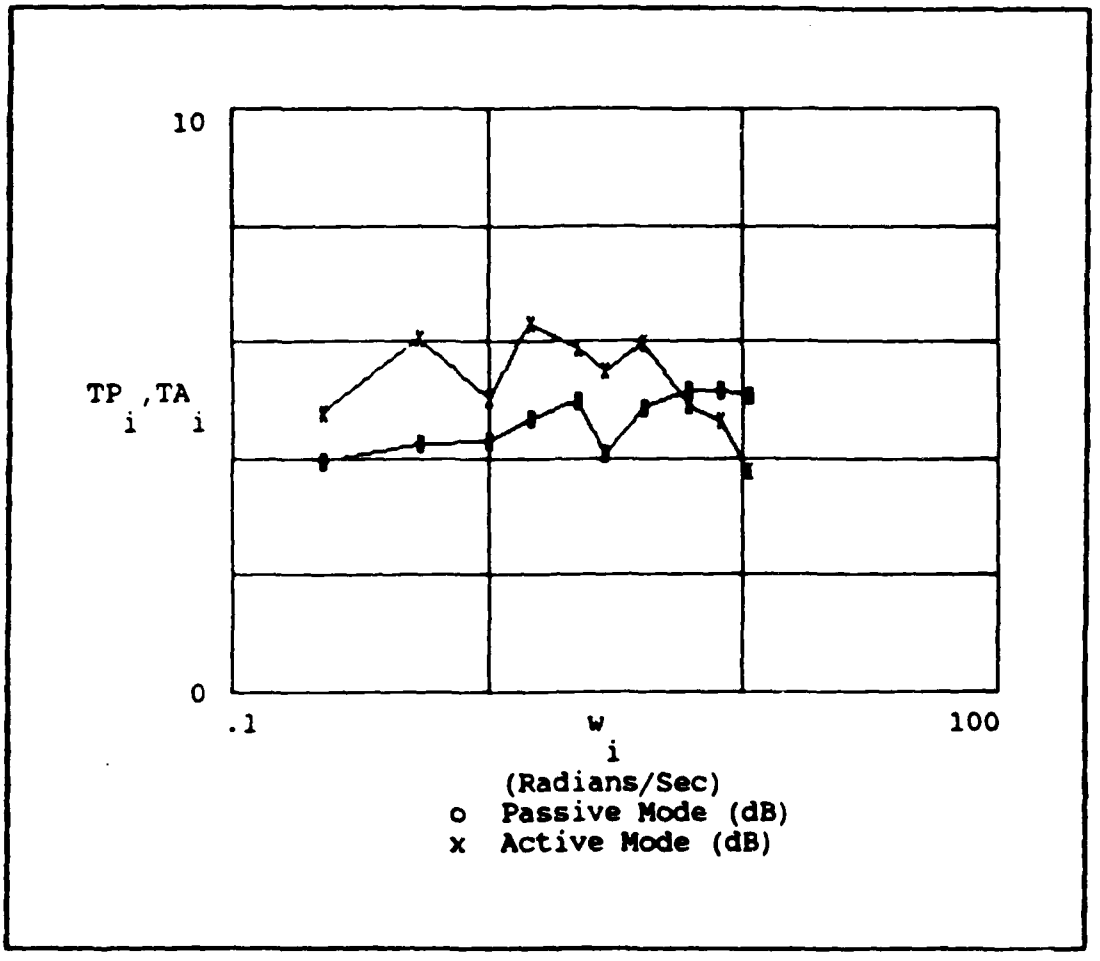

Figure D.11 - Transinformation Rate (FF #3)

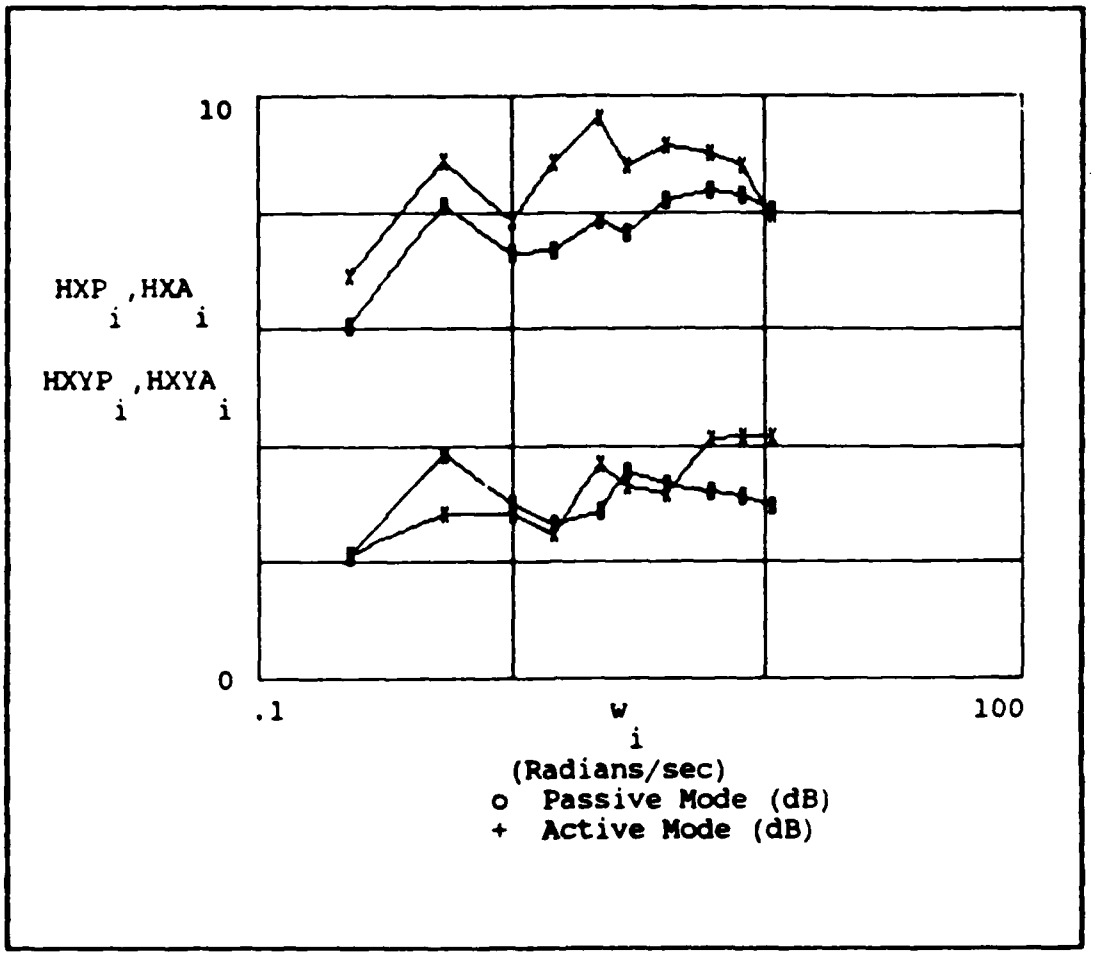

Figure D.12 - Display Error Entropy and Equivocation (FF #3)

Appendix E: Graphical Results For Subject #5

This appendix contains graphical representations of the results obtained by testing Subject #5. Each graph consists of a visual comparison of the active and passive modes of operation for a specific parameter under a specific forcing function.

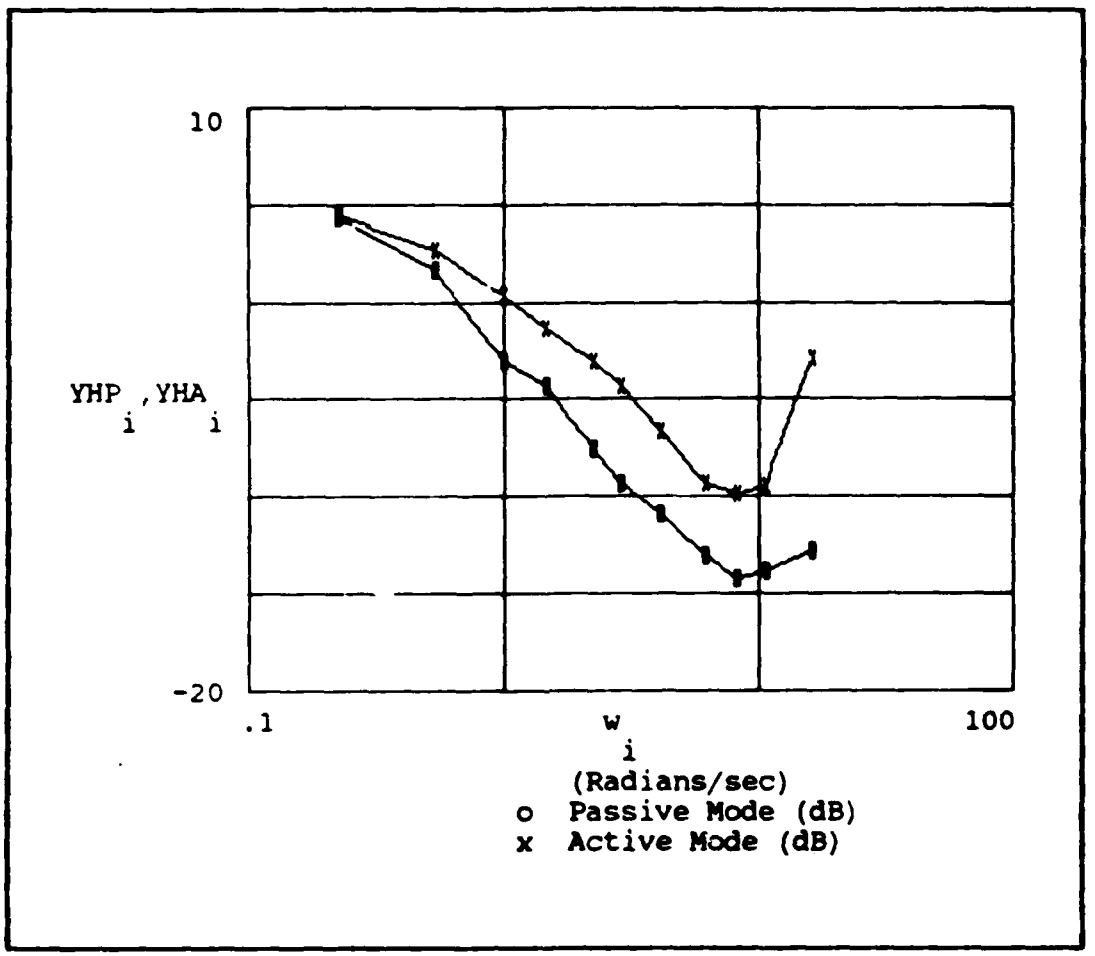

Figure E.1 - Human Operator Describing Function (FF #1)

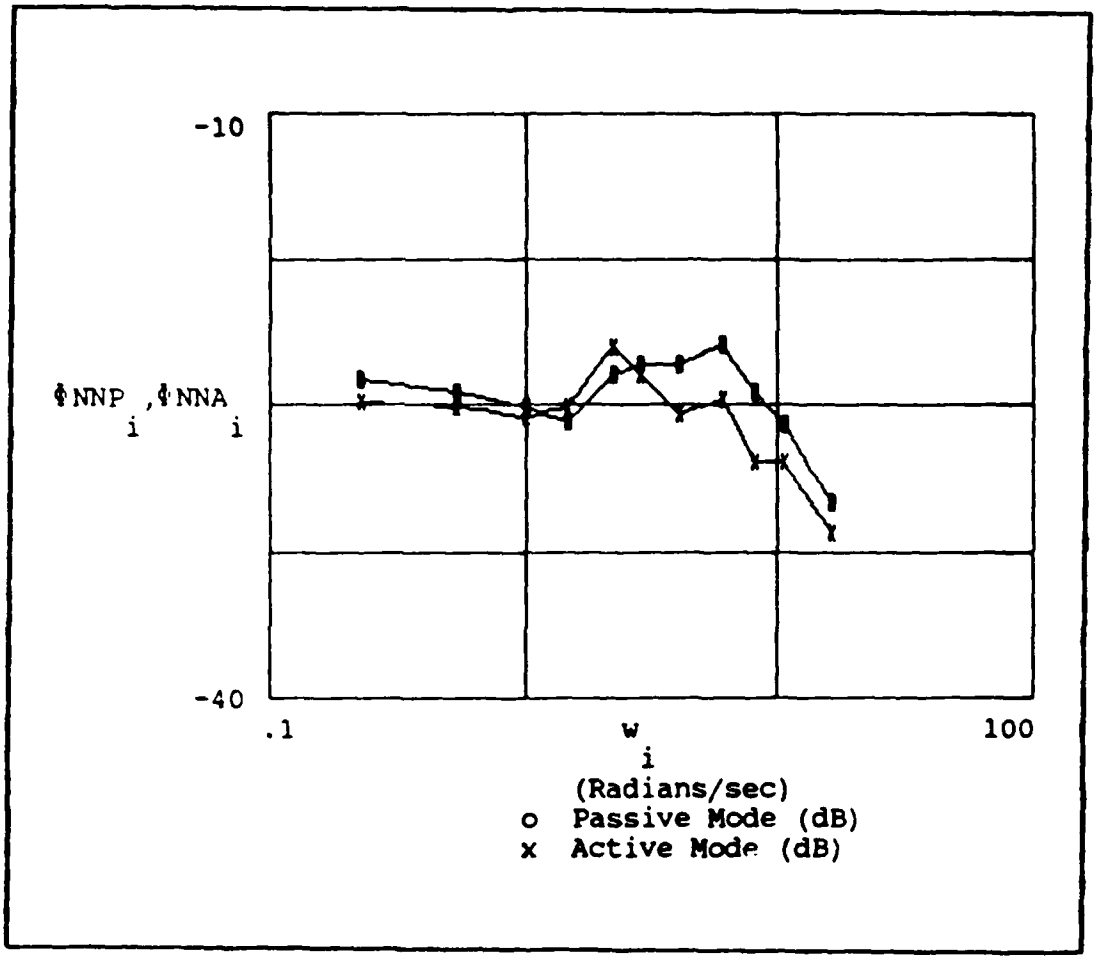

Figure E.2 - Operator Remnant/Noise (FF #1)

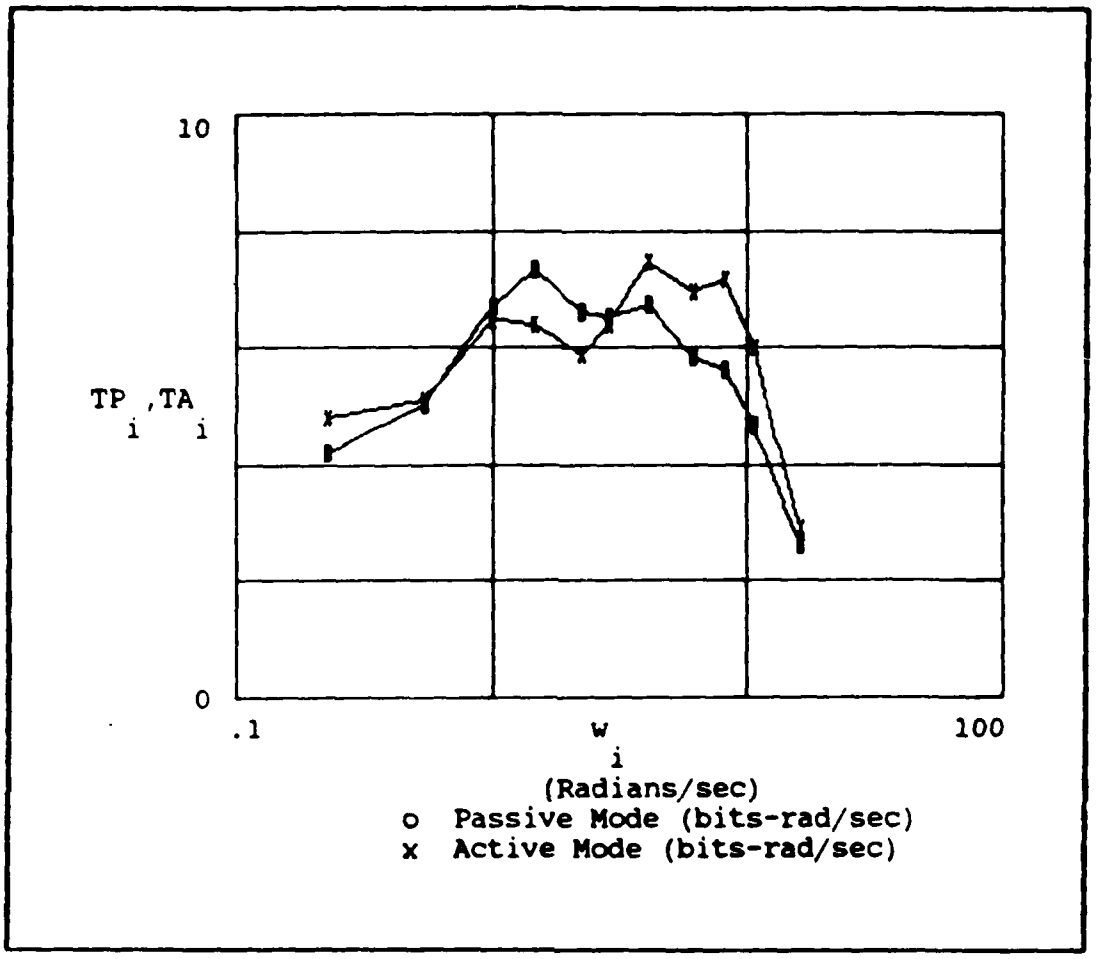

Figure E.3 - Transinformation Rate (FF #1)

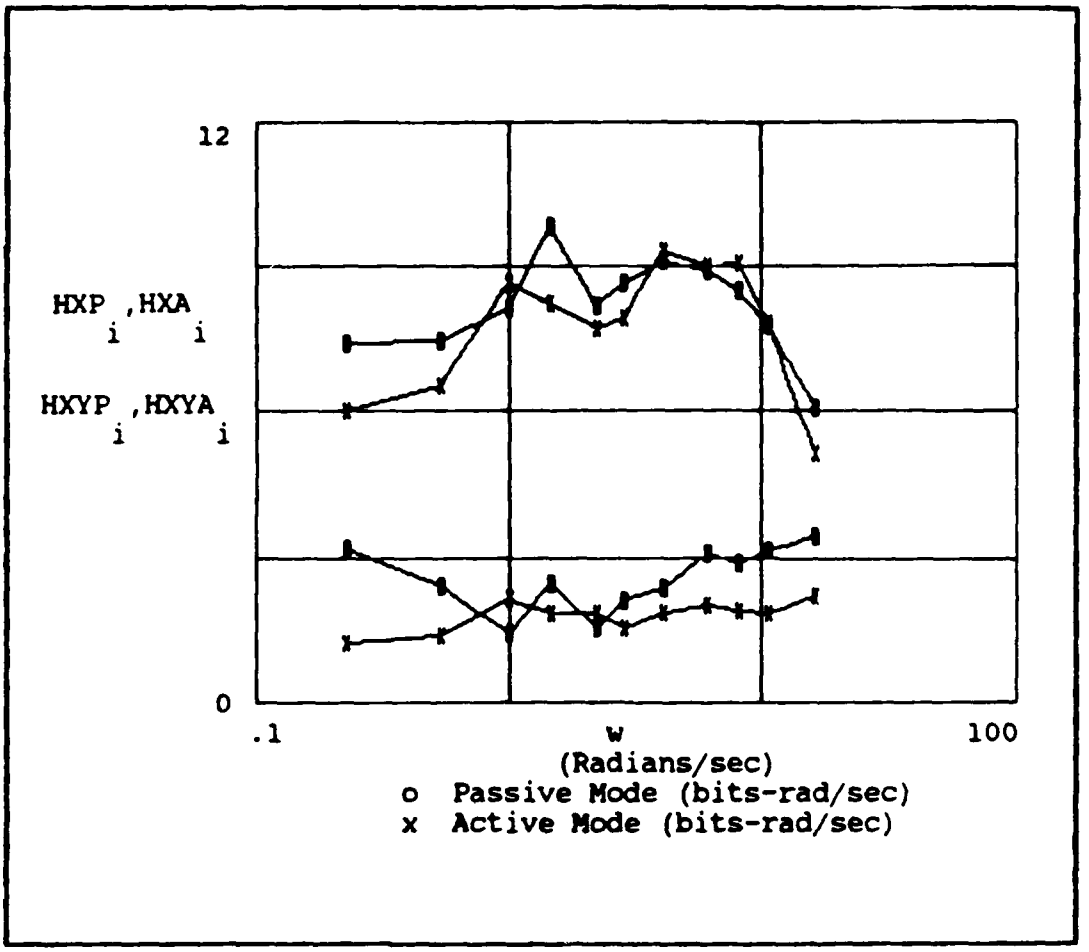

Figure E.4 - Display Error Entropy and Equivocation (FF #1)

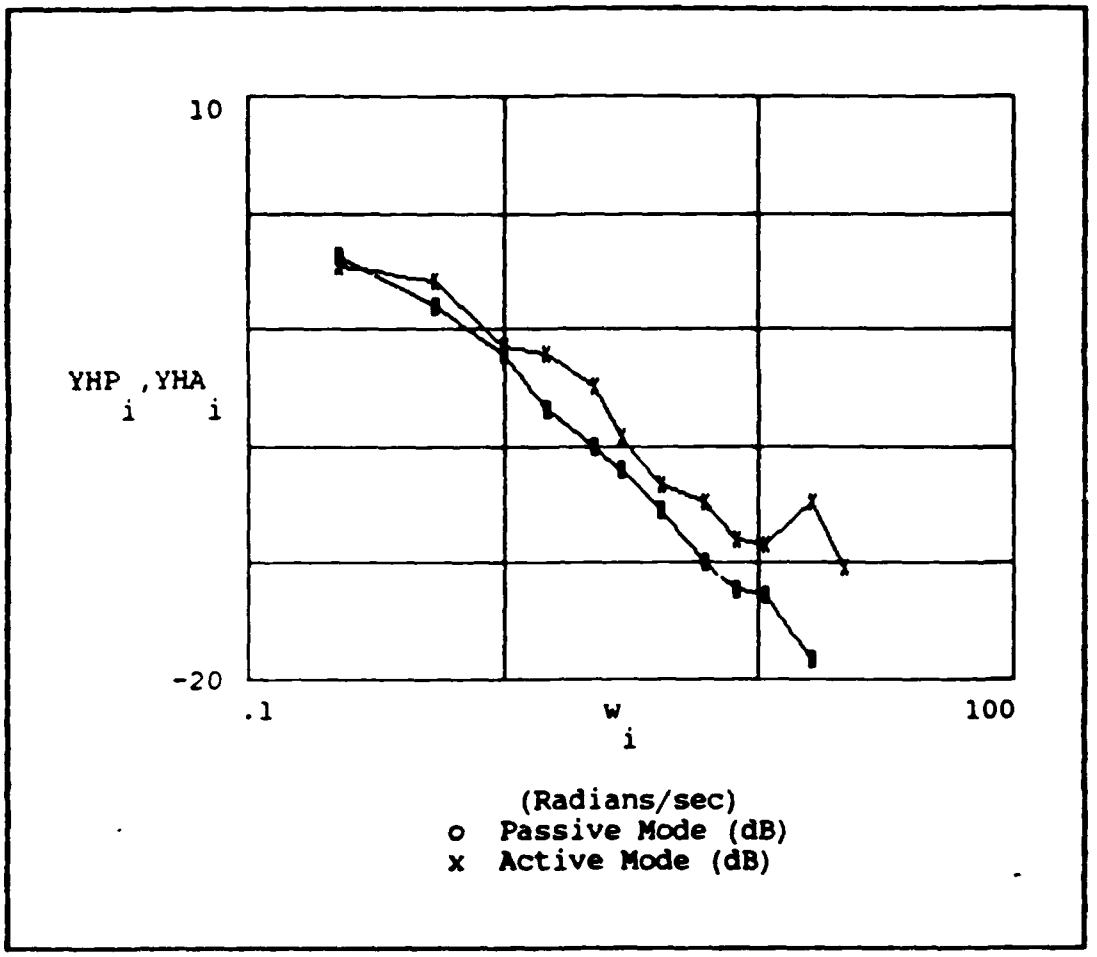

Figure E.5 - Human Operator Describing Function (FF #2)

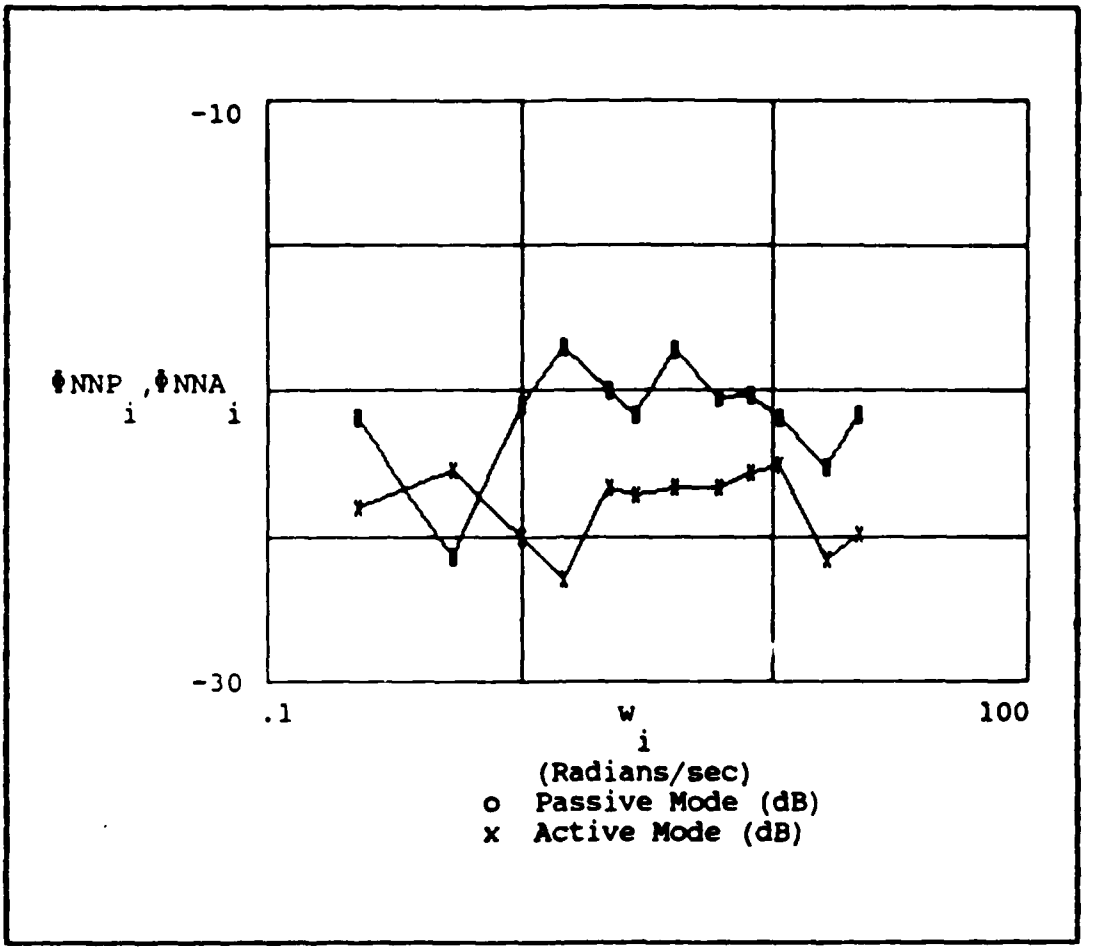

Figure E.6 - Operator Remnant/Noise (FF #2)

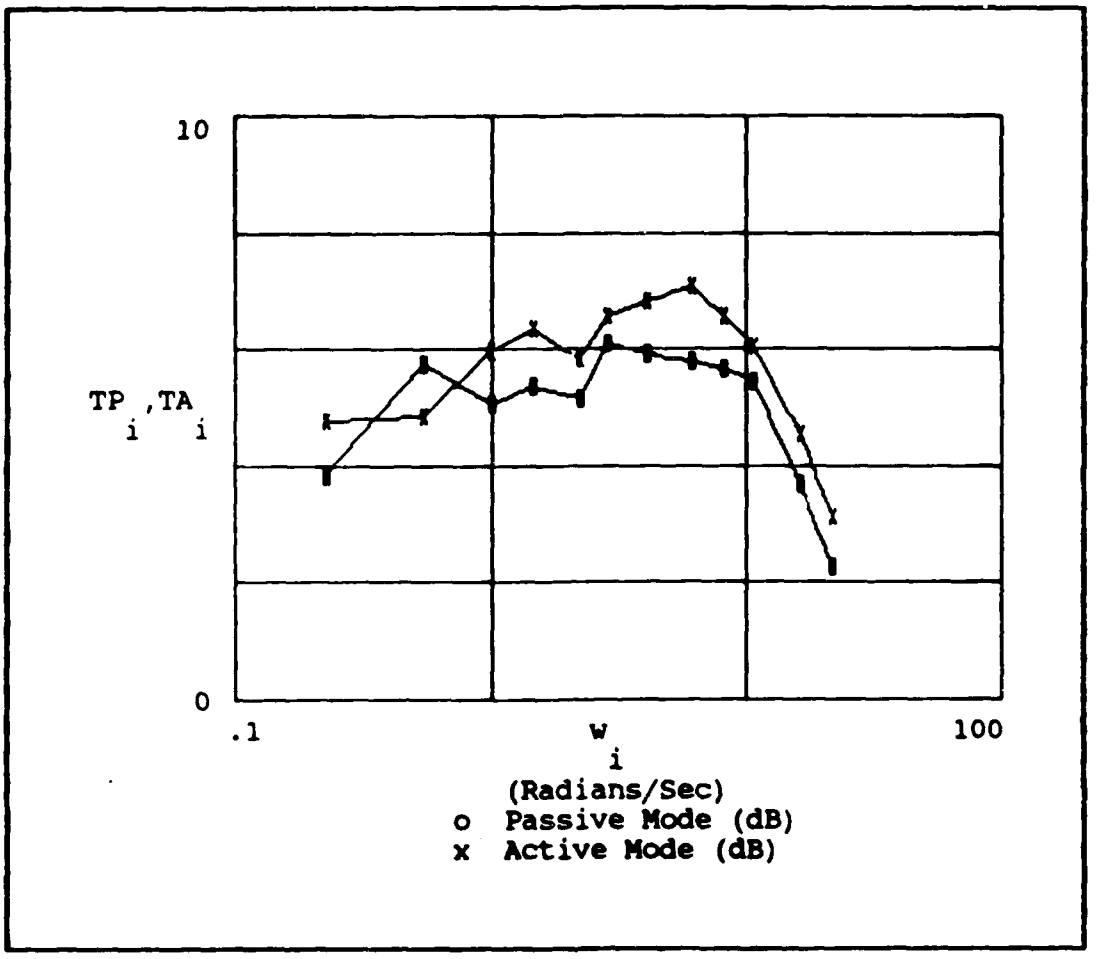

Figure E.7 - Transinformation Rate (FF #2)

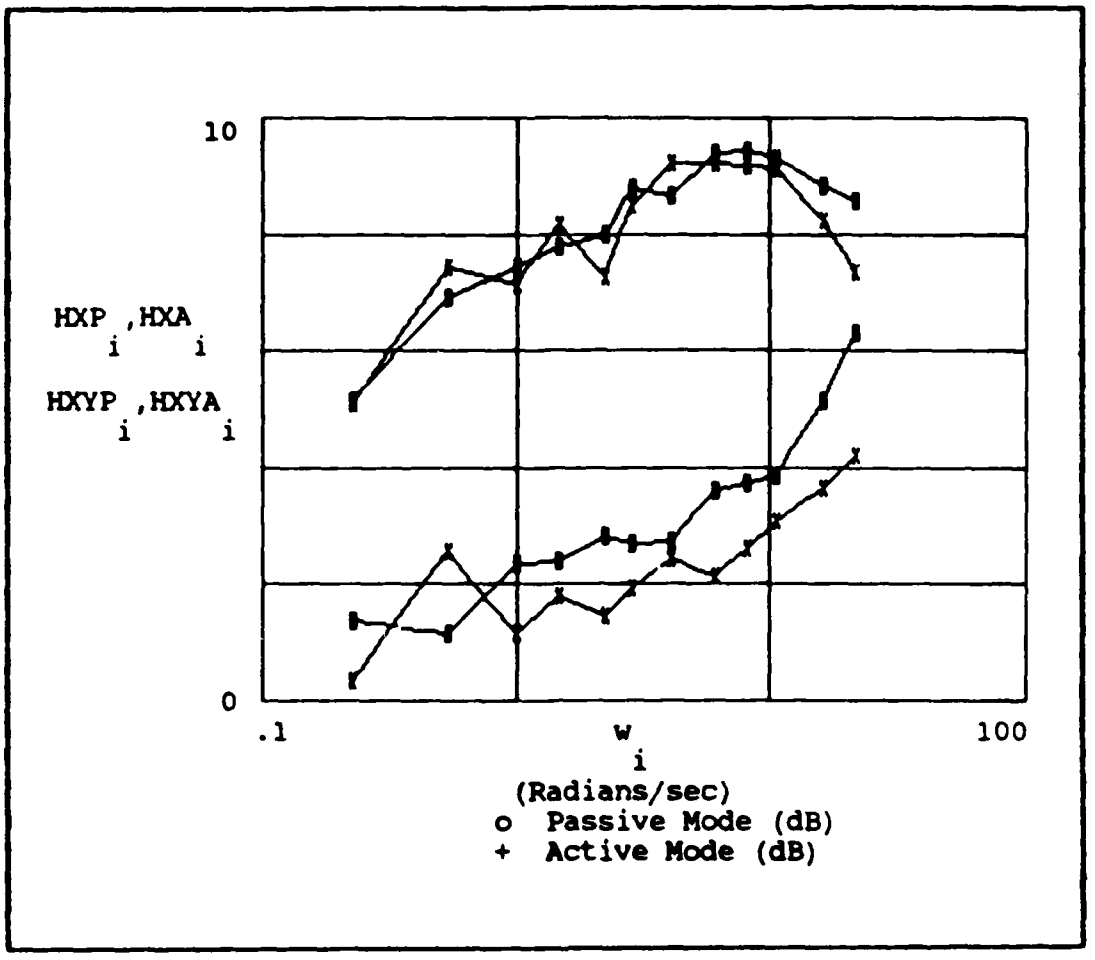

Figure E.8 - Display Error Entropy and Equivocation (FF #2)

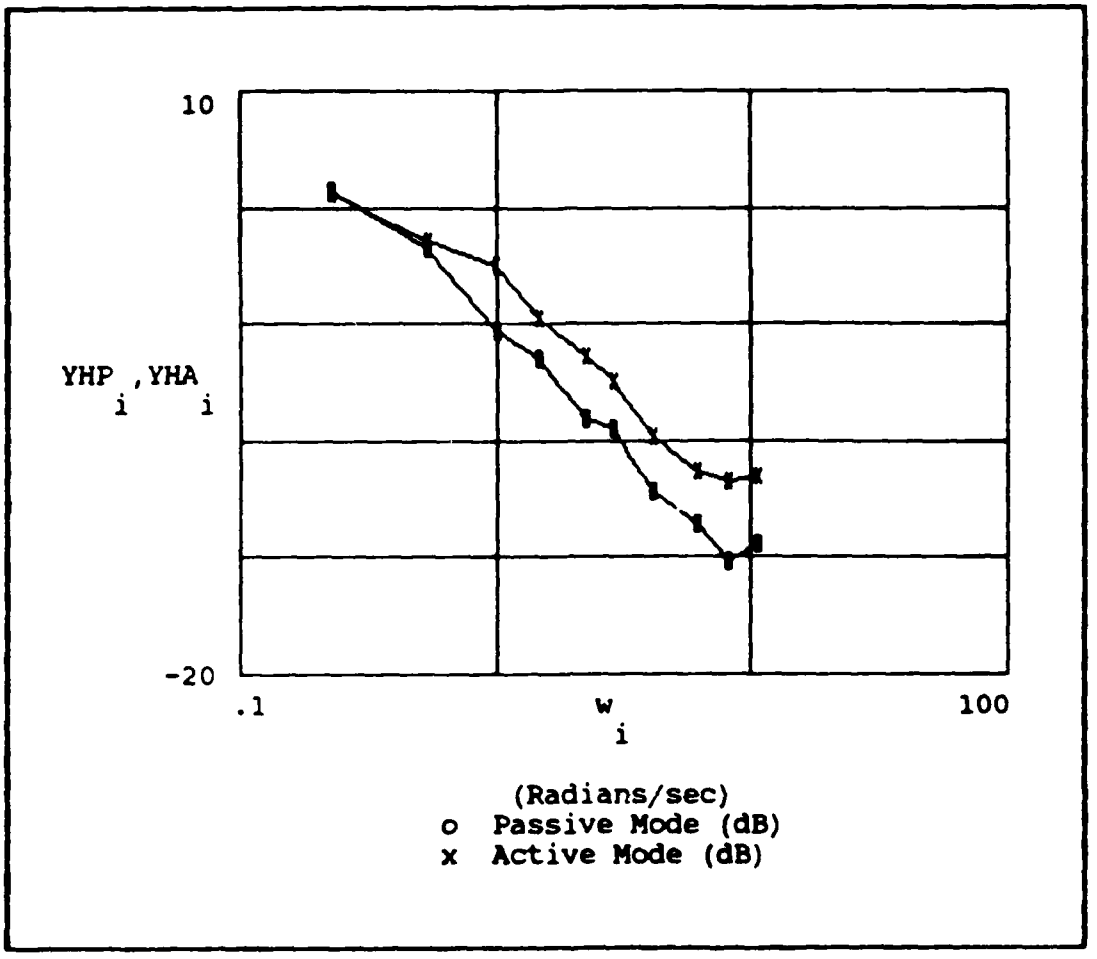

Figure E.9 - Human Operator Describing Function (FF #3)

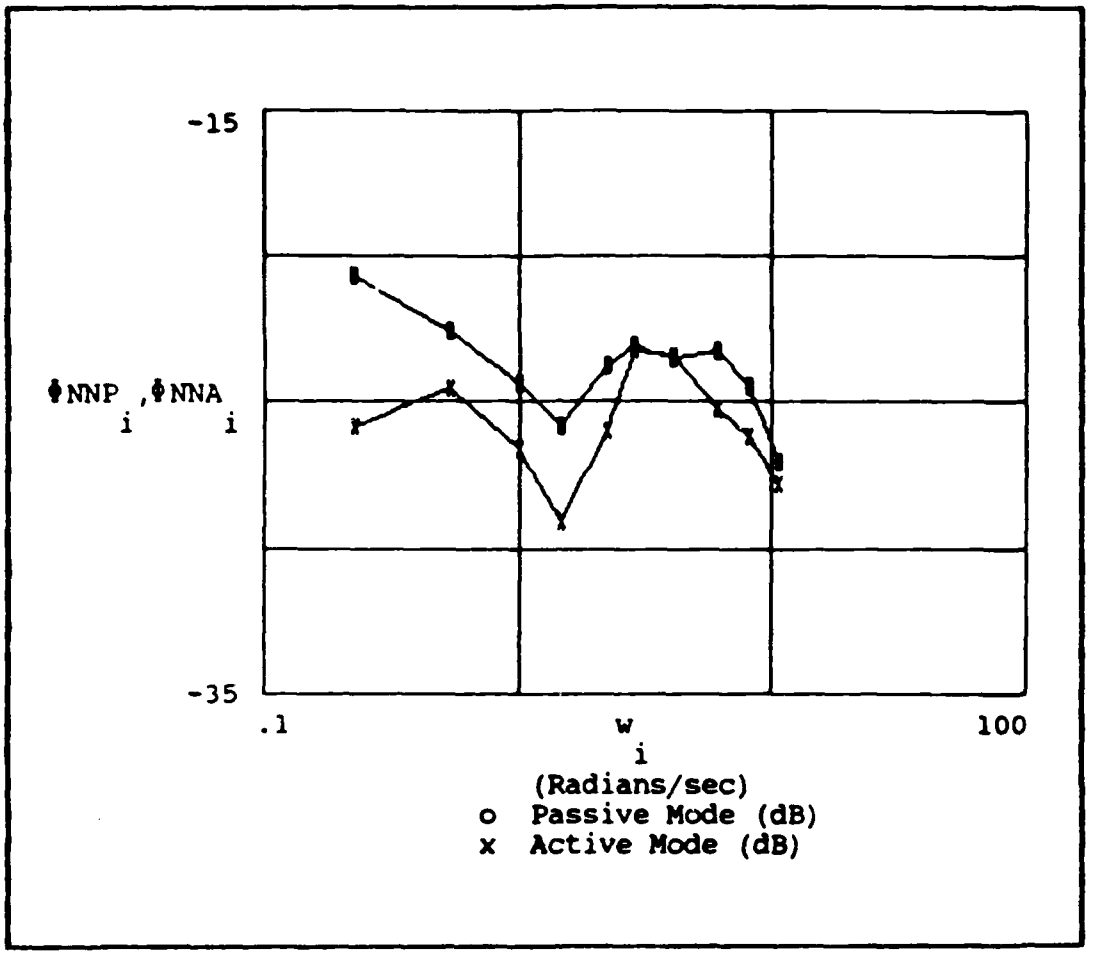

Figure E.10 - Operator Remnant/Noise (FF #3)

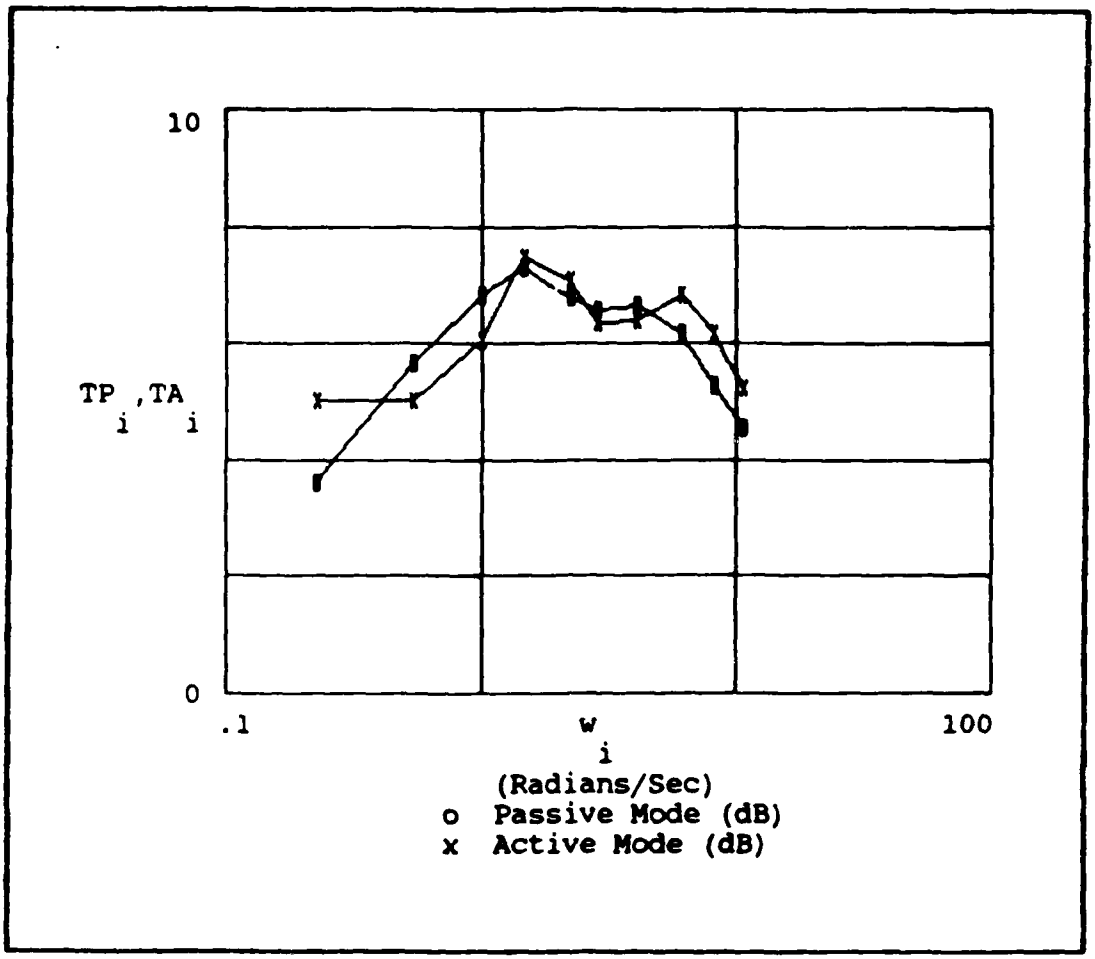

Figure E.11 - Transinformation Rate (FF #3)

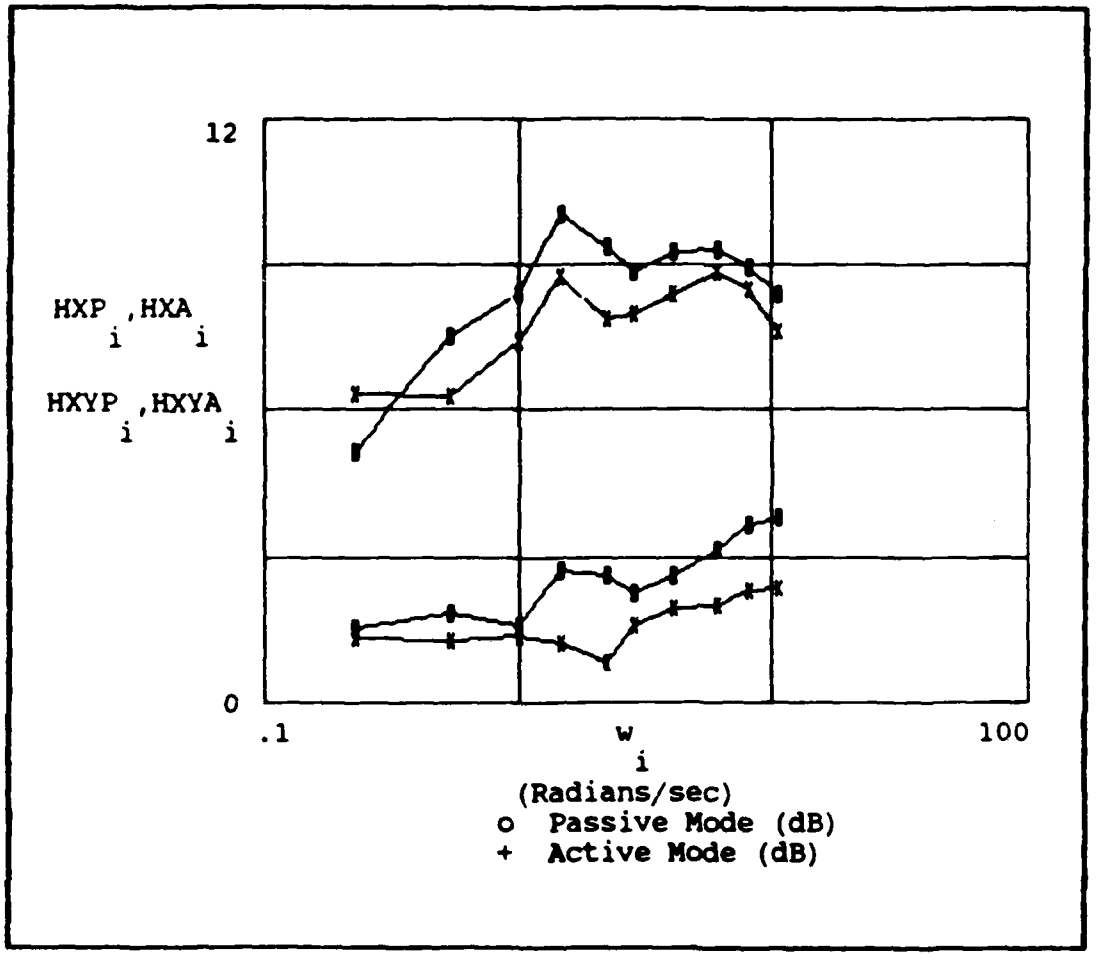

Figure E.12 - Display Error Entropy and Equivocation (FF #3)

Appendix F: Graphical Results For Subject #6

This appendix contains graphical representations of the results obtained by testing Subject #6. Each graph consists of a visual comparison of the active and passive modes of operation for a specific parameter under a specific forcing function.

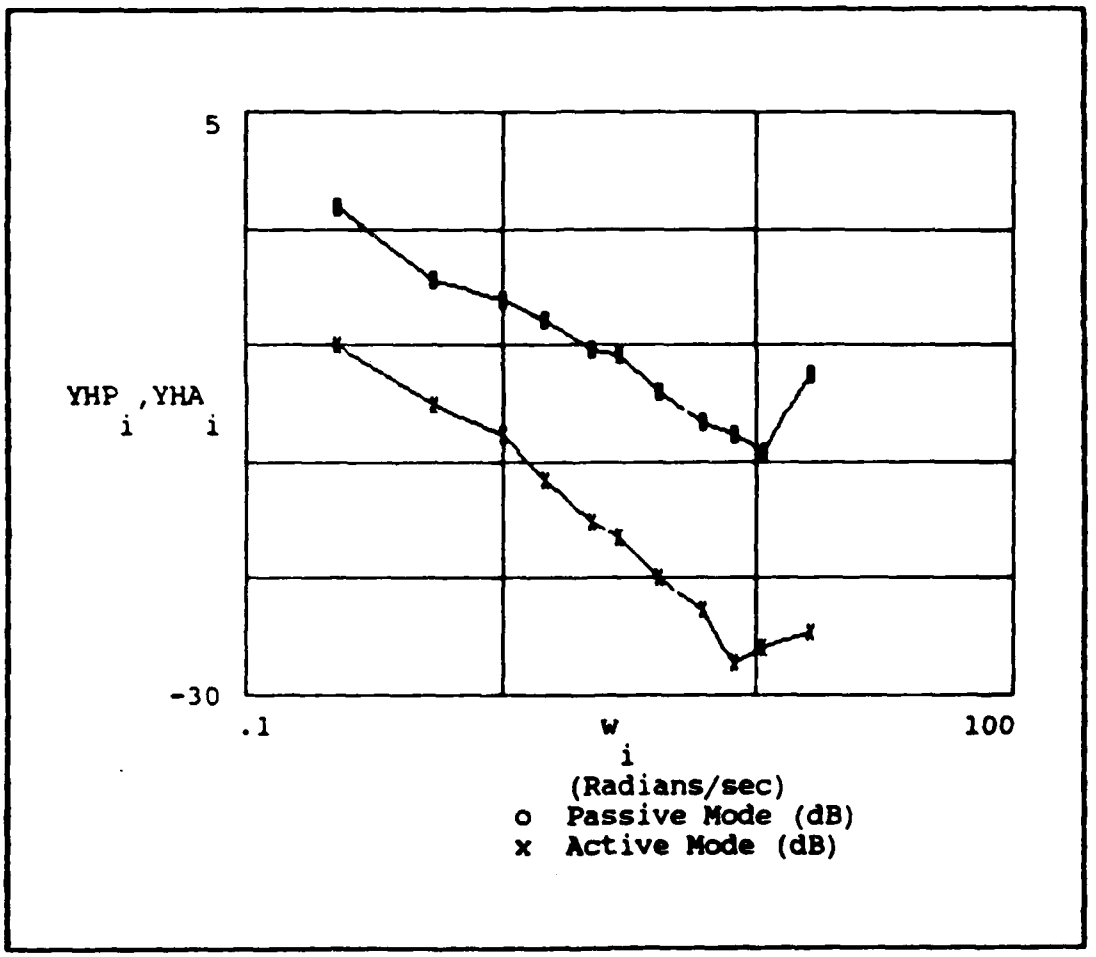

Figure F.1 - Human Operator Describing Function (FF #1)

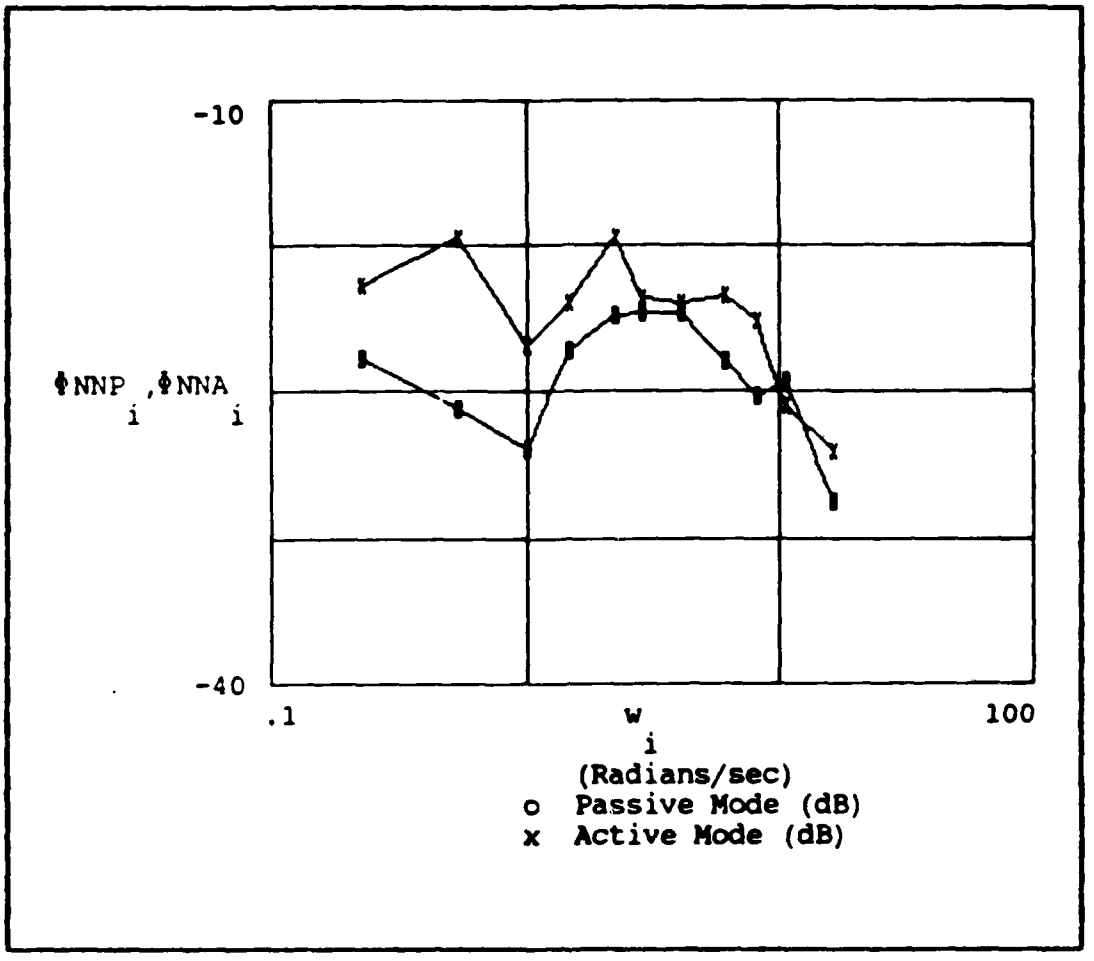

Figure F.2 - Operator Remnant/Noise (FF #1)

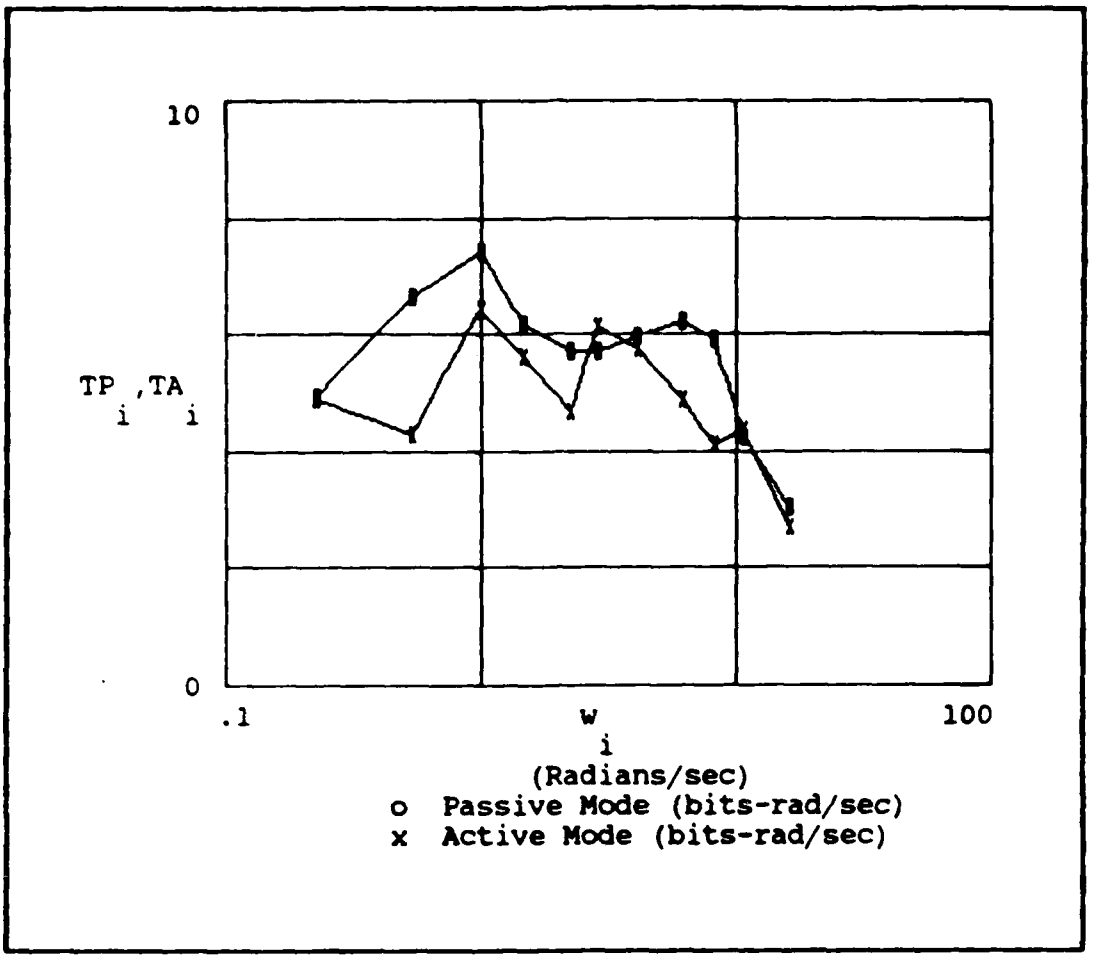

Figure F.3 - Transinformation Rate (FF #1)

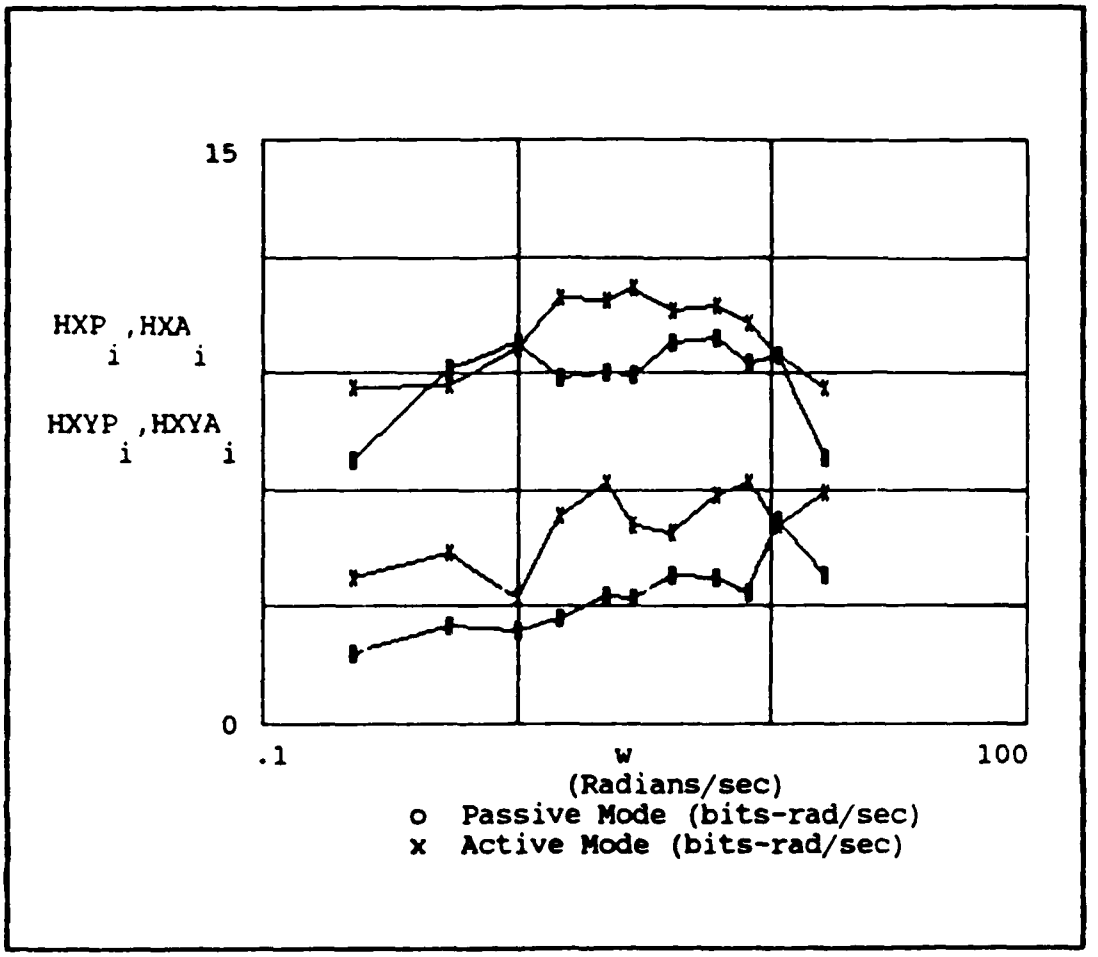

Figure F.4 - Display Error Entropy and Equivocation (FF #1)

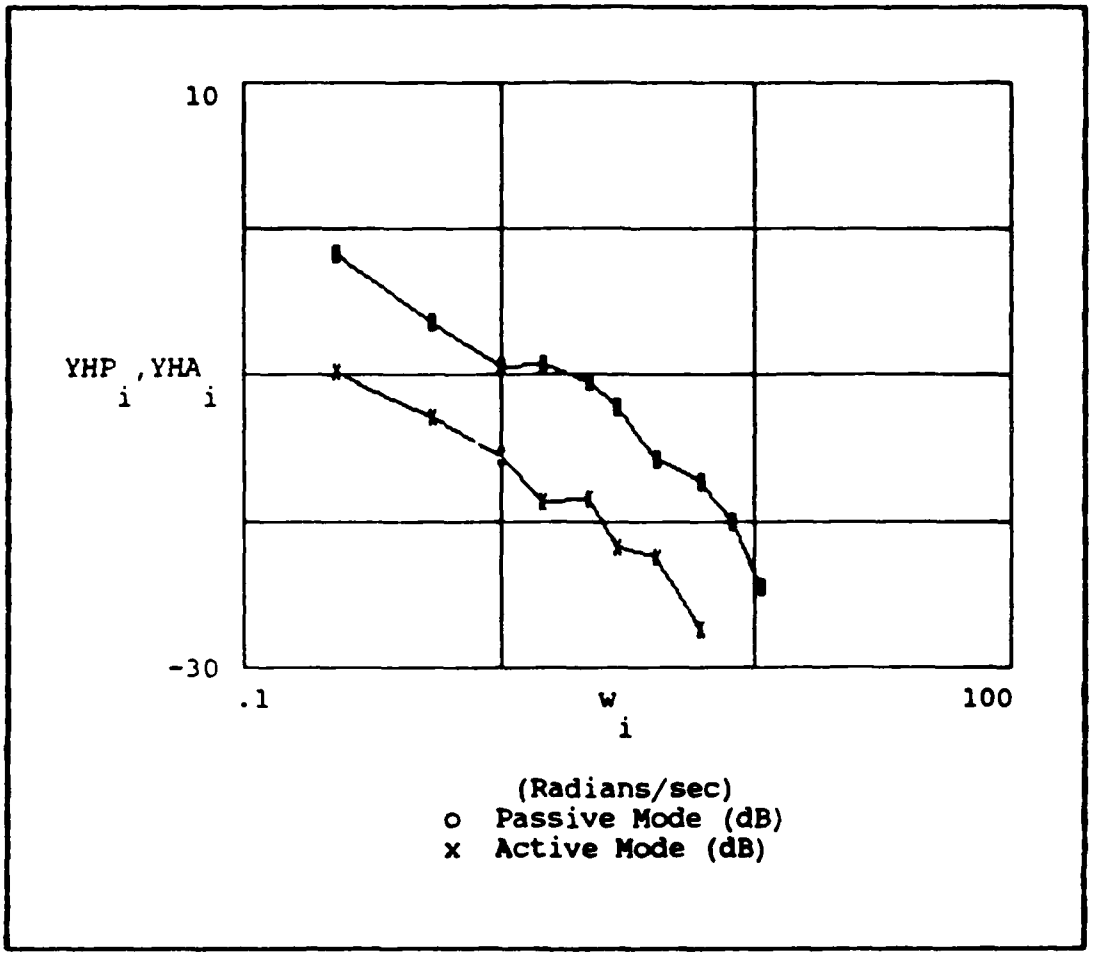

Figure F.5 - Human Operator Describing Function (FF #2)

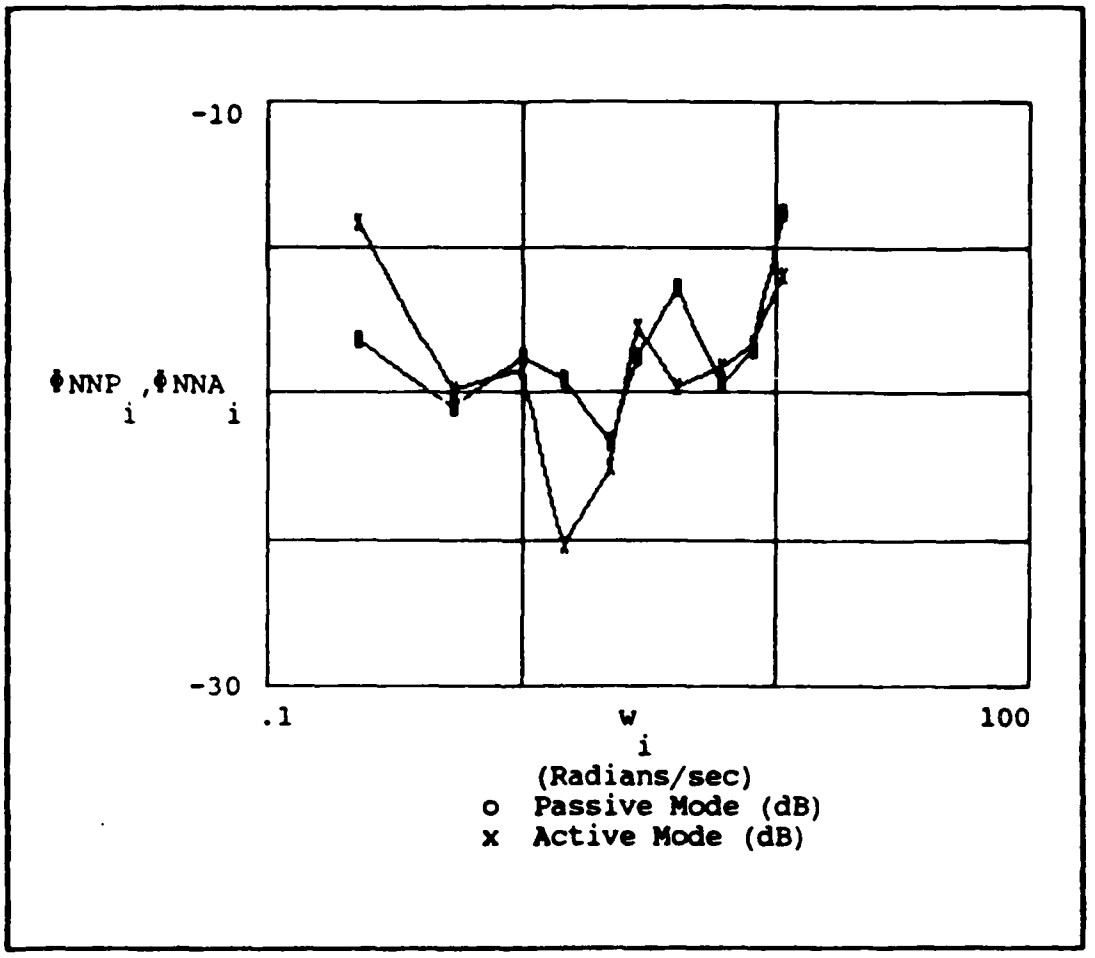

Figure F.6 - Operator Remnant/Noise (FF #2)

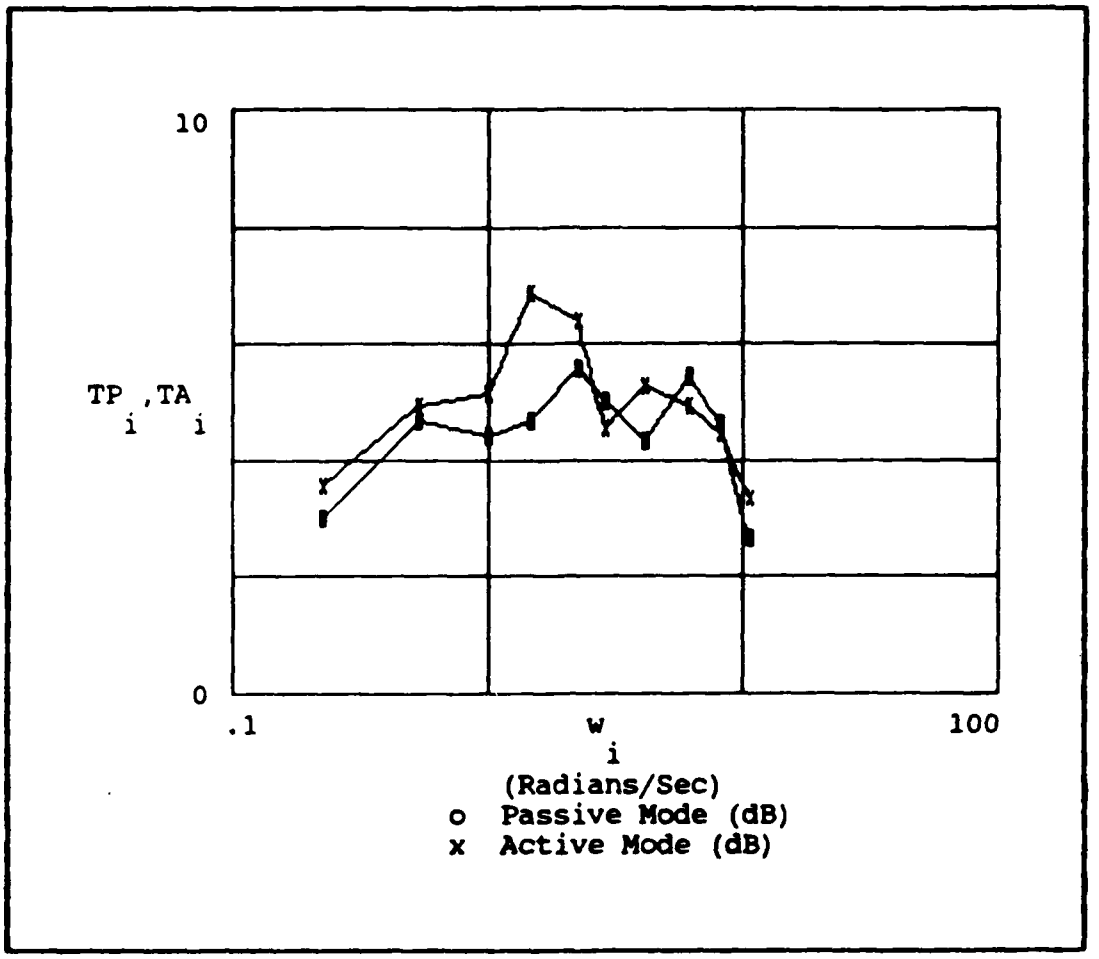

Figure F.7 - Transinformation Rate (FF #2)

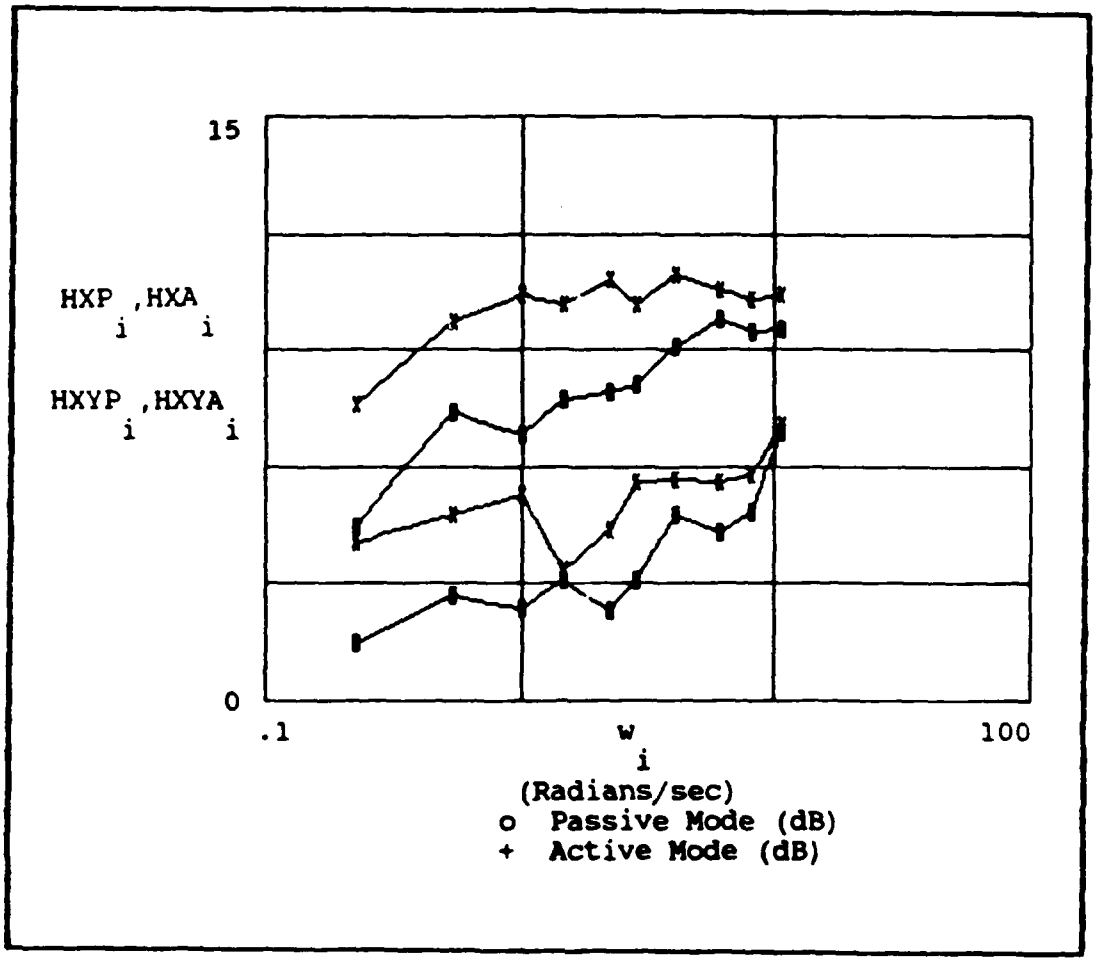

Figure F.8 - Display Error Entropy and Equivocation (FF #2)

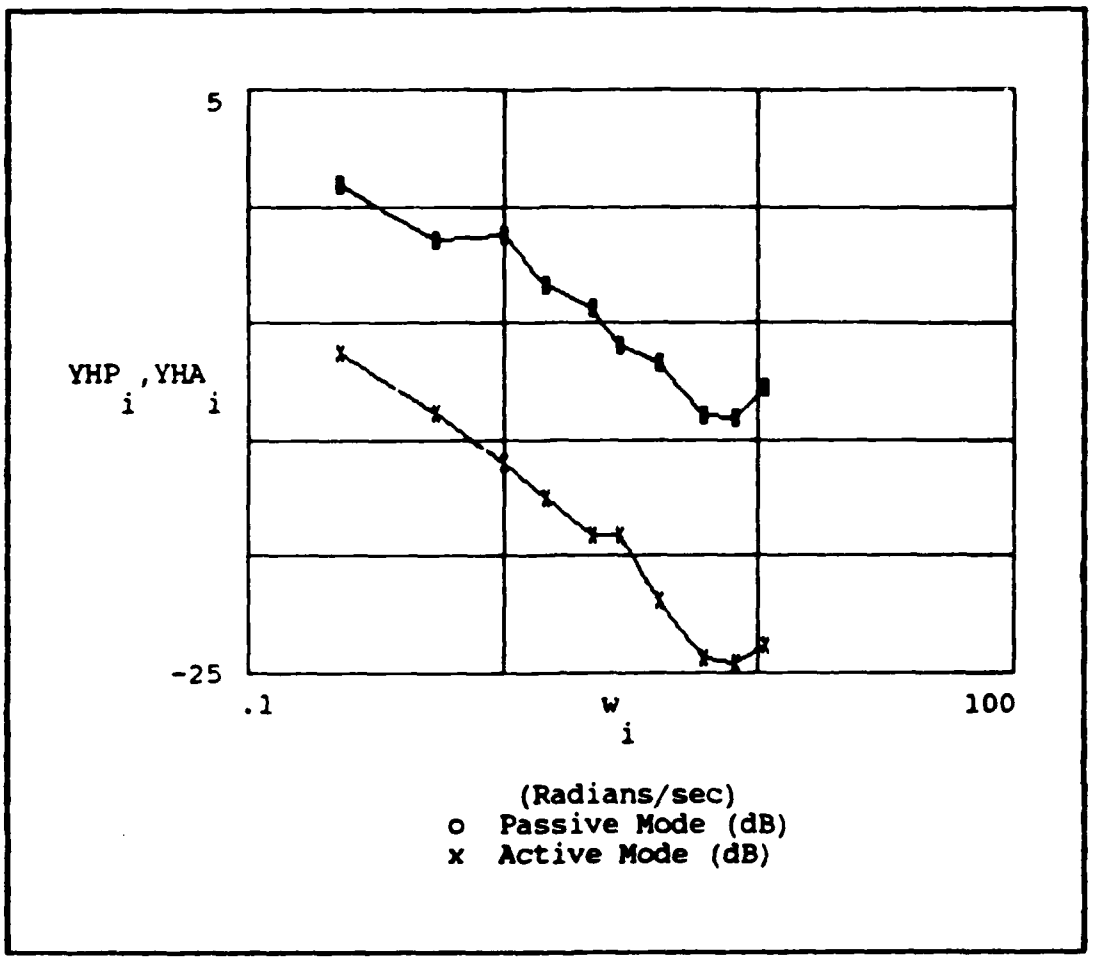

Figure F.9 - Human Operator Describing Function (FF #3)

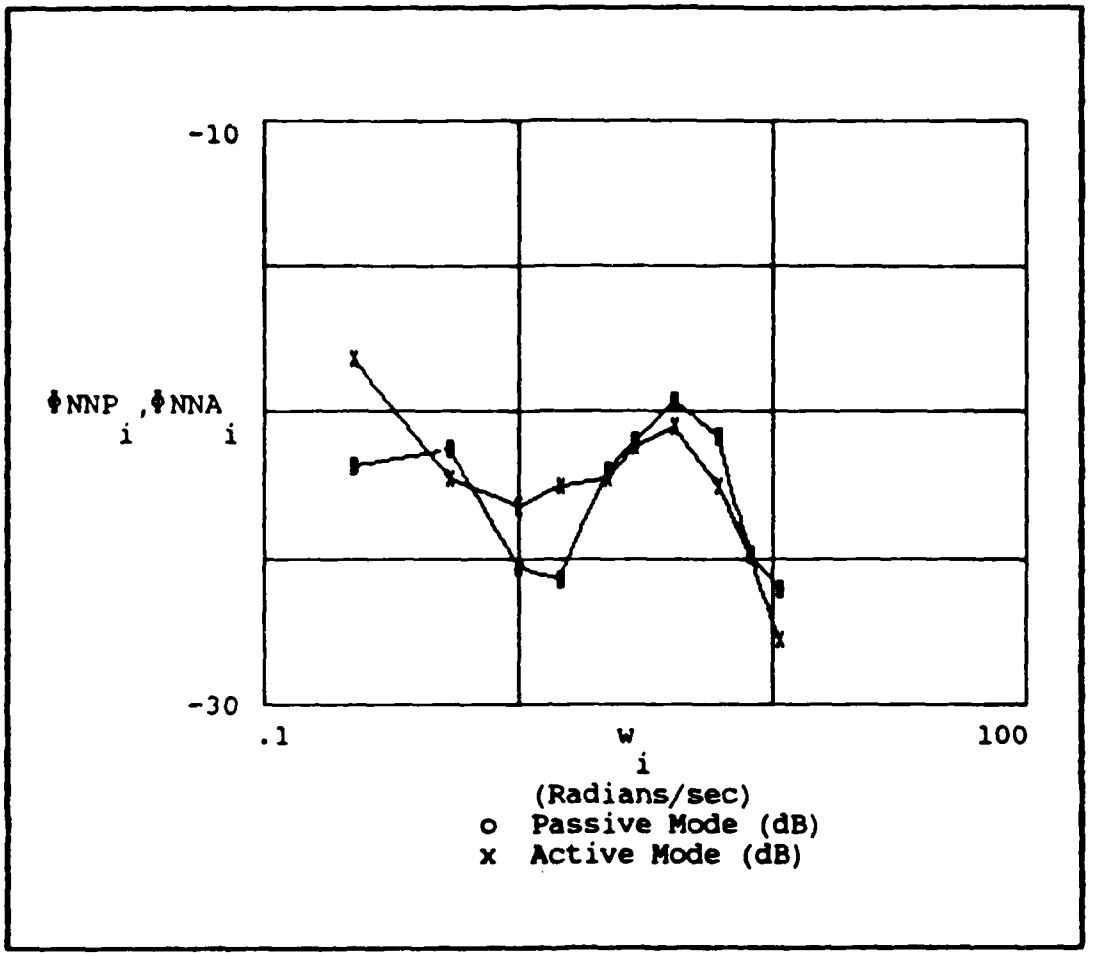

Figure F.10 - Operator Remnant/Noise (FF #3)

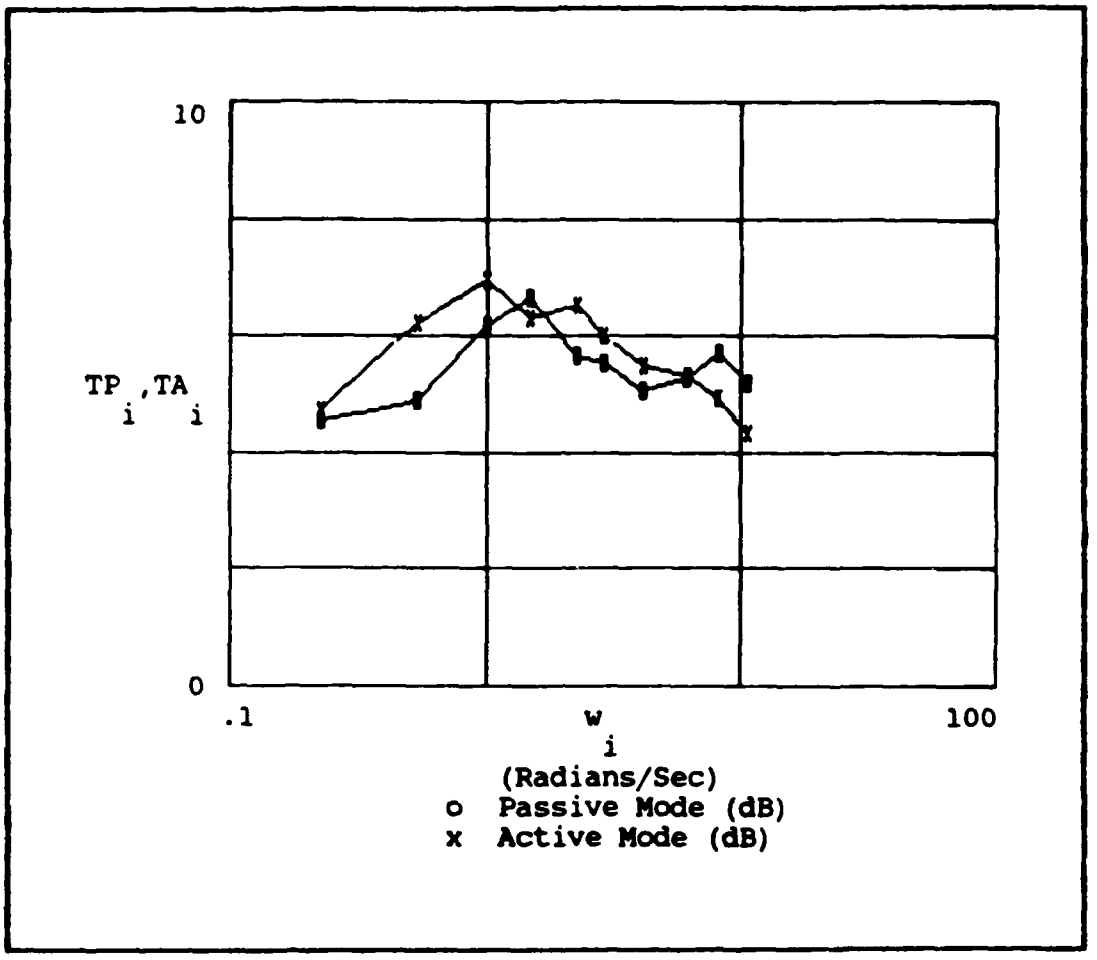

Figure F.11 - Transinformation Rate (FF #3)

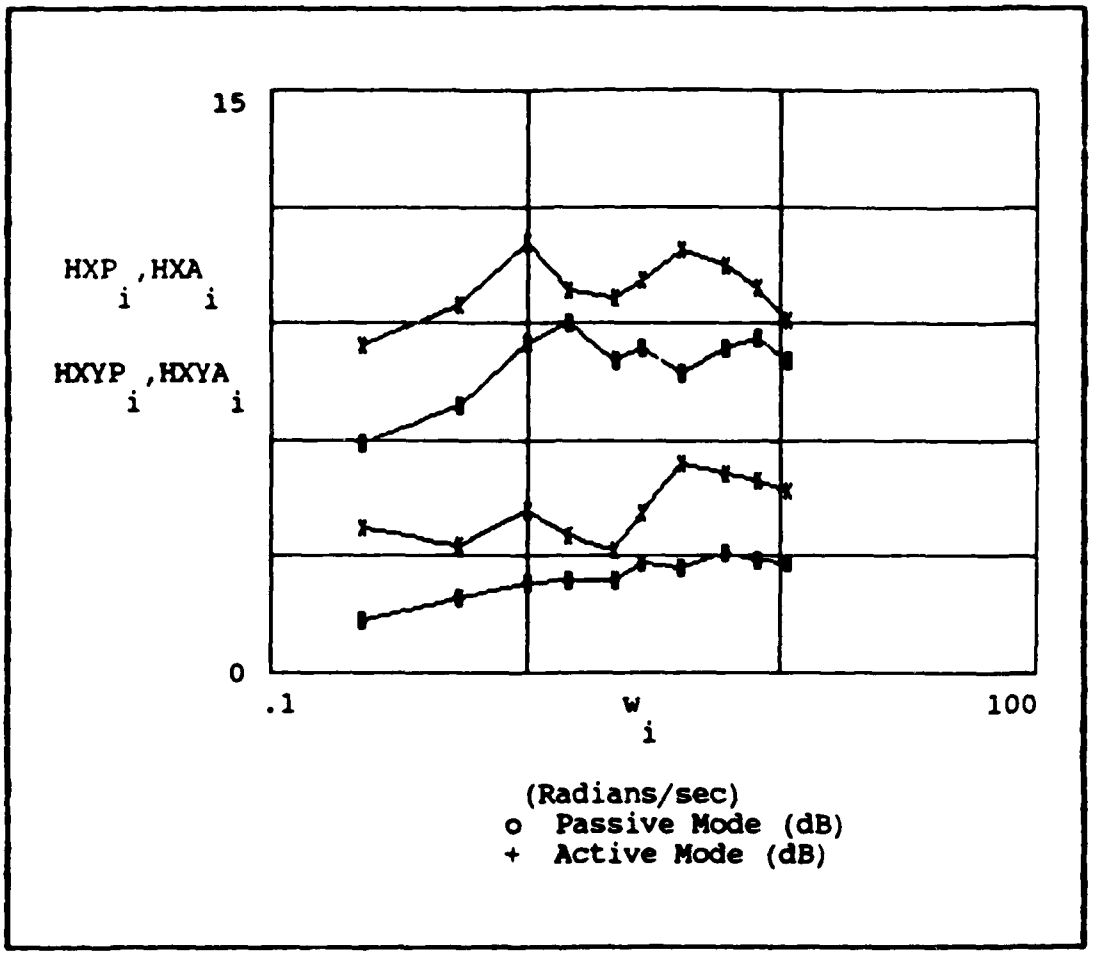

Figure F.12 - Display Error Entropy and Equivocation (FF #3)

Bibliography

1. Blahut, Richard E. Principles and Practice of Information Theory. Reading, MA: Addison-Wesley Publishing Company, 1987.

2. Crossman, E.R.F.W. "The Information Capacity of Human Motor System in Pursuit Tracking", The Quarterly Journal of Experimental Psychology. Volume XII, Part I: 1-16 (1960).

3. Fitts, Paul M. "The Information Capacity of the Human Motor System in Controlling the Amplitude of Movement", Journal of Experimental Psychology, Vol 47, 6:381-391

4. Fitts, Paul M. and Posner, Michael I. Human Performance. Belmont, CA: Brooks/Cole Publishing Company, 1967.

5. Elkind, J.I. and Sprague,L.T. "Transmission of Information in Simple Manual Control Systems", IRE Transactions on Human Factors in Electronics, 58-60 (March 1961).

6. Levison, William H. et al. "A Model for Human Controller Remnant", IRE Transactions on Man-Machine Systems, 4: 101-108 (1969).

7. Levison, William H. Techniques for Data Analysis and Input Waveform Generation for Manual Control Research. Technical Memorandum CSD-75-2. Control Systems Department, Bolt Beranek and Newman, Inc, Cambridge, MA, January 1975.

8. McRuer, D.T. et al. Human Pilot Dynamics in Compensatory Systems: Theory, Models, and Experiments With Controlled-Element and Forcing Function Variations. AFFDL-TR-65-15. Wright-Patterson Air Force Base, OH, July 1965.

9. Repperger, D.W. and McCollor,D. "Active Sticks - A New Dimension in Controller Design", Proceedings of the 20th Annual Conference in Manual Control (June 1984).

10. Repperger, D.W. Controllers With Force and Position Prio-Prioceptive Feedback. Protocol 88-10, AAMRL, Wright-Patterson Air Force Base, OH (March 1988).

11. Sheridan, T.B. and Ferrell, W.R. Man-Machine Systems: Information, Control, and Decision Models of Human Performance. Cambridge, MA: MIT Press, 1974.

12. Wempe, T. and Baty, Y. "Usefulness of Transinformation as a Measure of Human Tracking Performance", Conference on Manual Control, pp111-126 (circa 1966)

VITA

Captain John Pracher [redacted] on 3 May 1953. He earned a Bachelor of Science in Mathematics in 1975 from the State University College at Oneonta, New York. After attending Officer Training School at Lackland AFB, Texas in 1979, he was selected to attend the Bachelor Conversion Program at the Air Force Institute of Technology where he received a Bachelor of Science in Electrical Engineering in 1981. He was then assigned to Scott AFB, Illinois where he worked as a microwave and satellite systems engineer at the 1842nd Electrical Engineering Group, and subsequently, at Headquarters Air Force Communications Command as program manager for the ground terminal segment of the Defense Satellite Communications System. In 1984 Capt Pracher was assigned to Tinker AFB, Oklahoma as Chief of the Tactical Engineering Division of the 3rd Combat Communications Group. He later transferred to the Engineering and Installation Division to serve as the Air Force Program Manager for the Department of Defense Red Switch Project. In May 1987 he was selected to attend AFIT to pursue a Master's Degree in Electrical Engineering.

[redacted]

SECURITY CLASSIFICATION OF THIS PAGE

REPORT DOCUMENTATION PAGE

Form Approved
OMB No. 0704-0188

1a. REPORT SECURITY CLASSIFICATION UNCLASSIFIED	1b. RESTRICTIVE MARKINGS
2a. SECURITY CLASSIFICATION AUTHORITY	3. DISTRIBUTION/AVAILABILITY OF REPORT Approved For Public Release; Distribution Unlimited
2b. DECLASSIFICATION/DOWNGRADING SCHEDULE	
4. PERFORMING ORGANIZATION REPORT NUMBER(S) AFIT/GE/ENG/88D-38	5. MONITORING ORGANIZATION REPORT NUMBER(S)
6a. NAME OF PERFORMING ORGANIZATION School of Engineering 6b. OFFICE SYMBOL (If applicable) AFIT/ENG	7a. NAME OF MONITORING ORGANIZATION
6c. ADDRESS (City, State, and ZIP Code) Air Force Institute of Technology Wright-Patterson AFB OH 45433-6583	7b. ADDRESS (City, State, and ZIP Code)
8a. NAME OF FUNDING/SPONSORING ORGANIZATION AAMRL 8b. OFFICE SYMBOL (If applicable) BBS	9. PROCUREMENT INSTRUMENT IDENTIFICATION NUMBER
8c. ADDRESS (City, State, and ZIP Code) Wright-Patterson AFB OH 45433-6583	10. SOURCE OF FUNDING NUMBERS PROGRAM ELEMENT NO. / PROJECT NO. / TASK NO / WORK UNIT ACCESSION NO.
11. TITLE (Include Security Classification) See Box 19	
12. PERSONAL AUTHOR(S) John M. Pracher, B.S.E.E., Captain, USAF	
13a. TYPE OF REPORT MSEE Thesis 13b. TIME COVERED FROM _____ TO _____ 14. DATE OF REPORT (Year, Month, Day) 1988 November 15. PAGE COUNT 149	
16. SUPPLEMENTARY NOTATION	

17. COSATI CODES			18. SUBJECT TERMS (Continue on reverse if necessary and identify by block number)
FIELD	GROUP	SUB-GROUP	
23	02		Control Sticks, Control Systems, Information Theory, Control Theory, Performance (Human), Capacity, Equivocation
12	09		

19. ABSTRACT (Continue on reverse if necessary and identify by block number)

Title: RESPONSE EQUIVOCATION ANALYSIS FOR THE SMART STICK CONTROLLER

Thesis Chairman: David M. Norman, Major, USAF

Approved for release in accordance with AFR 190-1
[illegible]

20. DISTRIBUTION/AVAILABILITY OF ABSTRACT ☒ UNCLASSIFIED/UNLIMITED ☐ SAME AS RPT. ☐ DTIC USERS	21. ABSTRACT SECURITY CLASSIFICATION UNCLASSIFIED
22a. NAME OF RESPONSIBLE INDIVIDUAL David M. Norman, Major, USAF	22b. TELEPHONE (Include Area Code) (513) 255-3576 22c. OFFICE SYMBOL AFIT/ENG

DD Form 1473, JUN 86 *Previous editions are obsolete.* SECURITY CLASSIFICATION OF THIS PAGE

This research provides an analysis of response equivocation (lost information) for subjects who use the "smart stick controller" -- an aircraft stick controller designed by the Armstrong Aerospace Medical Research Laboratory (AAMRL) to improve a pilot's tracking performance. First, a control theory model of a compensatory tracking task is developed and analyzed. Then, using an information theory model of the pilot, the results are used to develop expressions for information theory parameters (input entropy, transinformation, and equivocation).

Six subjects were tested using the smart stick controller and experimental an apparatus developed by the AAMRL. Each subject was tested twice: first in the passive stick mode (normal stick operation), and again in the active stick mode. In the active stick mode, the smart stick actively exerts a force in the direction opposite to the desired stick motion. Power spectral densities of the display error and the operator response were used to calculate the information theory parameters.

The results indicated that by viewing the response equivocation alone, it was not possible to ascertain any significant change in performance between passive and active stick mode operation. However, by viewing other parameters (entropy, transinformation, human operator transfer function, and human operator remnant), it is evident that a change in performance definitely occurs.